eISSN 2500-0632

MINING SCIENCE AND TECHNOLOGY (RUSSIA)

ТОМ VOL. 7, №1
2022

GORNYE NAUKI I TEKHNOLOGII
ГОРНЫЕ НАУКИ И ТЕХНОЛОГИИ

MISIS
НАЦИОНАЛЬНЫЙ ИССЛЕДОВАТЕЛЬСКИЙ ТЕХНОЛОГИЧЕСКИЙ УНИВЕРСИТЕТ «МИСИС»
NATIONAL UNIVERSITY OF SCIENCE AND TECHNOLOGY MISIS

MINING SCIENCE AND TECHNOLOGY (Russia)
Горные науки и технологии
SCIENTIFIC AND PRACTICAL E-JOURNAL

eISSN 2500-0632
2022
Vol. 7, no. 1
https://mst.misis.ru/

Activities of the ***Mining Science and Technology (Russia) (Gornye nauki i tekhnologii)*** international journal are aimed at developing international scientific and professional cooperation in the field of mining.
The journal target audience comprises researchers, specialists in the field of mining, representatives of academic and professional communities.
The journal publishes original papers describing research findings, experience in the implementation of projects in mining industry, review publications.
The journal seeks to develop interdisciplinary areas that contribute to progress in mining, for example, technological and environmental safety, project organization and management in mining industry, development of territories, legal aspects of natural resource use, and other areas studied by researchers and practitioners. The journal always welcomes new developments. Papers are accepted in English or Russian.

QUARTERLY

FOUNDED in 2016

REGISTRATION
The journal science and applied research journal is registered by the Federal Service for Communication, IT and Mass Communication Control on August 10, 2015.
Registration Certificate E-No. ФС77-62652

INDEXATION
Scopus, CAS, EBSCO, DOAJ, РИНЦ, ВИНИТИ РАН, Dimensions, BASE, J-Gate, Jisc Library Hub Discover.

FOUNDER AND PUBLISHER
The National University of Science and Technology MISiS (NUST MISiS)

CONTACT
4 Leninsky Prospect, Moscow 119049, Russian Federation
Phone: +7 (495) 955-00-77
e-mail: send@misis.ru

ГОРНЫЕ НАУКИ И ТЕХНОЛОГИИ

Mining Science and Technology (Russia)

ЭЛЕКТРОННЫЙ НАУЧНО-ПРАКТИЧЕСКИЙ ЖУРНАЛ

eISSN 2500-0632

2022

Т. 7, № 1

https://mst.misis.ru/

Деятельность научно-практического журнала «Горные науки и технологии» (Mining Science and Technology (Russia)) направлена на развитие международного научного и профессионального сотрудничества в области горного дела.

Целевая аудитория журнала – исследователи, специалисты в области горного дела, представители академического и профессионального сообществ.

В журнале публикуются оригинальные статьи, описывающие результаты исследований, опыт реализации проектов в горнопромышленном комплексе, обзорные публикации.

Журнал стремится развивать такие междисциплинарные направления, как технологическая и экологическая безопасность, организация и управление проектами в горной промышленности, развитие территорий, правовые аспекты использования природных ресурсов и другие, которые способствуют прогрессу в горном деле и реализуются исследователями и практиками.

ПЕРИОДИЧНОСТЬ 4 раза в год

ОСНОВАН в 2016 году

РЕГИСТРАЦИЯ

Зарегистрирован Федеральной службой по надзору в сфере связи, информационных технологий и массовых коммуникаций 10 августа 2015 года.
Свидетельство о регистрации Эл № ФС77-62652.

ИНДЕКСИРОВАНИЕ

Scopus, CAS, EBSCO, DOAJ, РИНЦ, ВИНИТИ РАН, Dimensions, BASE, J-Gate, Jisc Library Hub Discover.

OPEN ACCESS Журнал открытого доступа.

УЧРЕДИТЕЛЬ И ИЗДАТЕЛЬ

МИСиС Национальный исследовательский технологический университет «МИСиС» (НИТУ «МИСиС»)

АДРЕС УЧРЕДИТЕЛЯ И ИЗДАТЕЛЯ

119049, г. Москва, Ленинский проспект, д. 4

КОНТАКТЫ РЕДАКЦИИ

Адрес: 119049, г. Москва, Ленинский проспект, д. 4
Телефон: +7 (495) 955-00-77
e-mail: send@misis.ru

MINING SCIENCE AND TECHNOLOGY (Russia)
Горные науки и технологии
SCIENTIFIC AND PRACTICAL E-JOURNAL
eISSN 2500-0632
2022
Vol. 7, no. 1
https://mst.misis.ru/

CONTENTS

MINERAL RESOURCES EXPLOITATION
Evaluation of the efficiency and environmental impact (on subsoil and groundwater) of underground block leaching (UBL) of metals from ores 5
V. I. Lyashenko, V. I. Golik, R. V. Klyuev

GEOLOGY OF MINERAL DEPOSITS
Features of fluid dynamics in long-term heterogeneous gas reservoirs 18
A. A. Feyzullayev, A. G. Gojayev, I. M. Mamedova

MINING ROCK PROPERTIES. ROCK MECHANICS AND GEOPHYSICS
Amplitude-initiated open hysteresis loop of *P*-wave attenuation in sandstone: experimental study 30
E. I. Mashinsky

SAFETY IN MINING AND PROCESSING INDUSTRY AND ENVIRONMENTAL PROTECTION
Experimental study of transient thermal conditions in longwall faces 37
M. O. Perestoronin, A. B. Zaitsev, M. A. Semin, D. A. Borodavkin

CONSTRUCTION OF MINING ENTERPRISES AND UNDERGROUND SPACE DEVELOPMENT
Analysis of mechanized tunneling parameters to determine the overcutting characteristics........ 49
D. S. Konyukhov

POWER ENGINEERING, AUTOMATION, AND ENERGY PERFORMANCE
Automatic control system for walking dragline excavator digging........ 57
L. D. Pevzner, N. A. Kiselev

Improvement of the electric energy quality in underground electric networks in highly productive coal mines........ 66
L. A. Plashchansky, S. N. Reshetnyak, M. Y. Reshetnyak

Behaviour of electric drive of roller-bit drilling rig swivel head with fuzzy control 78
N. M. Kuznetsov, I. N. Morozov

ГОРНЫЕ НАУКИ И ТЕХНОЛОГИИ
Mining Science and Technology
ЭЛЕКТРОННЫЙ НАУЧНО-ПРАКТИЧЕСКИЙ ЖУРНАЛ
eISSN 2500-0632
2022
Т. 7, № 1
https://mst.misis.ru/

СОДЕРЖАНИЕ

РАЗРАБОТКА МЕСТОРОЖДЕНИЙ ПОЛЕЗНЫХ ИСКОПАЕМЫХ

Оценка эффективности гидрогеологической и окружающей среды при подземном блочном выщелачивании металлов из руд ... 5
В.И. Ляшенко, В.И. Голик, Р.В. Клюев

ГЕОЛОГИЯ МЕСТОРОЖДЕНИЙ ПОЛЕЗНЫХ ИСКОПАЕМЫХ

Особенности флюидодинамики в длительно эксплуатирующихся неоднородных газовых резервуарах ... 18
А.А. Фейзуллаев, А.Г. Годжаев, И.М. Мамедова

СВОЙСТВА ГОРНЫХ ПОРОД. ГЕОМЕХАНИКА И ГЕОФИЗИКА

Амплитудно-инициируемая открытая петля гистерезиса затухания *P*-волны в песчанике: экспериментальное исследование ... 30
Э.И. Машинский

ТЕХНОЛОГИЧЕСКАЯ БЕЗОПАСНОСТЬ В МИНЕРАЛЬНО-СЫРЬЕВОМ КОМПЛЕКСЕ И ОХРАНА ОКРУЖАЮЩЕЙ СРЕДЫ

Экспериментальное исследование переходных тепловых режимов длинных очистных забоев ... 37
М.О. Пересторонин, А.В. Зайцев, М.А. Семин, Д.А. Бородавкин

СТРОИТЕЛЬСТВО ГОРНЫХ ПРЕДПРИЯТИЙ И ОСВОЕНИЕ ПОДЗЕМНОГО ПРОСТРАНСТВА

Анализ параметров механизированной проходки тоннелей для определения характеристик перебора грунта ... 49
Д.С. Конюхов

ЭНЕРГЕТИКА, АВТОМАТИЗАЦИЯ И ЭНЕРГОЭФФЕКТИВНОСТЬ

Система автоматического управления процессом черпания шагающего экскаватора-драглайна ... 57
Л.Д. Певзнер, Н.А. Киселев

Повышение качества электрической энергии в подземных электрических сетях высокопроизводительных угольных шахт ... 66
Л.А. Плащанский, С.Н. Решетняк, М.Ю. Решетняк

Исследование динамики электропривода вращателя бурового станка шарошечного бурения с нечетким управлением ... 78
Н.М. Кузнецов, И.Н. Морозов

MINERAL RESOURCES EXPLOITATION

Research article

https://doi.org/10.17073/2500-0632-2022-1-5-17

Evaluation of the efficiency and environmental impact (on subsoil and groundwater) of underground block leaching (UBL) of metals from ores

V. I. Lyashenko[1] ✉, **V. I. Golik**[2,3], **R. V. Klyuev**[3]

[1] *Ukrainian Research and Design and Survey Institute of Industrial Technology, Yellow Waters, Ukraine*
[2] *North Caucasus Mining and Metallurgical Institute (GTU), Vladikavkaz, Russian Federation*
[3] *Moscow Polytechnic University, Moscow, Russian Federation*
✉ *vilyashenko2017@gmail.com*

Abstract
One of the most problematic aspects of underground block leaching (UBL) of metals from ores is the possibility of pollution of water and air in the affected zone. Therefore, proving the possibility of mitigating environmental impact of metal leaching from ores by managing production processes with the implementation of nature- and resource-saving technologies is an important objective. The purpose of this study is to justify underground development effectiveness of ore deposits by traditional and integrated methods with leaching of metals from substandard and off-balance ores. This will allow the raw material base for extraction of metals from off-balance ores to be expanded and the environmental impact on subsoil and groundwater (hydrogeological systems) to be mitigated. A distinctive feature of a UBL (underground site for leaching of metals from shrunk ores) is that leaching solutions are supplied from sorption column placed in mining workings of the leaching level in the immediate vicinity of the extracting block. The pregnant solutions in the form of resin are discharged from the sorption column, placed in the leaching level mine workings, then winded in mine cars and further supplied to hydrometallurgical plant in tanks. A still rare attempt to justify the efficiency and environmental safety of underground metal leaching (UBL) from off-balance and substandard rock ores in installations mounted in mine workings, on the basis of monitoring and evaluation of subsoil and groundwater conditions was investigated. The average value of uranium concentration by level was established: 210 m – 3.6 mg/L; 225 m – 3.58 mg/L; 280 m – 0.91 mg/L. At the same time no contamination of underground mine waters was detected. Levels of sulfuric acid aerosols and radon decomposition products did not exceed the maximum allowable concentration (MAC) values. It is recommended that the hydrogeological environment be protected through silting the bottom of the stope for collection of pregnant solutions with clay mud and construct semi-active water-permeable chemically active barriers. The mentioned BIL process was implemented during the development of pilot block 5-86 and recommended for blocks 5-84-86 and 5-88-90 of Michurinskoye deposit of SE VostGOK, Ukraine, as well as during for development of ore deposits in Russia, Kazakhstan, and other developed mining countries.

Keywords
ore deposits, underground block leaching (UBL), installations, mine workings, monitoring, hydrogeological systems and environment, groundwater, performance

Acknowledgements
The authors are grateful to Y.N. Tarkhin, N.A. Khudoshina, L.A. Lyashenko, A.H. Dudchenk, A.A. Tkachenko (SE "UkrNIPIpromtekhnologii"), V.N. Pukhalsky, P.M. Kucha, A.V. Kopanev, V.V. Sinchuk, V.A. Merkulov (SE "Vostochny GOK"), and other specialists of these enterprises for assistance in the implementation of the obtained scientific and practical findings of the research.

For citation
Lyashenko V.I., Golik V.I., Kluev R.V. Evaluation of the efficiency and environmental impact (on subsoil and ground-water) of underground block leaching (UBL) of metals from ores. *Mining Science and Technology (Russia)*. 2022;7(1):5–17. https://doi.org/10.17073/2500-0632-2022-1-5-17

РАЗРАБОТКА МЕСТОРОЖДЕНИЙ ПОЛЕЗНЫХ ИСКОПАЕМЫХ

Научная статья

Оценка эффективности гидрогеологической и окружающей среды при подземном блочном выщелачивании металлов из руд

В.И. Ляшенко[1] ✉, **В.И. Голик**[2,3], **Р.В. Клюев**[3]

[1] *Украинский научно-исследовательский и проектно-изыскательский институт промышленной технологии, г. Желтые Воды, Украина*

[2] *Северо-Кавказский горно-металлургический институт (ГТУ), г. Владикавказ, Российская Федерация*

[3] *Московский политехнический университет, г. Москва, Российская Федерация*

✉ *vilyashenko2017@gmail.com*

Аннотация

Одним из самых проблемных мест подземного блочного выщелачивания (ПБВ) металлов из руд является возможность загрязнения водной и воздушной среды в зоне их влияния. Поэтому доказательство возможности минимизации последствий ПБВ металлов из руд путем управления технологическими процессами в рамках реализации природо- и ресурсосберегающих технологий актуально. Цель исследования – обоснование эффективности подземной разработки рудных месторождений традиционными и комбинированными технологиями с выщелачиванием металлов из скальных некондиционных и забалансовых руд. Это обеспечит повышение сырьевой базы добычи металлов из забалансовых руд и улучшит охрану недр, гидрогеологической и окружающей среды. Отличительной особенностью ПБВ (подземного участка по выщелачиванию металлов из замагазинированных руд) является то, что выщелачивающие растворы подают из сорбционной колонны, размещенной в горных выработках горизонта орошения в непосредственной близости от эксплуатационного блока. Выдачу продуктивных растворов в виде смолы осуществляют из сорбционной колонны, размещенной в горных выработках горизонта орошения, в вагонетках на дневную поверхность и далее в цистернах на гидрометаллургический завод. Исследованию подвергается пока еще редкий опыт обоснования эффективности и экологической безопасности ПБВ металлов из забалансовых и некондиционных скальных руд в установках, смонтированных в горных выработках, на основании мониторинга и оценки охраны недр, гидрогеологической и окружающей среды. Выявлено усредненное значение концентрации урана по горизонтам: 210 м – 3,6 мг/л; 225 м – 3,58 мг/л; 280 м – 0,91 мг/л. При этом загрязнения подземных шахтных вод не обнаружено. Уровень аэрозолей серной кислоты и продуктов распада радона не превышал значений предельно-допустимой концентрации. Рекомендовано охрану гидрогеологической среды производить заиливанием глинистым раствором днища камеры по сбору продуктивных растворов, сооружать полуактивные водопроницаемые химически активные барьеры. Указанная технология ПБВ внедрена при отработке опытного блока 5–86 и рекомендована для блоков 5–84–86 и 5–88–90 Мичуринского месторождения ГП «ВостГОК», Украина, а также при разработке рудных месторождений Российской Федерации, Республики Казахстан.

Ключевые слова

рудные месторождения, подземное блочное выщелачивание, установки, горные выработки, мониторинг, гидрогеологическая и окружающая среда, эффективность

Благодарности

Авторы выражают благодарность Ю.Н. Тархину, Н.А. Худошиной, Л.А. Ляшенко, А.Х. Дудченку, А.А. Ткаченко (ГП «УкрНИПИИпромтехнологии»), В.Н. Пухальскому, П.М. Куче, А.В. Копаневу, В.В. Синчуку, В.А. Меркулову (ГП «Восточный ГОК») и другим специалистам этих предприятий за содействие во внедрении полученных научных и практических результатов исследований.

Для цитирования

Lyashenko V.I., Golik V.I., Kluev R.V. Evaluation of the efficiency and environmental impact (on subsoil and ground-water) of underground block leaching (UBL) of metals from ores. *Mining Science and Technology* (*Russia*). 2022;7(1):5–17. https://doi.org/10.17073/2500-0632-2022-1-5-17

Introduction

With the increase in the volume of underground ore mining, the volume of waste on the surface and in underground workings increases, enhancing environmental pollution [1, 2]. Many areas of operating deposits are a fragmented rock mass, forming the basis for uncontrolled process of natural leaching [3, 4]. Therefore, proving the possibility of minimizing the consequences of natural leaching by managing technological processes as part of the implementation of resource-saving technologies is relevant. Therefore, proving the possibility of mitigating environmental impact of natural metal leaching from ores through managing production processes as part of the implementation of resource-saving technologies is an important objective [5, 6]. The main scientific and practical results of the studies of integrated methods for development of ore deposits, relating to both processes of beneficiation and hydrometallurgy, and methods of underground mining of minerals (physical-and-chemical geotechnologies), are presented below [7, 8]. This work is a continuation of the authors' research, the main scientific and practical findings of which are most fully presented in [9, 10–12].

Goal of research

The purpose of the study is to justify underground development effectiveness of ore deposit by traditional and integrated methods with leaching of metals from substandard and off-balance ores. This will allow expanding raw material base for extraction of metals from off-balance ores and mitigating environmental impact on subsoil and groundwater (hydrogeological systems).

In order to achieve this goal, the following tasks need to be undertaken:

1. To analyze the factors affecting the performance and environmental safety of underground development of ore deposits with metal leaching.

2. To identify the conditions and sources of possible pollution of water and air in the in the block in-situ leaching affected zone.

3. To develop measures for mitigating the adverse environmental impact of block in-situ leaching of metals from ores.

4. To outline promising areas of study aimed at increasing performance and environmental safety of underground block leaching of metals from ores.

Research Methods

Continuum mechanics, mathematical statistics, and wave processes research using standard and new techniques were used to summarize, critically analyze, and outline promising areas of scientific advances in the methods and technical means of underground ore mining, underground geotechnology, and blasting rupture of solid media.

Findings Discussion

Technology audit of block in-situ leaching

The known methods of extracting metals from ores are not waste-free. More and more money and energy are being spent in fully utilizing the tailings. These methods produce obvious environmental impact, since secondary tailings are activated and migrate into the environment during storage and processing. Significant economic efficiency distinguishes new method from known ones by the fact that there is no need to wind ore to the surface [11, 12].

Underground block leaching (UBL) has been carried out at the Gumeshevskoye deposit since 2005. The mines of the Priargunsky Industrial Mining and Chemical Association (Krasnokamensk, Russia) use mining methods involving metal leaching from shrinked (in stopes) ores on industrial scale. Geotechnological methods of metal production in RNO-Alania have been known since the second half of the last century [13, 14].

The environmental impact of ore natural leaching was studied based on the experience of enterprises in the North Caucasus. Here the contents of products of natural leaching of ores exceed the sanitary norms by 2-3 orders of magnitude. For instance, the Baksan River (Kabardino-Balkaria) at the Tyrnyauz deposit site receives effluents from the tungsten-molybdenum complex, containing tungsten and molybdenum. In the Alagirsky District of the Republic of North Osetia-Alania, the Ardon River is polluted with copper, lead, and zinc at the Sadon deposit site [15, 16].

The process of in situ dissolution of ore with transfer of useful components to the solution is an alternative to the traditional methods of development of these deposits The ore is shrunk into blocks. After percolating through the ore mass the pregnant solution of reagents is collected in the bottom, and from there directed to processing facilities (Fig. 1).

During block in-situ leaching of ores with grades of lead of 0.99 %, and zinc, 0.71 % at Kakadurskoye deposit (North Osetia), a method for development of the whole deposit (instead of development of a separate area of substandard (for conventional methods) reserves) was proposed. Professor I.A. Ostroushko proved its feasibility and achieved its implementation. The new method of mineral leaching in a disintegrator is based on the fact that at an impact velocity of 250 m/s their processing properties change. The processing of tailings of Sadon ores in the disintegrator allowed extraction of 22 % of lead and 76 % of zinc (from their initial content in the primary tailings). By means of multiple processing, the ultimate content was brought to the required level [17, 18]. The content of metals in natural leaching solutions corresponds to the content of the process accelerants, iron-bearing minerals, and retarders, calcium and magnesium minerals. In order to evaluate the characteristics of mine drainage in the Ardon River, its water samples were examined (Fig. 2).

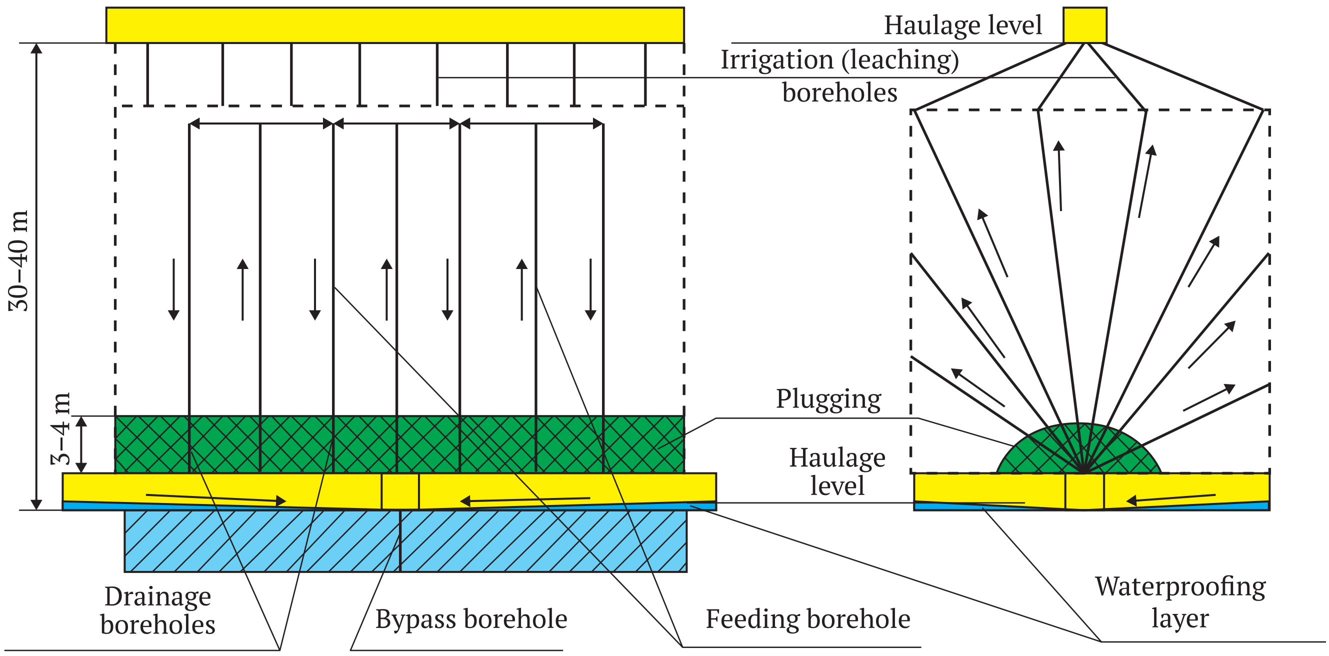

Fig. 1. Preparation of ore bodies for leaching without ore crushing

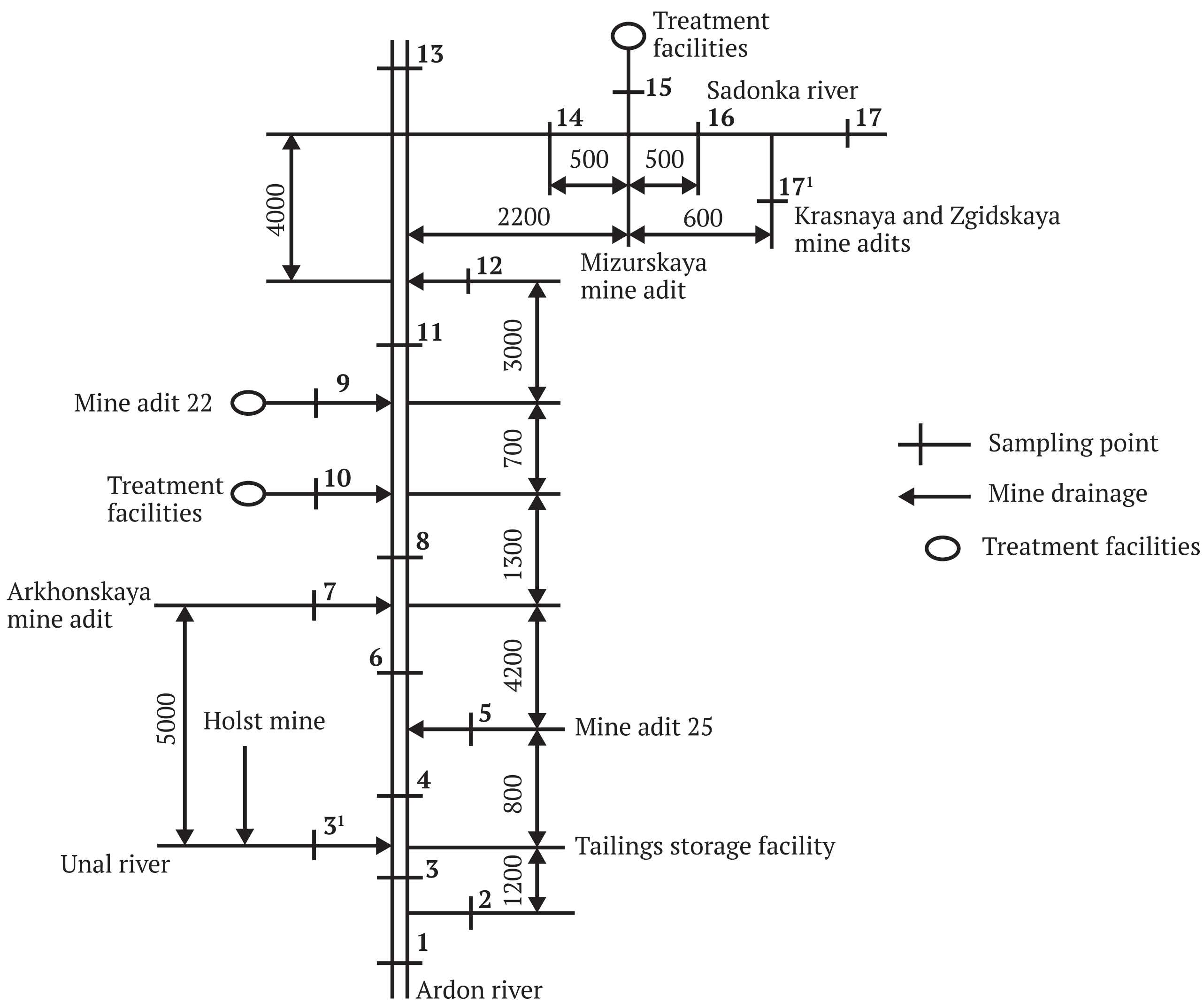

Fig. 2. The Ardon river sampling schematic

Combining the activities of enterprises, for example, the lead-zinc complex and JSC "Kavdolomit" (RNO-Alania, Russia) allows for the environmental impact to be mitigated. This includes backfilling of the mined-out space with backfilling mixture on the basis of dolomite-based binders to reduce losses of ores in the course of breaking. In order to produce the dolomite binder fraction, mills are used. They allow the dolomite specific surface to be increased up to 3000 cm^2/g thus raising the activity of binding additives by 20–30 % [19, 20]. Underground block leaching of metals from the broken ores is one of the best ways to reduce the amount of radioactive waste on the surface, decrease the backfill volume and increase the enterprise performance in the production process (Fig. 3).

Process flow sheet for metal leaching from ores in the installations placed in mine workings is illustrated in Fig. 4.

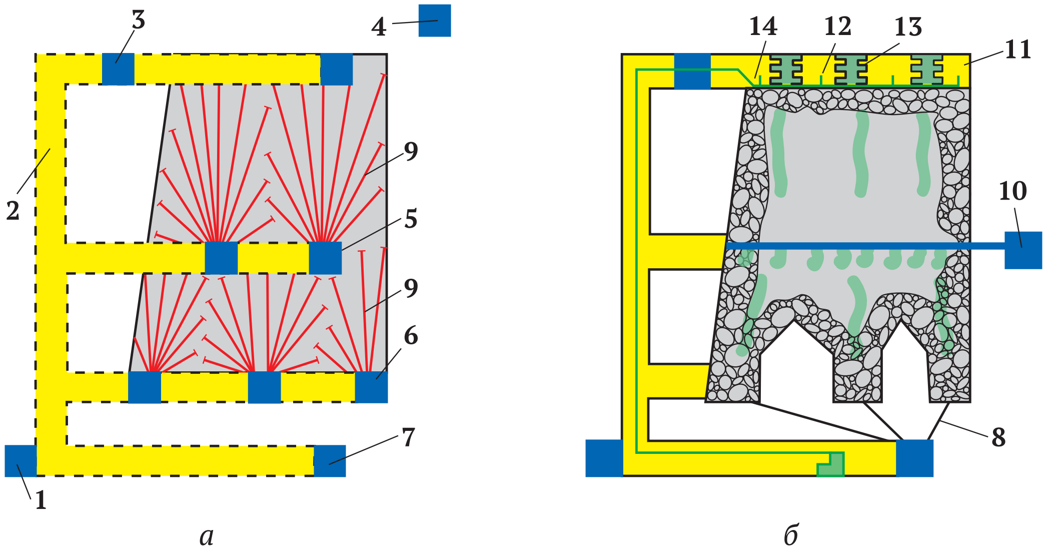

Fig. 3. Method of underground block leaching of metals from broken ores:
a and *b* – drilling and leaching of shrinked ores in a block:
1 – drift; *2* – raise; *3* – drift for leaching; *4* – drift; *5* – drill drifts; *6* – drill drifts; *7* – drainage drift; *8* – drainage boreholes; *9* – intermediate leaching level; *10* – intermediate leaching level; *11* – drift for leaching; *12* – top undercut; *13* – cribwork; *14* – leaching system

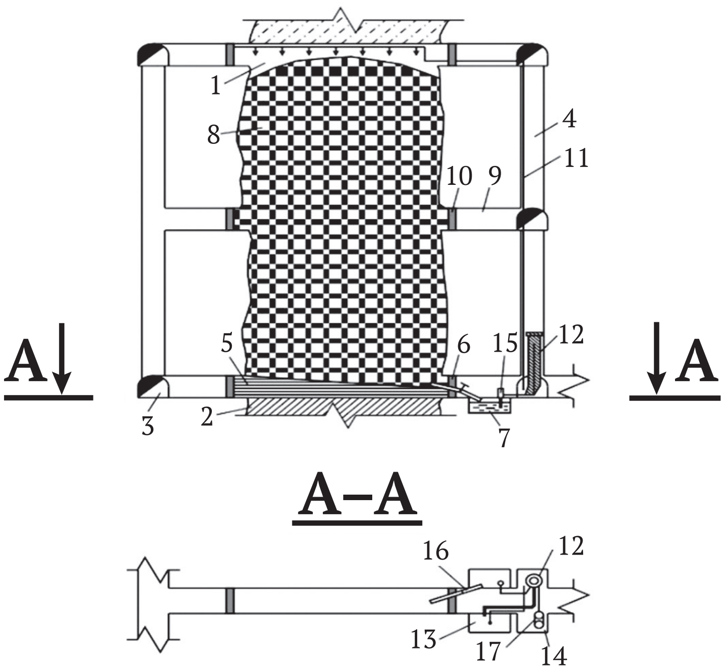

Fig. 4. Process flow sheet for metal leaching from ores in underground installations:
1 – stope; *2* – ore body; *3, 4* – horizontal and vertical workings; *5* – liner; *6* – stopping; *7* – tank; *8* – shrunk ore; *9* – working; *10* – stopping; *11* – pipeline; *12* – pregnant solution processing sorption units; *13* – tank for preparation of leaching solution; *14* – niches; *15* – pumps; *16* – pipe; *17* – metal desorption unit

eISSN 2500-0632
https://mst.misis.ru/

The ore body 2 is divided into extraction blocks, then secondary development and face-entry drivage are performed. Drilling of 50–85 mm (in diameter) boreholes from sub-level workings 9 is carried out. Partial shrunk ore drawing 8 is performed to the haulage level. The leaching system consisting of pipes 11 and nozzles is mounted in the upper part of stope 1. Workings 7 for collecting of pregnant solutions are prepared in the lower part [21, 22].

A process flow diagram of the underground block leaching commercial implementation is shown in Fig. 5. It includes: railway tank; pumps F430 PP-50/38, X 80-50-250 E, PR63, AX 125-100-400E, and X50-32-125 types; tank for low-quality acid; discharge device; road tanker and tank for resin; submersible pump of F-706 PP-185 type; sump for pregnant, neutralization, and leaching solutions; hydraulic hoist; 0.4 and 0.8 m^3 tanks; SNK-type sorption column; pipeline; ejector; free tanks; tanks for acidizing and neutralization; hand hoist with load-carrying capacity up to 1 ton.

Leaching and pregnant solutions are pumped from the lower to the upper levels without the solutions winding to the day surface. At the day surface, the products are wound as resin for further processing at the hydrometallurgical plant. In fact, an underground area for the leaching of metals from ores in UBL blocks with processing of solutions in units is placed in the underground workings. The authors point out that this method allows for a significant reduction in the list of operations required, when compared with the traditional mining methods [23, 24] (except for such operations as: creation of compensation space, drawing and delivery of up to 30 % of the shrunk ore from the UBL stope, etc.).

Hydrogeological and environmental monitoring

The system of environmental monitoring includes three-step control and allows the following tasks to be resolved: monitoring of the conditions of the mine waters; determining zones of mine air pollution; detecting emergency environment pollution; providing company management with necessary information.

a

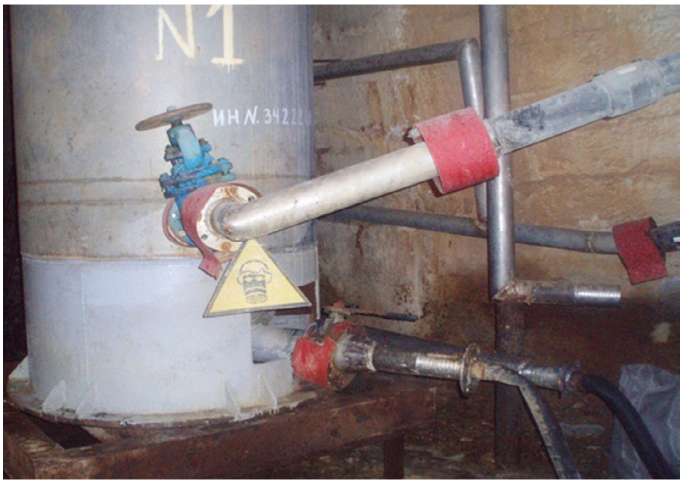

b

c

d

Fig. 5. Process equipment for UBL at Ingulskaya mine of SE VostGOK (photo):
a and *b* – sorption columns of SNK type; *c* – pump room with a 0.4 m^3 tank and AX pump;
d – train of tanks with ion exchange resin and diluted sulfuric acid

Research Findings

In order to monitor possible migration from the stope of the block and sump towards the block bottom, six rising observation boreholes were drilled (Fig. 6). The first level of water environment monitoring was implemented on a monthly basis. This requires measuring the hydrogen index (pH) of the mine water in observation boreholes by the staff of the pilot block.

During the testing 18,630 water pH measurements were performed. The observation boreholes remained dry during the testing. The water pH was practically neutral of 6.5–7.5, and only in 5 cases pH was measured at 1.5–2.0, which was explained by pipeline failures and stop valve wear. The halo of spreading the process solutions was local and neutralized by lime milk.

The second level of the monitoring aquatic environment included measuring the following indicators: uranium concentration; alkalinity; and hydrogen index (pH). During the block development, 882 samples of mine water were taken. Table 1 shows the monitoring results averaged on quarterly basis. The analyses show the average uranium concentrations of 3.6 mg/L at 210 m level; 3.58 mg/L at 225 m level; 0.91 mg/L at 280 m level. The water pH was neutral. The observations indicate no negative impact of the testing block on mine water quality, and the observation boreholes remained completely dry [25, 26].

The third level also included air monitoring. Full chemical analysis of the mine water samples for calcium, magnesium, sodium, potassium, total iron, carbonates, bicarbonates, sulfates, chlorides, nitrates, nitrites, ammonium, dry residue, uranium was carried out on monthly basis, and radiochemical analysis for radium-226, thorium-230, polonium-210, lead-210, uranium was performed on quarterly basis (Table 1).

Table 1

The third level monitoring results for mine water

Designation	Sample Location	Control parameters		
		Alkalinity, mg-eq/L	pH	Uranium, mg/L
Pre-testing	P – 1 P – 2 P – 3 P – 4 p – 5 P – 6	2.70 0.50 5.75	7.8 7.8 7.9	6.7 0.64 1.32
Averaged value for 3 years of testing	P – 1 P – 2 P – 3 P – 4 P – 5 P – 6	2.60 3.21 5.37	7.3 7.5 7.7	3.60 3.58 0.91

During the testing, 210 samples of mine water for ultimate analysis and 60 samples for radiochemical analysis were taken and analyzed. The results of the chemical and radiochemical analysis of the mine water, as well as those of the mine water immediately before the mine water treatment (in the unit at 210 m level) are given in Table 2.

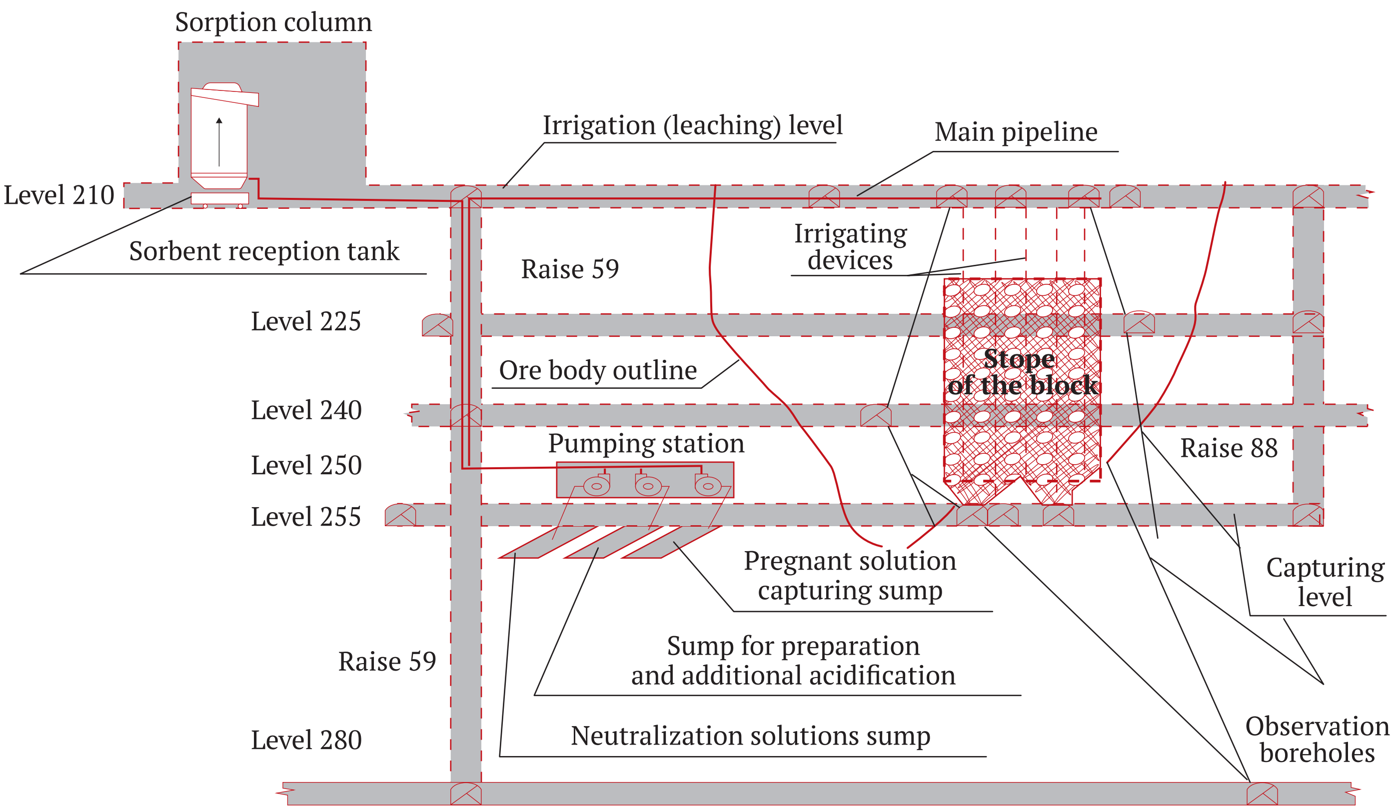

Fig. 6. Process flow diagram of block preparation for leaching:
Pc.59 – ore chute of 59-th axis; Raise 59, Raise 88 – ventilation and manway raise of 59-th and 88-th axis, respectively

Data on the chemical composition of the mine water samples showed that up to the moment of block acidification the mine water, the chemical composition varied considerably both spatially and depending on time of sampling. For example, sulfate ion concentration varied from 403.0 to 998.0 mg/L, that of uranium, from 0.35 to 7.30 mg/L. Comparing the water analysis data, it can be concluded that the average concentrations of sulfate-ion, chloride-ion, uranium, pH, dry residue in the samples taken during the UBL testing did not exceed those in the samples taken before the acidizing (leaching) of the shrunk ore. No essential changes in composition and concentrations of elements in mine water discharged into Ingul River during UBL operation (blocks 5-86; 5-84-86; 5-88-90) were observed. Samples were collected once a month for the following parameters: sulfuric acid aerosols; radon concentration; gamma exposure rate. Since the beginning of block 5-86 operation only, 576 samples were collected. Review of the data presented in Table 3 showed that the determined indicators did not exceed those of the samples taken before the testing [27, 28].

Review of Findings

Initial findings of the study showed significant dependence of the leaching process performance (based on time factor) on the working volume of the sump for pregnant solutions. Optimal volume was found to be 70–80 m^3, while design volume was 20 m^3 only. The

Table 2

The third level monitoring results for mine water

Subject of research and measurement component	Mine water	Average Value		
		pre-testing	testing	post-testing
Uranium, mg/L	90	6.7	6.2	4.4
Ra – 226 × 10^{-11}, Ci/L	20	8.37	6.24	6.7
Th – 230 × 10^{-11}, Ci/L	20	3.03	2.46	2.2
Pb – 210 × 10^{-11}, Ci/L	20	32.05	9.53	10.4
Po – 210 × 10^{-11}, Ci/L	20	2.5	1.18	2.8
$SO^{2-}{}_4$, mg/L	70	614	659	691
CI, mg/L	70	172	166	142
PH, unit	70	7.6	7.7	8.2
Ca^{2f}, mg/L	70	145	133	124
Md^{2f}, mg/L	70	41.3	62.8	52
Na^f, mg/L	70	235	229	220
K^f, mg/L	70	15.5	13,2	12
Fe_{tot}, mg/L	70	0.05	0.05	0,05
NH_4, mg/L	70	1.1	0.15	0.1
NO_3, mg/L	70	40	15	9
NO_2, mg/L	70	26	0.2	0.1
HCO_3, mg/L	70	92	157	132
Dry residue, mg/L	70	1588	1560	1366

Table 3

The third level monitoring results for air

Subject of research and measurement component	Air	Average Value		
		pre-testing	testing	post-testing
Level 210 m				
Sulfuric acid aerosols, mg/m^3	640	–	0.5	–
Radon, Bq/m^3	64	580	645	110
EDR, μR/hr (gamma radiation exposure dose)	64	146	206	227
Level 240 m				
Sulfuric acid aerosols, mg/m^3	128	–	0.26	–
Radon, Bq/m^3	128	513	490	439
EDR, μR/hr (gamma radiation exposure dose)	128	454	331	312

initial operating experience revealed a negative factor in terms of a significant amount of sand and debris in the regenerated resin at the hydrometallurgical plant. Subsequently the decision was taken to install an autonomous resin regeneration unit at the plant for the UBL pilot areas [29, 30].

During development of block 5-86, in accordance with the recommendations issued, the previously driven workings were used as much as possible. The same approach was used at preparation of pilot blocks 5-84-86 and 5-88-90, as well as pilot-commercial block 1-75-79, for UBL at Michurinskoye deposit. The required volume of remedial work as in previously driven mine workings was carried out. At the same time the issues of stability of mine workings of the leaching level located in the area of intensive influence of worked-out blocks require special attention. The ore mass in level 197–210 m was already weakened by the development workings and stopes, constructed before the preparation of blocks for UBL, as well as by the network of boreholes of the leaching system currently being created. In these workings, a systematic monitoring of their stability and the stress-strain state of the near-contour rock mass was organized (geotechnical and seismic monitoring). The results of UBL commercial testing showed that the system of stockpile preparation for extraction existing at VostGOK only change in the drilling while blasting parameters allowed ores of optimal granulometric composition to be produced in the pilot block. During the testing, about 54 % of the metal reserves in the block were transferred into the solution at an acid consumption rate of 36 % of the design value. Thus, extraction and processing of ores with the use of traditional methods under current economic conditions is inexpedient if the metal content in the extracted ordinary ore is less than 0.070 c.u. (Table 4).

Advantages of block leaching

There are no costs for individual operations as compared with the traditional ore mining and processing methods, namely:

Mining: secondary crushing and drawing of ore; in-mine transportation of ore; ore winding to the surface; crushing and beneficiation of ore; backfilling of mined-out space; loading into rail cars and transportation of ore to hydrometallurgical plant;

Table 4

Main indicators of metal block leaching

Designation	Value
Volume of ore being leached, kt	8.248
Grade of metal, c.u.	0.065
Acid H_2SO_4 used, t	231.1
Acid specific consumption, kg/t	28.0
Acid consumption for acidizing, t	27.8
Oxidant specific consumption, kg/t	3.3
Acidification time, day	40
Volume of solutions fed to leaching, m^3	66106
Density of leaching, L/m^2 x hr	9.6
L/S ratio, units	8:1
Leaching time, day	166
Sorption duration, day	398
Volume of solutions for sorption, m^3	25756
Characteristics of pregnant solutions: a) metal concentration, average, mg/L b) average acidity, g/L	 220 13.5
Characteristics of irrigation solutions: Fe^{+3} /Fe^{+2}, concentration, g/l Mineralization (dry residue), g/l	 1.9/0.38 43.2
Volume of metal-saturated anionite, m^3	101.3
Average capacity of saturated sorbent, kg/m^3	27.3
Residual capacity of regenerated sorbent for metal, kg/m^3	0.66
Tailings washing in block: duration, days	65
Washing water volume, m^3	5775
Specific water consumption for washing, m^3/t	0.7

Processing at hydrometallurgical plant: ore rehandling; ore crushing; leaching; sorption; resin regeneration; tailings storage.

The phenomenon of natural leaching is a consequence of the insufficient sophistication of mining methods used. The mechanism of the natural metal leaching processes is known and controllable/applicable. The radical approach to the mitigation of the environmental impact of natural leaching is the complete utilization of metal-containing raw materials. The concept of environmental protection of subsoil use provides for the replacement of uncontrolled natural leaching with artificial leaching in a controlled workspace. The level of knowledge on the theory and practice of metal extraction from metal ores allows the methods with leaching to restore the previous potential of mining industries [31, 32].

Performance

The maximized performance of the integrated method of development with leaching of metals from ores is provided through increasing the extraction of useful components from the subsoil:

$$M' \geq \frac{\varepsilon_n - \varepsilon_T}{\varepsilon_n - \varepsilon_2 \varepsilon_3} M, \qquad (1)$$

where M – amount of useful component in situ; M' – amount of useful component extracted; ε_n – extraction of metals from ores by the methods with leaching; ε_T – extraction of metals by traditional methods (TS):

$$\varepsilon_T = \frac{M_m}{M} \varepsilon_1 \varepsilon_2 \varepsilon_3, \qquad (2)$$

where M_m – TS quantity of metals; ε_1 – extraction of metals from subsoil by TS; ε_2 – extraction of metals into concentrate; ε_3 – extraction of useful component from concentrate to the final product.

The profit from the use of substandard reserves (low-grade ores) in production at the expense of increasing ore production volumes, output of finished products (metals), and ROI through implementation of integrated methods with leaching is determined according to the following mathematical model:

$$Profit = \sum_{1}^{n} \left[\begin{array}{l} \left(C_{ore}^{b} - C_{ext}^{b} - C_{enr}^{b} - C_{met}^{b}\right) \cdot V_{b}^{sel} + \\ + \left(C_{ore}^{comb} - C_{ext}^{comb} - C_{enr}^{comb} - C_{met}^{comb}\right) - D_0 \end{array} \right] \cdot V_{comb}^{sel}, \qquad (3)$$

where *Profit* is annual profit from combination (integration) of the methods, MU; C_{ore}^{b}, C_{ore}^{comb} – proceeds from metal sales (produced from balance and combined, respectively, ore reserves, MU/t; C_{ext}^{b}, C_{enr}^{b}, C_{met}^{b} – ccosts of mining, processing, and metallurgical treatment of balance ores, respectively, MU/t; C_{ext}^{comb}, C_{enr}^{comb}, C_{met}^{comb} – costs of mining, processing, and metallurgical treatment of combined ore reserves, respectively, MU/t; V_{b}^{sel}, V_{comb}^{sel} – volume of selectively extracted balance and combined ores, respectively, tons; n – the mix of extracted metals; D_0 – total damage (economic consequences) to the environment, effected (−), or preventable (+), taking into account the costs of storage of pollutants and protection of the population living in the mining affected zone, MU.

Thus, UBL implementation on commercial scale will significantly improve economic performance of production. Through the modernization of fixed assets, this would allow for the technical re-equipping of production involving reserves of low-grade and substandard ores in production, thus prolonging LoM (for existing mines). The research established that chemical mining methods could be used for development of low-grade and substandard ores, thus increasing profitability. Furthermore, the use of substandard ores could allow the raw-material base of metals at operating mines to be raised 1.4–1.6 times. It was shown that performance of different options of methods for metal leaching from ores was defined in terms of the completeness of its extraction. The experience accumulated in the world practice shows that under other equal conditions, such as mineralization type, structure, porosity of ore, diffusion coefficient, temperature, concentration of process solutions, etc., the completeness of leaching directly depends on the ore crushing quality and uniformity of its density distribution when shrunk. The possibility of underground block leaching of metals from shrunk ores was proved, and the dependence of metal recovery on the average linear size of the blast-crushed ore mass fragments was established [33, 34].

Advanced research directions

In order to prevent groundwater pollution (hydrogeological environment protection) the base of the stope needs to be silted for the collection of pregnant solutions with clay mud. Semi-active water permeable chemically active barriers (VPChAB) need to be constructed and biological technologies in UBL to be used. The main advantages of using iron-oxide composites based on natural clay minerals to clean water from contamination with uranium compounds are their environmental friendliness, cheapness, availability, and manufacturability. This should ensure that the degree of metal contamination of ground and surface waters, soils and sediments, including the main Michurinsky Fault (Kropivnitsky, Ukraine), is reduced. Research needs to be continued to develop such methods that would satisfy both economic and environmental requirements [35, 36].

Conclusions and recommendations

Based on the scientific and practical results of the tests on integrated leaching of metals from off-balance and substandard ores for their subsequent processing at hydrometallurgical plant, the following conclusions were made.

1. Semi-commercial (pilot-plant) testing on leaching of metals from ores of operational block 5-86 of Michurinskoye deposit (Ukraine) was implemented with observations at three levels: 210; 225; and 280 meters. In the tests, the pH of water was at a neutral level of 6.5–7.5, and only in 5 cases were its values 1.5-2.0. This was explained by pipeline failures and stop valve wear and tear. The halo of spreading the process solutions was local and neutralized by lime milk.

2. Environmental monitoring with water analysis showed the average uranium concentrations of 3.6 mg/L at 210 m level, 3.58 mg/L at 225 m level, 0.91 mg/L at 280 m level. No contamination of underground mine waters was detected. The levels of sulfuric acid aerosols and radon decomposition products did not exceed the maximum allowable concentration (MAC) values.

3. It is recommended that the worked-out ore mass be treated with lime milk and mine water through the boreholes for feeding leaching solutions (leaching system), in order to neutralize and wash it. The hydrogeological environment (groundwater) should be protected through silting the bottom of the stope for collection of pregnant solutions with clay mud. Groundwater monitoring should be performed in observation boreholes drilled in the bottom of the production block and at contacts with the ore body, as well as in zones of fracturing and hydraulic fracturing of rocks.

4. The phenomenon of natural leaching of metals from crude ore is a consequence of the insufficient sophistication of mining methods used and can be minimized. This will provide increased financial viability, the rational use of subsoil, groundwater and environmental protection, and increase raw material base for metals production by 1.4–1.6 times.

References

1. Mosinets V.N., Lobanov D.P., Tedeev M.N. et al. *Construction and operation of ISL mines*. Monograph. Under the general editorship of Mosinets V. N. Moscow: Nedra Publ.; 1987. 304 p. (In Russ.)

2. Chernov A.P. (ed.) *Mining and processing of uranium ores in Ukraine*. Kyiv: Adef-Ukraine Publ.; 2001. 238 p. (In Russ.)

3. Lyashenko V.I., Golik V.I., Kozyrev E.N. Integrated mining methods with underground leaching. *Gornyi Zhurnal*. 2008;(12):37–40 (In Russ.)

4. Dzaparov V.Kh. Life threat of RSO-Alaniya reion. *Vestnik of Nosov Magnitogorsk State Technical University*. 2009;(3):75–76. (In Russ.). URL: http://vestnik.magtu.ru/content/%D0%92%D0%B5%D1%81%D1%82%D0%BD%D0%B8%D0%BA%20%D0%9C%D0%93%D0%A2%D0%A3%20%D0%B7%D0%B0%202009%20%D0%B3%D0%BE%D0%B4,%20%D0%9D%D0%BE%D0%BC%D0%B5%D1%80%203.pdf

5. Ahrens V.Zh., Babichev N.I., Bashkatov A.D. et al. *In situ leaching*. 2nd ed. Moscow: Gornaya Kniga Publ.; 2011. 295 p. (In Russ.)

6. Lyashenko V.I., Kisly P.A., Djatchin V.Z. Radiometrical preconcentration of uranium ores. *Obogashchenie Rud*. 2015;(1):3–9 (In Russ.)

7. Lyashenko V.I., Khomenko O.E., Golik V.I. Friendly and resource-saving methods of underground ore mining in disturbed rock masses. *Mining Science and Technology* (*Russia*). 2020;5(2):104–118. (In Russ.). https://doi.org/10.17073/2500-0632-2020-2-104-118

8. Ghorbani Y., Franzidis J.-P., Petersen J. Heap leaching technology – current state, innovations, and future directions: a review. *Mineral Processing and Extractive Metallurgy Review*. 2016;37(2):73–119. https://doi.org/10.1080/08827508.2015.1115990

9. Oxley A., Smith M.E., Caceres O. Why heap leach nickel laterites. *Minerals Engeneering*. 2016;88:53–60. https://doi.org/10.1016/j.mineng.2015.09.018

10. Vrancken C., Longhurst P.J., Wagland S.T. Critical review of real-time methods for solid waste characterisation: Informing material recovery and fuel production. *Waste Management*. 2017;61:40–57. https://doi.org/10.1016/j.wasman.2017.01.019

11. Li J., Li D., Xu Z., Liao C., Liu Y., Zhong B. Selective leaching of valuable metals from laterite nickel ore with ammonium chloridehydrochloric acid solution. *Journal of Cleaner Production*. 2018;179:24–30. https://doi.org/10.1016/j.jclepro.2018.01.085

12. Gabaraev O.Z., Dmitrak Yu.V., Drebenshtedt K., Savelkov V.I. Regularities of interaction of destroyed geo-materials and ore-bearing massif in the processing of processed deposited ore. *Sustainable Development of Mountain Territories*. 2017;9(4):406–413. (In Russ.). https://doi.org/10.21177/1998-4502-2017-9-4-406-413

13. Komashchenko V.I. Environmental-economical expediency of utilizing mining-industrial wastes for their converting. *Izvestija Tulskogo Gosudarstvennogo Universiteta. Nauki o Zemle*. 2015;(4):23–30. (In Russ.). URL: https://tidings.tsu.tula.ru/tidings/pdf/web/file/tsu_izv_earth_science_2015_04.pdf

14. Burdzieva O.G., Zaalishvili V.B., Beriev O.G., Kanukov A.S., Maysuradze M.V. Mining impact on environment on the North Ossetian territory. *International Journal of GEOMATE*. 2016;10(1):1693–1697. URL: https://geomatejournal.com/geomate/article/view/2012/1888

15. Karamushka V.P., Kamnev E.N., Kuzin R.Z. *Reclamation of uranium ore mining and processing facilities*. Moscow: Gornaya Kniga Publishing House; 2014. 183 p. (In Russ.)

16. Kachurin N., Komashchenko V., Morkun V. Environmental monitoring atmosphere of mining territories. *Metallurgical and Mining Industry*. 2015;(6):595–597. URL: https://www.metaljournal.com.ua/assets/Journal/MMI-6/083-Nikolai-Kachurin.pdf

17. Svyatetsky V.S., Solodov I.N. Technological advancement strategy of uranium mining industry in Russia. *Gornyi Zhurnal*. 2015;(7):68–77. (In Russ.). https://doi.org/10.17580/gzh.2015.07.10

18. Kaplunov D.R., Yukov V.A., Lavenkov V.S. The underground copper block and boreholes leaching methods comparison. *Mining Informational and Analytical Bulletin*. 2017;(3):7–14. URL: https://giab-online.ru/files/Data/2017/3/7_14_3_2017.pdf

19. Morozov A.A., Yakovlev M.V. Off-balance uranium ores formed at development of the Streltsovsky ore field involvement in processing. *Mining Informational and Analytical Bulletin*. 2016;(12):174–181. (In Russ.). URL: https://giab-online.ru/files/Data/2016/12/174_181_12_2016.pdf

20. Rylnikova M.V., Radchenko D.N. Methodological aspects of designing a system of mineral flow management in the full cycle of integrated development of ore deposits. *Ratsionalnoe Osvoenie Nedr*. 2016;(3):36–41. (In Russ.)

21. Chen T., Lei C., Yan B., Xiao X. Metal recovery from the copper sulfide tailing with leaching and fractional precipitation technology. *Hydrometallurgy*. 2014;147–148:178–182. https://doi.org/10.1016/j.hydromet.2014.05.018

22. Ghorbani Y., Franzidis J.-P., Petersen J. Heap leaching technology – current state, innovations, and future directions: a review. *Mineral Processing and Extractive Metallurgy Review*. 2016;37(2):73–119. https://doi.org/10.1080/08827508.2015.1115990

23. Kopbaeva M.P., Panova E.N., Prinzin N.A., Karmanov E.M. Optimization of uranium peroxide precipitation. *Gornyi Zhurnal*. 2016;(5):90–94. (In Russ.). https://doi.org/10.17580/gzh.2016.05.13

24. Solodov I.N., Kamnev E.N. (eds). *Uranium geotechnology (Russian experience)*. Moscow: KDU Publ.; 2017. 576 p. (In Russ.)

25. Svyatetskiy V.S., Polonyankina S.V., Ermakov A.G. Uranium-mining industry of Russia: the state and prospects of development. *Razvedka i Okhrana Nedr*. 2017;(11):22–26. (In Russ.)

26. Mashkovtsev G.A., Miguta A.K., Shchetochkin V.N. Uranium resource base. Problems of exploration and development. *Mineral Recourses of Russia. Economics and Management*. 2017;(3):67–78. (In Russ.)

27. Balikhin A.V. Uranium mineral-resources: the current state and perspectives for development. Review. *Kompleksnoe Ispol'zovanie Mineral'nogo Syr'a*. 2019;(1):36–50. (In Russ.). https://doi.org/10.31643/2019/6445.05

28. Sinclair L., Thompson J. In situ leaching of copper: Challenges and future prospects. *Hydrometallurgy*. 2015;157:306–324. https://doi.org/10.1016/j.hydromet.2015.08.022

29. Aben E., Markenbayev Zh., Khairullaev N., et al. Study of change in the leaching solution activity after treatment with a cavitator. *Mining of Mineral Deposits*. 2019;13(4):114–120. https://doi.org/10.33271/mining13.04.114

30. Malanchuk Z., Korniienko V., Malanchuk Ye., et al. Modeling the formation of high metal concentration zones in man-made deposits. *Mining of Mineral Deposits*. 2018;12(2):76–84. https://doi.org/10.15407/mining12.02.076

31. Stupnik M., Kalinichenko O., Kalinichenko V., et al. Choice and substantiation of stable crown shapes in deep-level iron ore mining. *Mining of Mineral Deposits*. 2018;12(4):56–62. https://doi.org/10.15407/mining12.04.056

32. Ovseychuk V.A., Zozulia A.M. Improvement of in-situ leaching: a case-study of the Streltsovo ore field. *Mining Informational and Analytical Bulletin*. 2021;(3–1):26–33. (In Russ.) https://doi.org/10.25018/0236_1493_2021_31_0_26

33. Kovalchuk I., Tobilko V., Kholodko Yu., Zahorodniuk N., Kornilovych B. Purification of mineralized waters from U(VI) compounds using bentonite/iron oxide composites. *Technology Audit and Production Reserves*. 2020;3(3):12–18. https://doi.org/10.15587/2706-5448.2020.205146

34. Antoninova N. Yu., Sobenin A. V., Shubina L. A. Assessment of usability of industrial waste in construction of geochemical barriers. *Mining Informational and Analytical Bulletin*. 2020;(12):78–88. (In Russ.). https://doi.org/10.25018/0236-1493-2020-12-0-78-88

35. Kamnev E. N., Karamushka V. P., Seleznev A. V., et al. Ecology of uranium mine closure: problems and solutions (in terms of Russia, CIS Countries and Germany). *Mining Informational and Analytical Bulletin*. 2020;(5):26–39. (In Russ.). https://doi.org/10.25018/0236-1493-2020-5-0-26-39

36. Podrezov D. R. Issues of improving control and increasing efficiency of production blocks at an ISL uranium mine. *Mining Science and Technology (Russia)*. 2020;5(2):131–153. (In Russ.). https://doi.org/10.17073/2500-0632-2020-2-131-153

Information about the authors

Vasiliy I. Lyashenko – Cand. Sci. (Eng.), Senior Research Fellow, Ukrainian Research and Design Insitute for Industrial Technology, Zholti Vody, Ukraine; ORCID 0000-0001-8361-4179, Scopus ID 8915855500; e-mail vilyashenko2017@gmail.com

Vladimir I. Golik – Dr. Sci. (Eng.), Professor of the Mining Department, North Caucasian Mining and Metallurgical Institute, Vladikavkaz, Russian Federation; ORCID 0000-0002-1181-8452, Scopus ID 6602135324; e-mail v.i.golik@mail.ru

Roman V. Klyuev – Dr. Sci. (Eng.), Professor of the Department of the Technique of Low Temperature name P.L. Kapitza, Moscow Polytechnic University, Moscow, Russian Federation; ORCID 0000-0003-3777-7203, Scopus ID 57194206632; e-mail kluev-roman@rambler.ru

Received 21.11.2021
Revised 28.12.2021
Accepted 01.02.2022

GEOLOGY OF MINERAL DEPOSITS

Research article

https://doi.org/10.17073/2500-0632-2022-1-18-29

Features of fluid dynamics in long-term heterogeneous gas reservoirs

A.A. Feyzullayev[1, 2] SC ✉, A.G. Gojayev[3] SC, I.M. Mamedova[4] SC

[1] *Institute of Geology and Geophysics of the National Academy of Sciences of Azerbaijan, Baku, Republic of Azerbaijan*

[2] *Institute of Oil and Gas of the National Academy of Sciences of Azerbaijan, Baku, Republic of Azerbaijan*

[3] *Gas Storage Facility Operation Department of "Azneft" Production Association, State Oil Company of the Azerbaijan Republic (SOCAR), Baku, Republic of Azerbaijan*

[4] *«Oil and Gas» Research Projective Institute, SOCAR, Baku, Republic of Azerbaijan*

✉ *fakper@gmail.com*

Abstract

Geological features are characterized by macro- and micro-heterogeneity, manifested by the spatial variability of material composition and lithophysical properties of rocks. This, in turn, determines the spatial and temporal variability of hydrocarbon (HC) fluid dynamics both during the reservoir formation and during its development and, subsequent operation as an underground gas storage facility (UGSF). The long-term operation of underground gas reservoirs at the Galmas and Garadagh areas in the South Caspian Basin (SCB), serving as a reservoir of commercial gas accumulations, and subsequent underground gas storage (UGSF) is characterized by significant peculiarities. Analysis of monitoring data on volumes of gas injection and extraction at the Galmas/Garadagh UGSF in the period of 2020–2021 showed their spatial variability, as well as the variability of wells deliverability during the gas reservoir development. This suggests the inherited nature of UGSF operation mode in relation to the gas reservoir development mode. The heterogeneous nature of spatial variability of these parameters is determined by the reservoir rock poroperm properties. A formation pressure drop during reservoir development is accompanied by decreasing rock permeability. When operating UGSF, the lithofacial properties of rocks determine the ratio of volumes of injected and extracted gas. In this regard, a necessary condition for selecting the optimal system of UGSF operation is to take into account the spatial heterogeneity of the underground reservoir. The irregular nature of variation of rock poroperm properties, the origination of isolated zones in the reservoir with considerable residual gas volumes, as well as unpredictable directions of fluid movement are the main reasons for decreased efficiency of field development and underground gas storage facility operation. In order to determine the optimal system of operation of UGSF in depleted underground oil and gas reservoirs, the features of the spacial variations resulting from the rocks poroperm properties need to be taken into account.

Keywords

underground gas storage facility, reservoir, rocks, reservoir poroperm properties, porosity, permeability, spatial heterogeneity, gas-condensate reservoir, fluid dynamics, South Caspian Basin

Acknowledgements

This study was carried out with the financial support of the Fund of the State Oil Company of Azerbaijan Republic (SOCAR) - Grant No. 06LR – AMEA.

For citation

Feyzullaev A.A., Godzhaev A.G., Mammadova I.M. Features of fluid dynamics in long-term heterogeneous gas reservoirs. *Mining Sciences and Technology* (*Russia*). 2022;7(1):18–29. https://doi.org/10.17073/2500-0632-2022-1-18-29

ГЕОЛОГИЯ МЕСТОРОЖДЕНИЙ ПОЛЕЗНЫХ ИСКОПАЕМЫХ

Научная статья

Особенности флюидодинамики в длительно эксплуатирующихся неоднородных газовых резервуарах

А. А. Фейзуллаев[1, 2] SC ✉, А. Г. Годжаев[3] SC, И. М. Мамедова[4] SC

[1] *Институт геологии и геофизики, Национальная Академия наук Азербайджана, г. Баку, Республика Азербайджан*

[2] *Институт нефти и газа Национальной Академии наук Азербайджана, г. Баку, Республика Азербайджан*

[3] *ПО «Азнефть», Государственная нефтяная компания Азербайджана, г. Баку, Республика Азербайджан*

[4] *НИПИ «Нефтегаз», Государственная нефтяная компания Азербайджана, г. Баку, Республика Азербайджан*

✉ *fakper@gmail.com*

Аннотация

Геологические объекты характеризуются макро- и микронеоднородностью, что проявляется изменчивостью в пространстве вещественного состава и литофизических свойств пород. Это, в свою очередь, определяет пространственно-временную изменчивость динамики углеводородных (УВ) флюидов как при формировании залежи, так и при ее разработке, а в последующем и эксплуатации в качестве подземного хранилища газа (ПХГ). Длительная эксплуатация подземных газовых резервуаров на площадях Галмас и Гарадаг в Южно-Каспийском бассейне (ЮКБ), служащих вместилищем промышленных скоплений газа, а в дальнейшем для подземного хранения газа (ПХГ) характеризуется существенными особенностями. Анализ данных мониторинга объемов закачки-отбора газа на ПХГ Галмас и Гарадаг в период 2020–2021 гг. показал изменчивость в пространстве их значений, так же, как и продуктивности скважин при разработке газового резервуара. Это позволяет предположить унаследованный с режимом разработки газового резервуара характер режима эксплуатации ПХГ. Неоднородный характер изменения в пространстве этих параметров определяется фильтрационно-емкостными свойствами пород. Падение пластового давления в процессе разработки залежи сопровождается снижением проницаемости пород, а при эксплуатации ПХГ литофациальные свойства пород определяют соотношение объемов закачиваемого и отбираемого газа. В связи с этим необходимым условием выбора оптимальной системы эксплуатации ПХГ является учет пространственной неоднородности подземного резервуара. Неравномерный характер изменения по площади фильтрационно-емкостных свойств горных пород (ФЕС), формирование изолированных зон в резервуаре со значительными остаточными объемами газа, а также непрогнозируемые направления движения флюидов являются основными причинами снижения эффективности разработки залежи и эксплуатации ПХГ. Для определения оптимальной системы эксплуатации ПХГ, созданных в истощенных подземных нефтегазовых резервуарах, необходимо учитывать особенности изменения в пространстве ФЕС слагающих его пород.

Ключевые слова

подземное хранилище газа, резервуар, горные породы, фильтрационно-емкостные свойства, пористость, проницаемость, пространственная неоднородность, газоконденсатная залежь, флюидододинамика, Южно-Каспийский бассейн

Благодарности

Данная работа выполнена при финансовой поддержке Фонда Государственной нефтяной компании Азербайджана (SOCAR) – Грант № 06LR – AMEA.

Для цитирования

Feyzullaev A.A., Godzhaev A.G., Mammadova I.M. Features of fluid dynamics in long-term heterogeneous gas reservoirs. *Mining Sciences and Technology* (*Russia*). 2022;7(1):18–29. https://doi.org/10.17073/2500-0632-2022-1-18-29

Introduction

There are no absolutely homogeneous geological features in the natural environment. All are characterized by macro- and micro-heterogeneity, manifested by spatial variability of the material composition and lithophysical properties of rocks. This, in turn, determines the spatial and temporal variability of hydrocarbon (HC) fluid dynamics both during reservoir formation and during its development and, subsequent operation as an underground gas storage facility (UGSF).

Irreversible changes in the reservoir during the long-term development of fields are caused by a continuous drop in formation (reservoir) pressure connected with extraction of significant volumes of fluids (oil, gas, water) from the underground reservoir [1, 2]. In comparison with the change in porosity of rocks, the formation pressure drop leads to more significant irreversible changes in their permeability [3-6].

Compared with the mode of reservoir development, changes in the reservoir during UGSF operation are connected with repeated alternating stresses on the formation (reservoir) (cyclic variations of the effective pressure), caused by seasonal injection and extraction gas.

The study of the above processes by the example of gas field development in Galmas and Garadagh areas of SCB, as well as the long-term operation of UGSFs created in them is the main objective of this paper.

Brief description of the assets to be investigated

Galmas field / UGSF

Galmas oil and gas field / UGSF (underground gas storage facility) is located in the northern part of Nizhnekurinsky depression, 75 km from Baku (Fig. 1).

The depression is complicated by longitudinal and transverse faults and, as a consequence, has a block structure. The main fault within the fold is a longitudinal disruption, upon which an extinct mud volcano of the same name is located.

The Productive Strata consists of alternating clayey and sandy-silty interlayers, the proportion of which varies significantly depending on the depth and area of spreading.

Commercial gas inflows were obtained from wells which penetrate into the formations of the local Absheron sequence (Lower Anthropogen), Akchagyl (Upper Pliocene), and Productive Strata (PS, Lower Pliocene). The Galmas field was brought into commercial development in 1956.

Since 1976 the previously commercially gas-bearing I and II horizons of the PS have been used as Underground Gas Storage Facilities (UGSF). Gas in small volumes is also injected into the sand reservoir of the Absheron formation (strata).

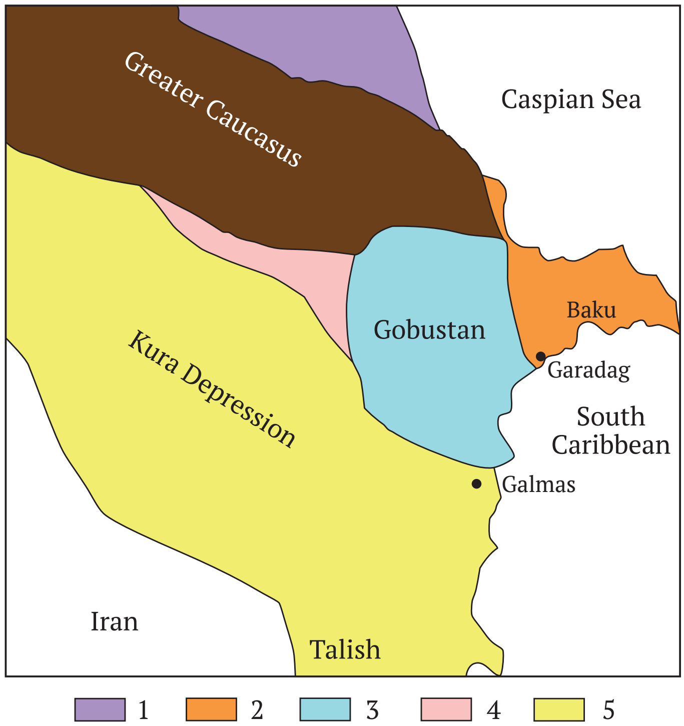

Fig. 1. Location of the Galmas and Garadagh fields / UGSFs and lithofacial types of the Productive Strata sediments: *1* – Pre-Caspian; *2* – Absheron; *3* – Gobustan; *4* – Geylar; *5* – Nizhnekurinsky

Garadagh field / UGSF

The Garadagh field/UGSF is located in the extreme southwestern part of the Absheron Peninsula, 30 km from Baku (see Fig. 1) and is confined to the southern flank of the asymmetric anticline with block structure [7].

The main targets of the Garadagh oil and gas field development are the I-VII horizons of the PS. A gas-condensate reservoir was identified in the VII-VIIa horizons of the PS (hereinafter the PS VII horizon). In the SE part of the southern limb they unite and form a single thick sandstone layer. The effective thickness of the VII horizon reaches 10–25 m in the northwest and 55–75 m in the southeast.

Exploitation of the PS VII horizon as a UGSF started in 1986.

Research techniques and factual material

Analysis of well productivity in the areas under study was performed for about 110 wells. The poroperm properties of rocks were studied in more than 150 core samples.

Gas injection/withdrawal dynamics analysis for Galmas and Garadagh UGSFs, covering the period of 2009–2011, was carried out based on the data of more than 100 and 60 wells, respectively.

The monitoring of formation pressure in the wells included more than 50 measurements.

The data processing and corresponding plotting were carried out using standard computer programs.

eISSN 2500-0632
https://mst.misis.ru/

Findings and Discussion

About the conditions of the PS rocks formation

Galmas and Garadagh fields / UGSFs, confined to the Lower Pliocene sediments, are located in different oil-gas bearing districts of SCB, Nizhnekurinsky and Absheron (see Fig. 1).

It is known that PS formation occurred within the South Caspian Sea, which was isolated from the Eastern Paratethys. PS formation covers the time interval from 5.5 million years ago to 3.5 million years ago, i.e. about 2 million years [8].

Sediments were accumulated under conditions of significant fluctuations of the Paleo-Caspian level, resulting in the origination of different types of paleo-conditions, from lacustrine to typically fluvial. The PS sequence is represented by rhythmic alternation of sand-silt-clay sediments, the thickness of which in the most submerged (buried) part of the basin reaches 7 km.

In connection with the fact that the sediments were brought to the basin simultaneously from several surrounding mountain groups, five lithofacial types of sediments were distinguished in the PS [8].

The Garadagh field / UGSF is located in the zone of PS Absheron facies. This is composed mainly of sediments brought by Paleo-Volga from the Russian platform. Other sources of the material midgration are of subordinate importance. The rocks of this facies are mostly sandy. The number of productive horizons in some fields reaches 40–50. The Absheron facies is the thickest in the South Absheron basin (up to 5 km). The mineralogical composition of the light fraction of the rocks is characterized be predominance of quartz, 95 %. Feldspars (up to 20 %) and rock fragments (up to 10 %) are also present.

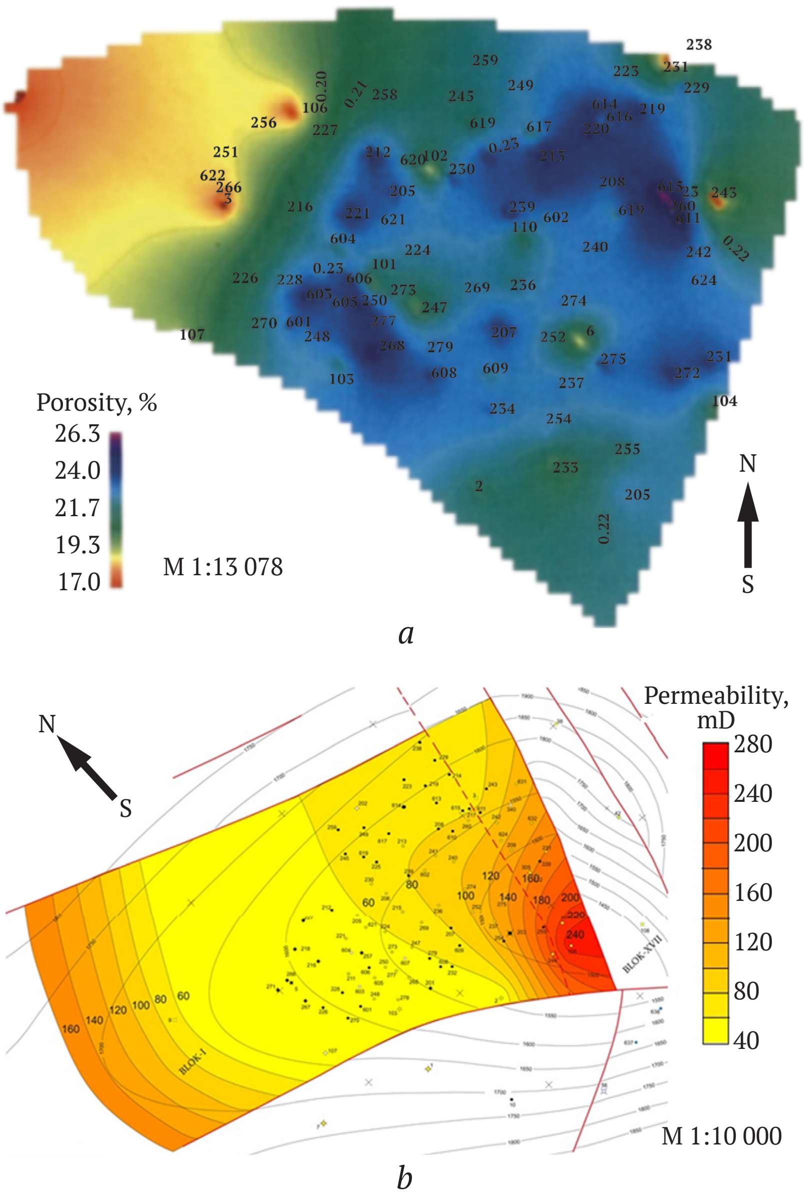

Fig. 2. Spatial variation of porosity (*a*) and permeability (*b*) of the rocks of the PS I horizon at the Galmas field

The PS rocks within the Galmas field/UGSF refer to the Nizhnekurinsky facies. During origination of this lithofacial type of PT, clastic material was brought to this part of the SCB mainly by the largest river. The Paleo-Kura, and the Paleo-Arax transported products of the erosion of the Kurinsky Lowland, the Great and Minor Caucasus, and the Talysh.

The total thickness of the sediments is 3,500–4,000 m. The sequence is represented by about 20 sand members, up to 20 m thick. The highest level of sandiness is observed in the upper 300–400 m, and the sand content decreases considerably down the sequence. The rocks of the Nizhnekurinsky facies differ from those of the Absheron facies by low quartz content and high feldspar content.

On spatial heterogeneity of gas reservoirs

Analysis shows that the Galmas and Garadagh underground gas reservoirs are characterized by geological heterogeneity (block structure, spatial variation of the material composition of rocks). This is also manifested in spatial variation of poroperm properties of the reservoir rocks (Fig. 2, 3).

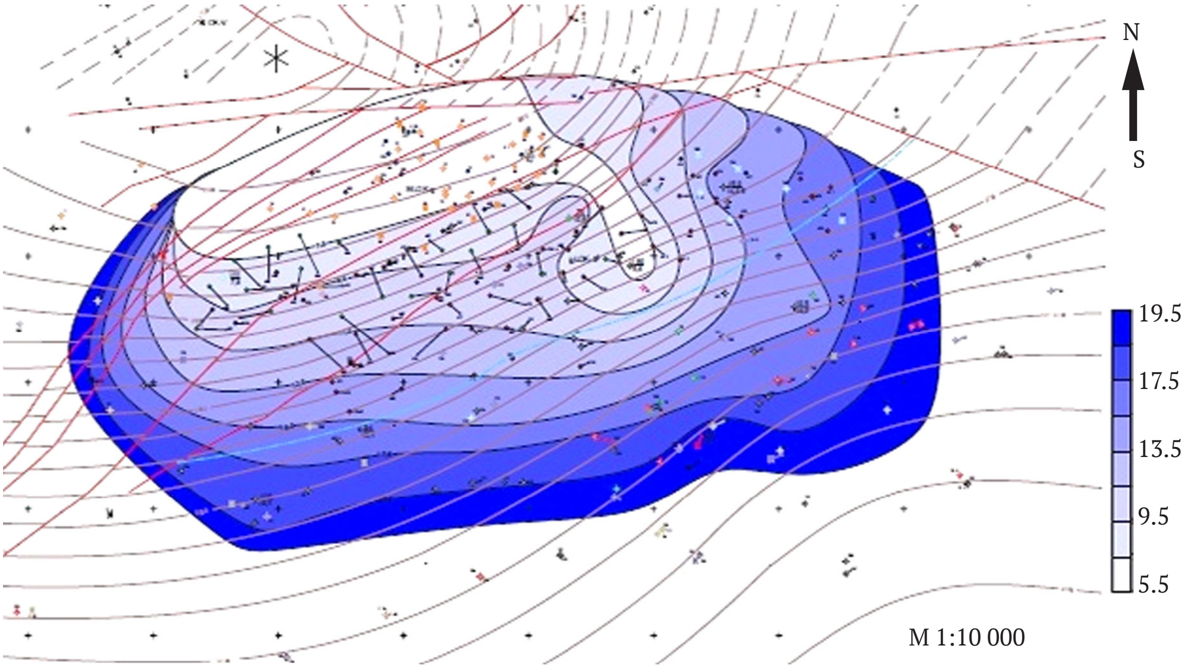

a

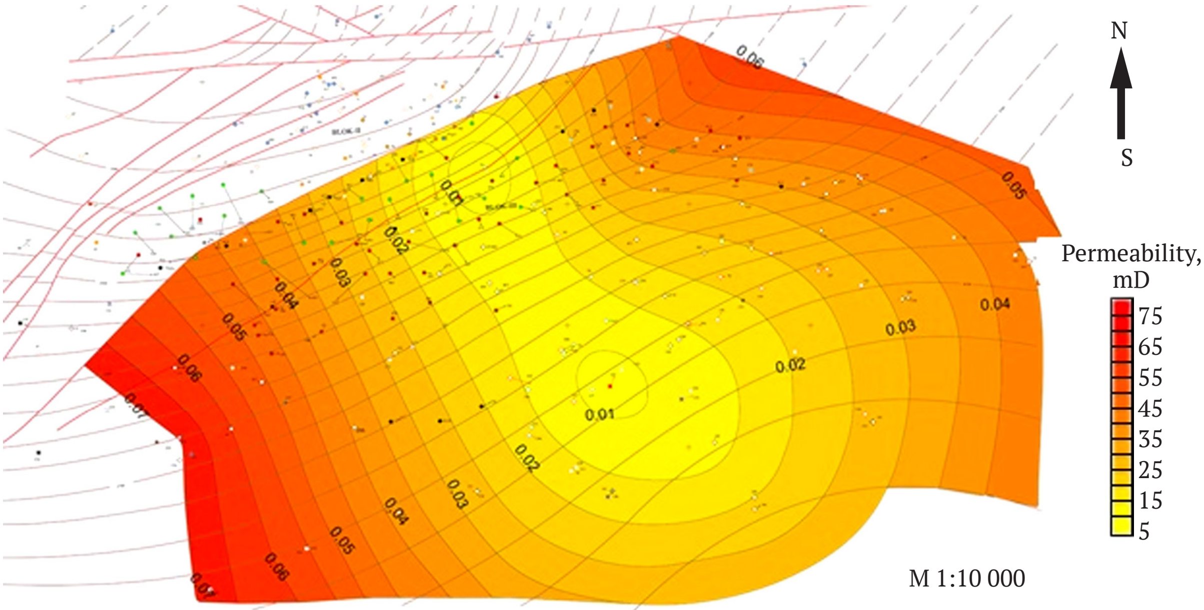

b

Fig. 3. Spatial variation of porosity (*a*) and permeability (*b*) of the rocks of the PS VII horizon at the Garadagh field

eISSN 2500-0632
https://mst.misis.ru/

Spatial heterogeneity is also manifested in the productivity of wells at the Galmas and Garadagh fields, Fig. 4.

The spatial irregularity of gas saturation of an underground reservoir also defines spatial variability of the subvertical gas dispersion intensity. This is clearly seen by the example of the Galmas field. Here less contrasting halos of HC gas dispersion were identified in the north-north-western part of the reservoir with relatively low gas saturation of rocks, in comparison with its southern part (uplifted pool) with higher gas saturation (Fig. 5).

Peculiarities of fluid dynamics in the course of the development of the fields

During the development of the Galmas gas condensate field (from 1958 to 1962) about 3.8 billion m³ of gas were extracted from the underground reservoir. This led to 13.5 MPa (from 21.1 to 7.6 MPa) drop in the reservoir pressure, averaging about 0.3 MPa per month (Fig. 5, *a*).

The development of the Garadagh gas-condensate field, which began in 1955, was carried out without maintaining reservoir pressure. By the end of the 1980s it was depleted. About 21 billion m³ of gas was

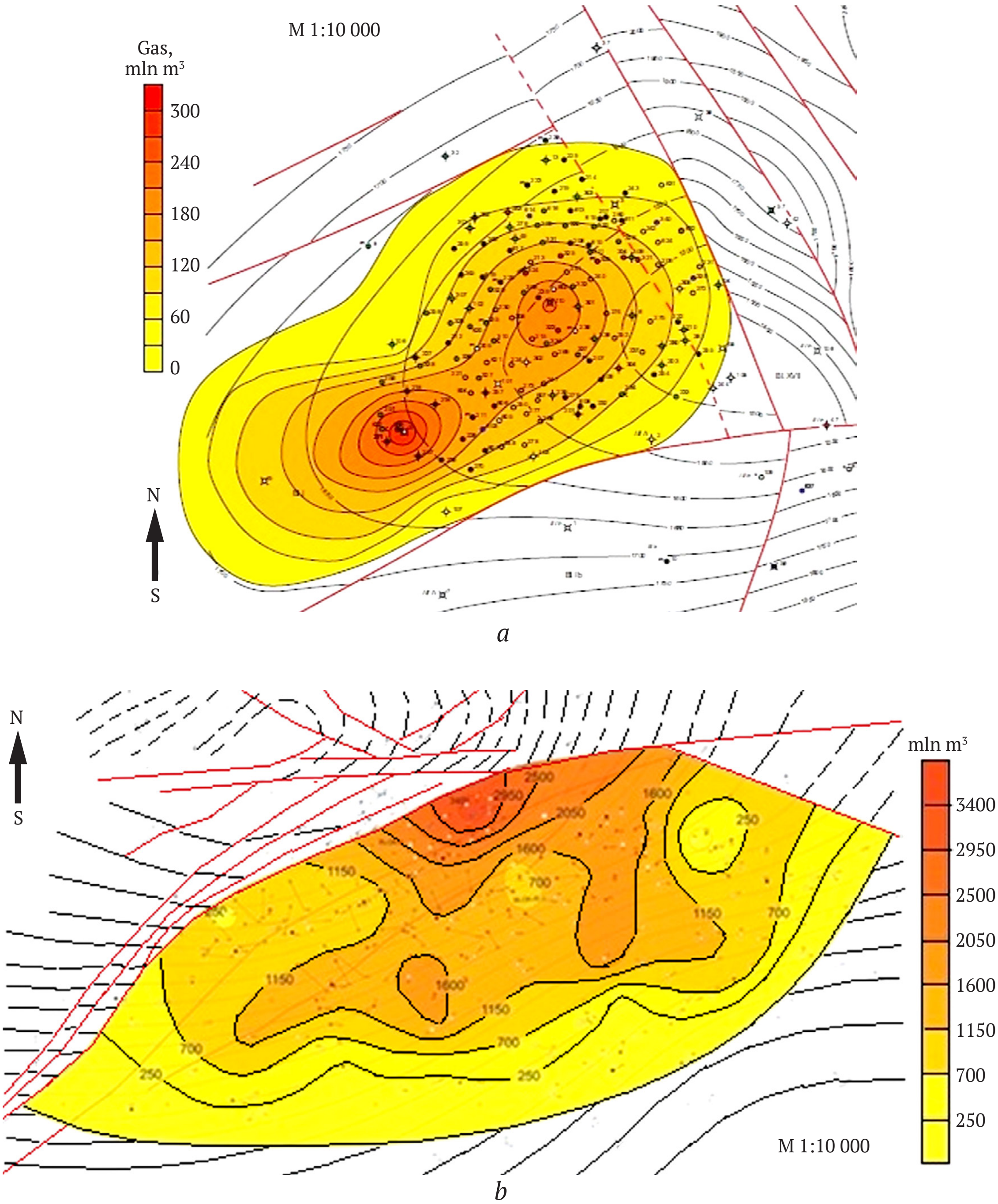

Fig. 4. Well productivity variation maps for the Galmas (*a*) and Garadagh (*b*) fields

withdrawn in total, leading to reservoir pressure drop from 39.8 to 3.6 MPa (Fig. 5, *b*)

The rate of reservoir pressure drop at the Galmas field is about 1.8 times higher than that at the Garadagh field. This is most likely due to the lower energy level of gas in the Galmas field due to its relatively smaller reserves compared to the Garadagh field.

The initial reservoir pressure in the wells within the Garadagh area exceeds hydrostatic pressure by an average of 1.2 times. Due to excess elastic energy of gas in the first 2 years of the field development, a permanent increase in production was observed accompanied by an insignificant drop in reservoir pressure (within the interval of 40-38 MPa). The cause-and-effect relationship between the two parameters during further reservoir development follows the exponential law, characterized by a steady decline in gas production and reservoir pressure drop (Fig. 7).

Based on the example of the Garadagh field, it was found that the value of the reservoir pressure drop change (from 2.4 to 11.7 MPa) was accompanied by decreased rock permeability (from 1.2 to 4.9 mD) (Fig. 8, Table 1). The permeability decline rate due to the reservoir pressure drop in the considered wells is equatable, except for wells 124 and 132, located in the near-fault zone. In these wells the permeability decline rate is relatively higher.

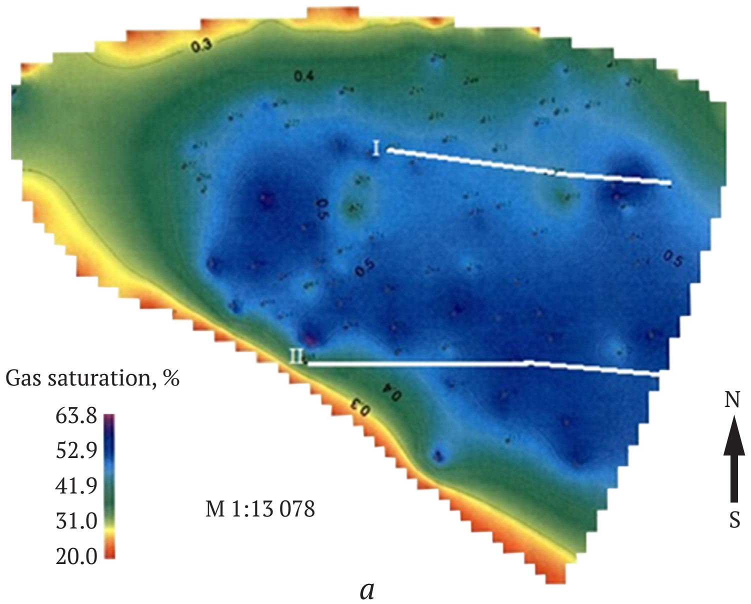

a

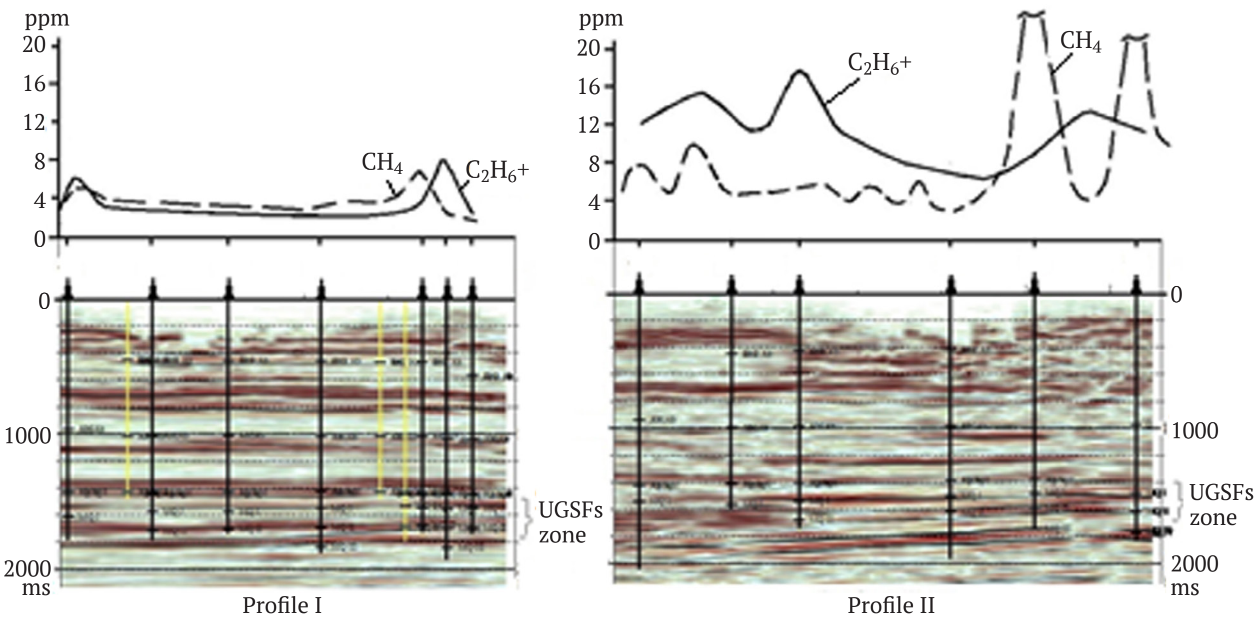

b

Fig. 5. Galmas field/UGSF: a – spatial variability of gas saturation of the PS I horizon rocks and location of gas survey profiles; b – distribution of HC gas concentrations in near-surface sediments (depth of about 1.2 m) along profiles I and II

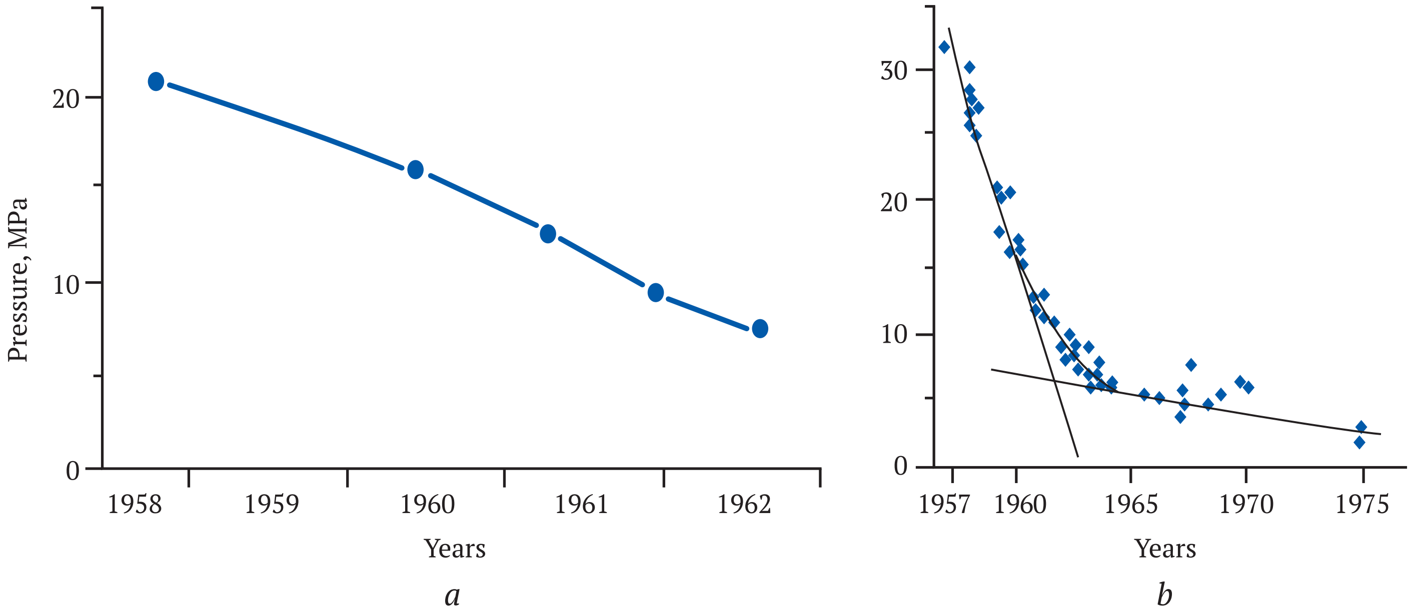

Fig. 6. Plots showing reservoir pressure drop rate during development of the Galmas (*a*) and Garadagh (*b*) fields (1)

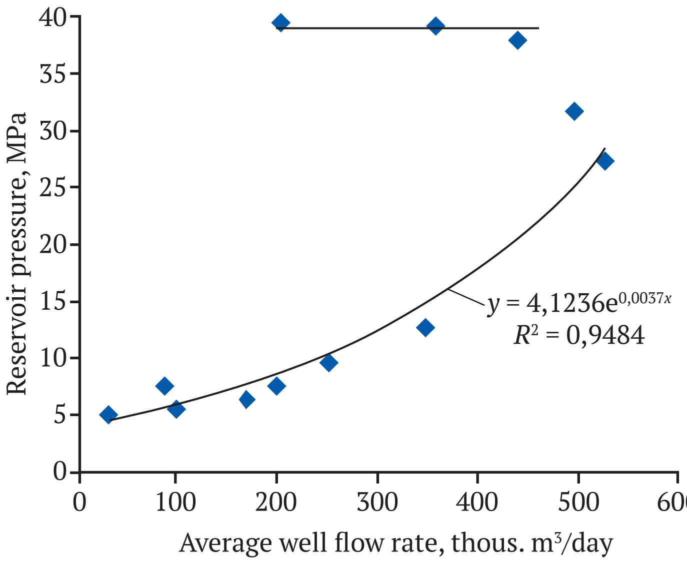

Fig. 7. Relationship between the reservoir pressure and the well flow rate at the Garadagh field

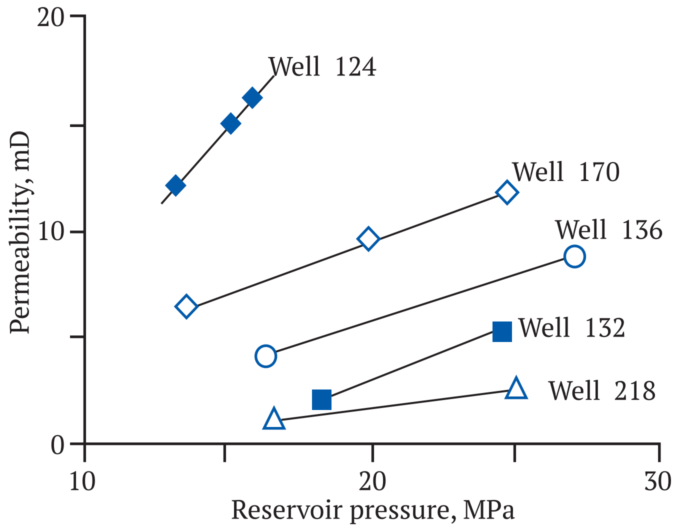

Fig. 8. Graphs of the PS rock permeability changes vs. the reservoir pressure drop at the Garadagh field. Well 124 is located near a fault

Table 1

Graphs of the PS rock permeability changes vs. the reservoir pressure drop during the Garadagh field development

Hole ID	Porosity, %	Measuring period, months	Pressure drop, MPa	Rock permeability decline, %
136	18.0	25	11	47
132 (close to fault)	18.5	15	3	56
218	17.4	14	1	44
170	16.7	13	5	41

Features of UGSF operation

Analysis of the monitoring data on the volumes of gas injected and extracted at the Galmas UGSF and Garadagh UGSF in 2020–2021 showed a spatial variability in their values (Fig. 9 and Fig. 10). A similar variability was demonstrated by productivity of the wells during the corresponding gas reservoir development (see Fig. 4). This suggests an inherited nature of UGSF operation in relation to the gas reservoir development mode. This is also confirmed by the positive correlation between the total volumes of gas extracted from individual wells since the beginning of the Galmas field development, and volumes extracted during operation of the UGSF created in the same reservoir (Fig. 11).

It is important to note that operating wells at the UGSF differ in terms of the ratio of injected and extracted gas volumes. This may be due to the influence of both technical and geological factors.

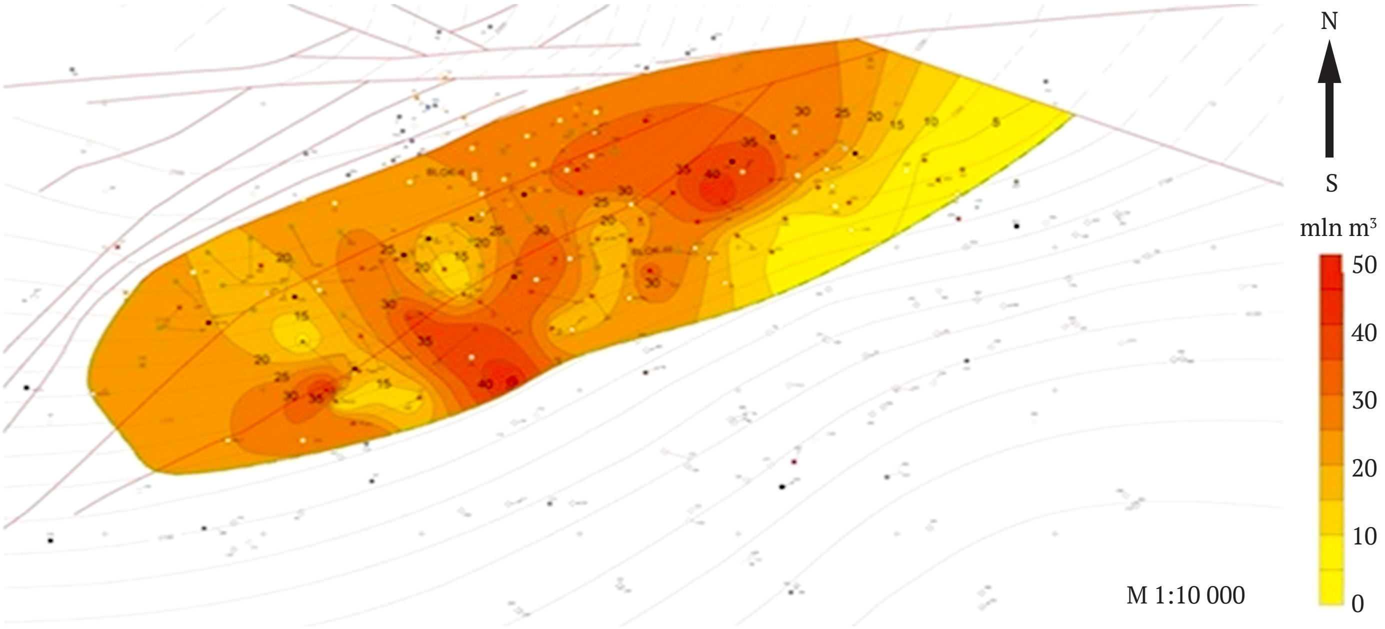

a

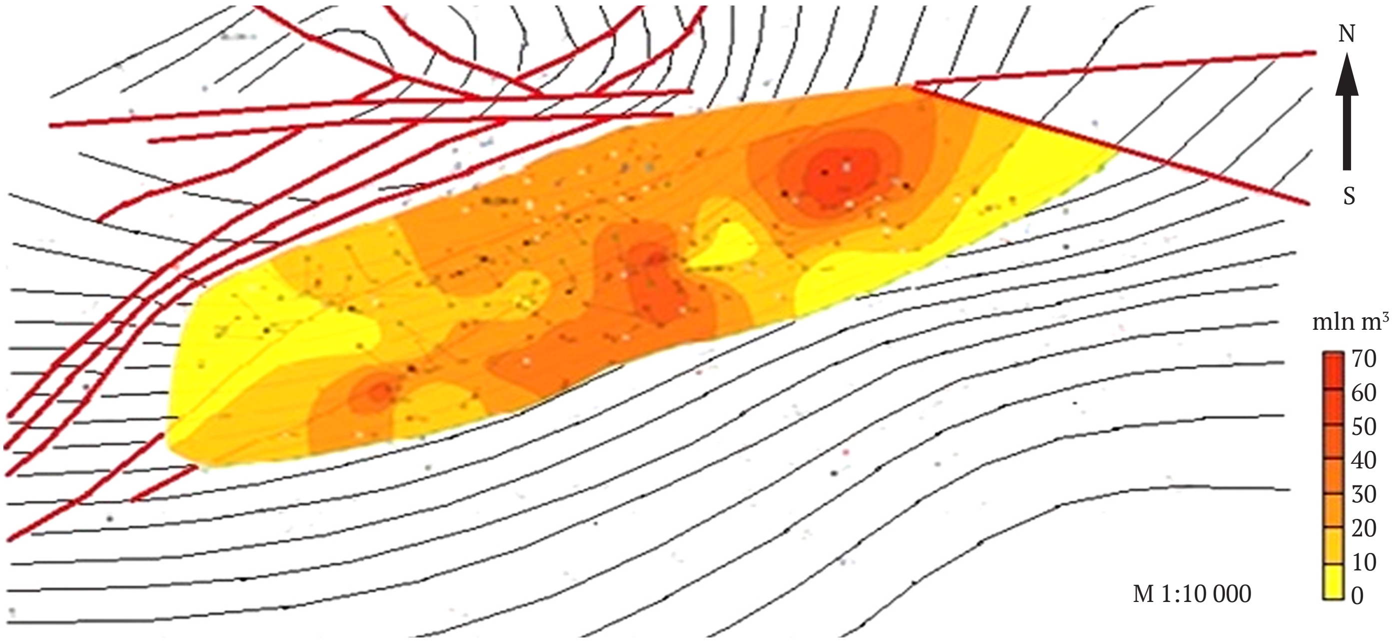

b

Fig. 9. Maps of spatial variation of the volumes of injected (*a*) and withdrawn (*b*) gas at the Garadagh UGSF for the period of 2020–2021

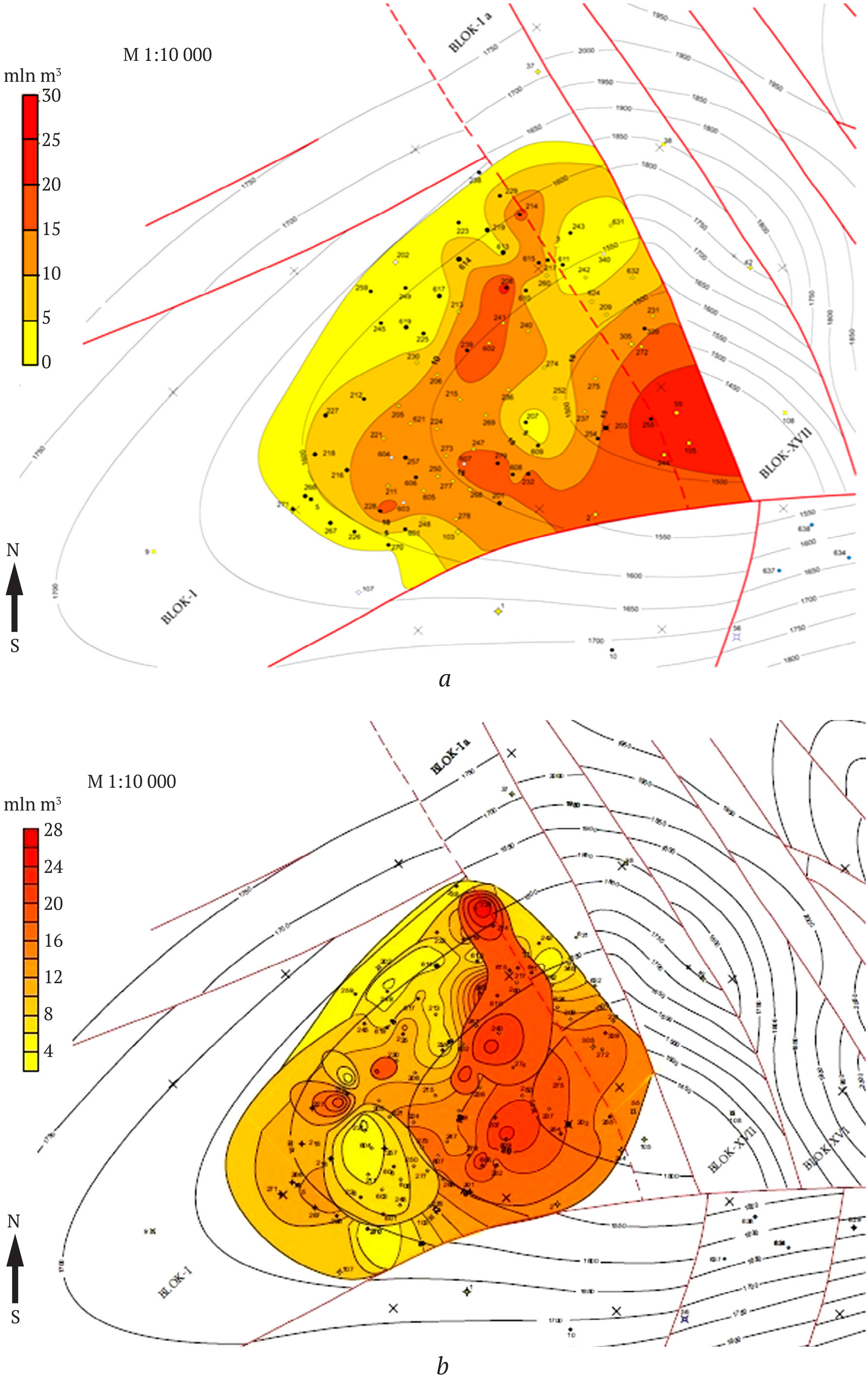

Fig. 10. Maps of spatial variation of the volumes of injected (*a*) and withdrawn (*b*) gas at the Galmas UGSF for the period of 2020–2021

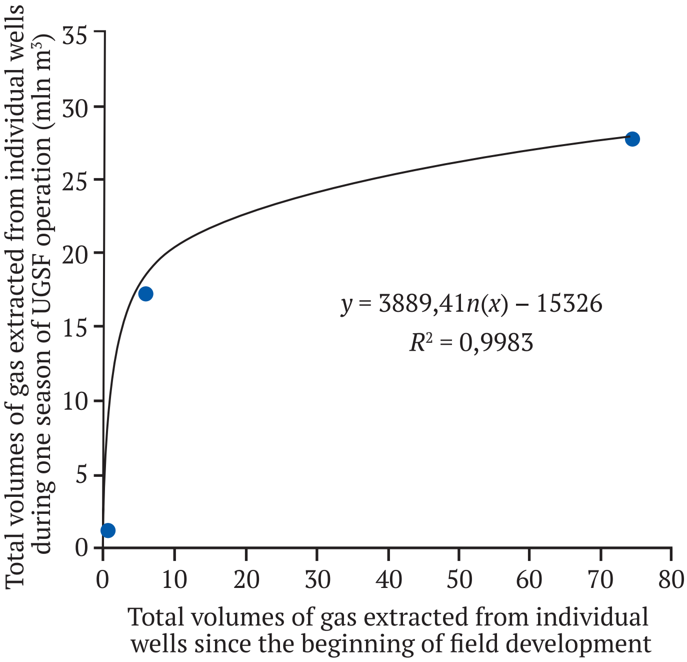

Fig. 11. Galmas Field/UGSF. Relationship between the total volumes of gas extracted from individual wells since the beginning of field development and during one season of UGSF operation

The analysis showed that in the wells with low rock poroperm properties the volumes of injected and withdrawn gas are close to the optimum (Garadagh UGSF), or the volumes of withdrawn gas exceed the volumes of injected gas (Galmas UGSF) (Fig. 12). In wells with relatively high rock poroperm properties, as a rule, the volumes of injected gas are greater than the volumes extracted (Table 2). A possible explanation for this phenomenon may be that rocks with relatively low rock poroperm properties are better at accumulating and retaining injected gas due to the low filtration properties and high adsorption properties of the rocks. Gas injection into relatively more permeable rocks with favorable fluid dynamics properties probably contributes to the dispersion (loss) in space of the injected gas.

Table 2

Galmas and Garadagh UGSFs. The ratio of extracted and injected volumes of gas for the wells with different rock poroperm properties

Well ID	Rock porosity, %	Rock permeability, μm²	Volumetric ratio of extracted and injected gas
Galmas UGSF			
240	27.8	0.130	0.7
252	29.2	0.145	0.7
275	29.3	0.183	0.8
624	27.5	0.198	0.9
273	24.8	0.065	1.3
219	25.6	0.068	4.1
606	24.7	0.084	1.3
277	24.5	0.069	1.4
Garadagh UGSF			
453	15	0.083	1.2
458	8.8	0.026	1.2
467	11.5	0.036	1.4
471	13.8	0.073	1.2
450	9.6	0.015	0.6
459	9.2	0.025	0.6
464	8.2	0.022	0.7
465	8.4	0.008	0.8

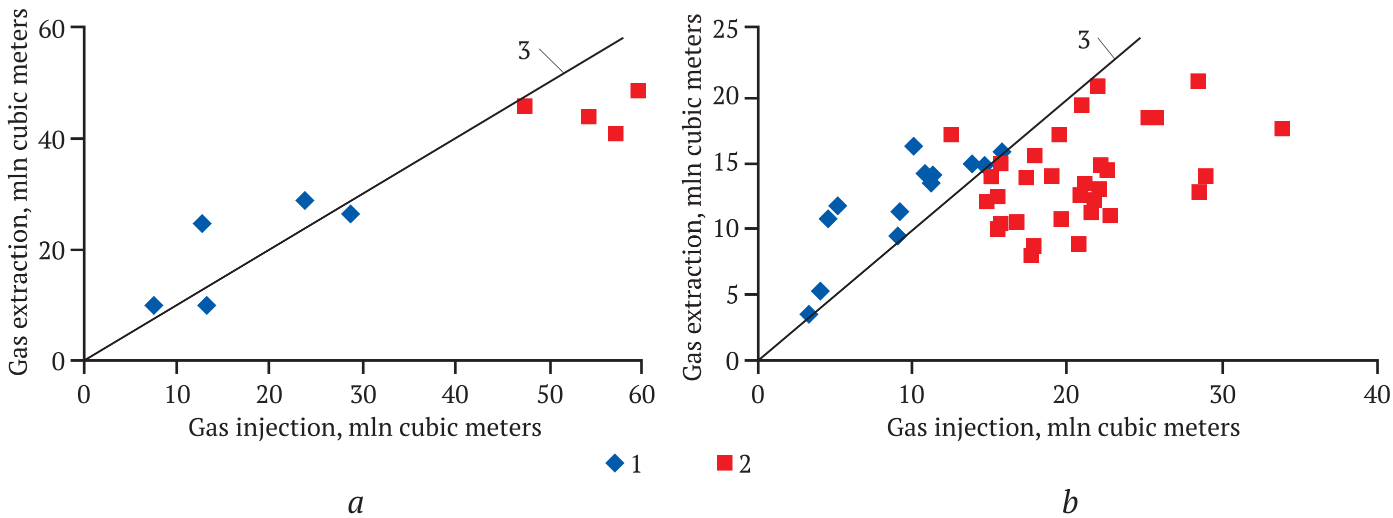

Fig. 12. Relationship between gas injection and extraction volumes at Garadagh (*a*) and Galmas (*b*) UGSFs:
1, *2* – wells with low and high rock poroperm properties, correspondingly;
3 – the line of equal values of gas injection and extraction volumes

Conclusion

Based on the example of the Garadagh and Galmas fields in the SCB, it was established that one of the main geological factors determining the mode of well operation both during the field development and in the course of UGSF operation is reservoir heterogeneity, as manifested in spatial variability of its geological structure and petrophysical properties of rocks.

The main reasons for decreased efficiency of field development and underground gas storage facility operation are: the irregular nature of variation of rock poroperm properties; origination of isolated zones in the reservoir with considerable residual gas volumes; as well as unpredictable directions of fluid movement.

In order to determine the optimal system of operation of UGSF in depleted underground oil and gas reservoirs, the features of the spacial variations resulting from the rocks poroperm properties need to be taken into account.

References

1. Kharroubi A., Layan B., Cordelier P. Influence of pore pressure decline on the permeability of North Sea sandstones. In: *International Symposium of the Society of Core Analysts*. 5-9 October. Abu Dhabi: UAE; 2004. URL: https://www.ux.uis.no/~s-skj/ipt/Proceedings/SCA.1987-2004/1-SCA2004-45.pdf

2. Kashnikov O. Yu. *Research and consideration of deformation processes during development of oil accumulations in terrigenous reservoirs*. [Ph.D. thesis in Engineering Science]. Tyumen; 2008. 23 p. (In Russ.)

3. Chan A. W. *Production-induced reservoir compaction, permeability loss and land surface subsidence*. [Dissertation for PhD degree]. Stanford University; 2004. 176 p.

4. Liu J. J., Feng X. T., Jing L. R. Theoretical and experimental studies on the fluid-solid coupling processes for oil recovery from low permeability fractured reservoirs. *International Journal of Rock Mechanics and Mining Sciences*. 2004;41(3):1–6. https://doi.org/10.1016/j.ijrmms.2003.12.032

5. Chan A. W., Zoback M. D. The role of hydrocarbon production on land subsidence and fault reactivation in the Louisiana Coastal Zone. *Journal of Coastal Research*. 2007;23(3):771–786. https://doi.org/10.2112/05-0553

6. Khuzhayarov B. Kh., Yuldashev T. R., Rustamov A. R. Changing of poroperm properties of bottomhole zone rocks due to rock deformation. *Molodoy Uchenyy*. 2018;(17):140–144. URL: https://moluch.ru/archive/203/49750/

7. Panakhov R. A., Kiyasbeyli T. N. Process flow diagram of Stage II Karadag UGSF pilot operation (big block). *Report of VNIPIgaz*. Baku: 1985. 213 p. (In Russ.)

8. Alizade A. A. (ed.) *Geology of Azerbaijan*. Vol. VII. Oil and Gas. Baku: Nafta-Press; 2008. 672 p. (In Russ.)

Information about the authors

Akper A. Feyzullayev – Dr. Sci. (Geol. and Mineral.), Professor, Head of Department of Institute of Geology and Geophysics, National Academy of Sciences of Azerbaijan, Baku, Republic of Azerbaijan. Scopus ID 24170958500; e-mail: fakper@gmail.com

Araz G. Gojayev – Cand. Sci. (Geol. and Mineral.), Chief Geologist of Gas Storage Facility Operation Department of "Azneft" Production Association, State Oil Company of Azerbaijan Republic (SOCAR), Baku, Republic of Azerbaijan; Scopus ID 57222324518

Irada M. Mamedova – Cand. Sci. (Geol. and Mineral.), Chief of Laboratory of «Oil and Gas» Research Projective Institute of SOCAR, Baku, Republic of Azerbaijan; Scopus ID 24178644200

Received	30.09.2021
Revised	20.12.2021
Accepted	01.02.2022

MINING ROCK PROPERTIES. ROCK MECHANICS AND GEOPHYSICS

Research article

https://doi.org/10.17073/2500-0632-2022-1-30-36

Amplitude-initiated open hysteresis loop of *P*-wave attenuation in sandstone: experimental study

E. I. Mashinsky SC

Trofimuk Institute of Petroleum Geology and Geophysics,
Siberian Branch of the Russian Academy of Sciences, Novosibirsk, Russian Federation

✉ *MashinskiiEI@ipgg.sbras.ru*

Abstract

In the area of solid state physics and materials science, new knowledge has been attained in recent years about micro-nano-plasticity using high-precision measurements at low stresses and strain. Rock microplasticity is currently poorly understood, but in the future it may prove useful in resolving problems of a fundamental and applied nature. This study examines the effect of cyclically varying pulse amplitude and wave velocity on the attenuation parameters of longitudinal wave (P-wave) in sandstone. Laboratory measurements were performed on rock specimens using the reflected wave method in the frequency range of 0.5–1.4 MHz at five values of strain amplitude ~ (0.5-2.0)10^{-6}. Trial simulations were performed, in order to establish the effect of amplitude-dependent wave velocity on the parameters of wave attenuation in the sandstone. Wave attenuation behavior under combined action of the amplitude-dependent factor and wave velocity deviation is complex. The change in strain amplitude shifts the attenuation peak $1/Q_p(f)$ in the attenuation-frequency coordinates. The maximum change in peak attenuation value due to the amplitude factor and wave velocity deviation reaches 3–4 %. An open wave attenuation hysteresis loop was identified as a consequence of the closed amplitude cycle A1(+) --- A1(+) --- A1(–), where A1(+) = A1(–). Open attenuation hysteresis occurs both in the cases of constant and variable wave velocities. The length of the open part of the attenuation hysteresis loop relative to the peak value of the attenuation is as follows: for constant wave speed, 62.63 %, in the mode of increasing wave speed, 91.58 %; and, in the mode of decreasing wave speed, 47.01 %. The effect of open hysteresis of wave attenuation in sandstone can be explained by the action of microplastic deformation detected in the experiments.

Keywords

rock physics, amplitude-dependent wave velocity, open hysteresis of wave attenuation, microplastic strain, jump inelasticity, elastic modulus, nano-strain

Acknowledgments

I express my gratitude to B.V. Pashkov and G.V. Egorov for performing the experiments and further discussion of the results obtained.

For citation

Mashinsky E.I. Amplitude-initiated open hysteresis loop of *P*-wave attenuation in sandstone: experimental study. *Mining Science and Technology* (*Russia*). 2022;7(1):30–36. https://doi.org/10.17073/2500-0632-2022-1-30-36

СВОЙСТВА ГОРНЫХ ПОРОД. ГЕОМЕХАНИКА И ГЕОФИЗИКА

Научная статья

Амплитудно-инициируемая открытая петля гистерезиса затухания *P*-волны в песчанике: экспериментальное исследование

Э.И. Машинский SC

Институт нефтегазовой геологии и геофизики им. А.А. Трофимука,
Сибирское отделение Российской академии наук, г. Новосибирск, Российская Федерация

✉ *MashinskiiEI@ipgg.sbras.ru*

Аннотация

В физике твердого тела и материаловедении с использованием высокоточных измерений на малых напряжениях и деформациях были получены новые знания о микро-нанопластичности. В настоящее время свойство микропластичности горных пород мало изучено, но в перспективе оно может быть полезно для решения задач фундаментального и прикладного характера. В этом исследовании изучено влияние циклически изменяемой амплитуды импульса и скорости волны на параметры затухания продольной волны в песчанике. Лабораторные измерения выполнены на образцах породы методом отраженных волн в диапазоне частот 0,5–1,4 МГц на пяти значениях амплитуды деформации ~ $(0{,}5–2{,}0)10^{-6}$. Проведено пробное моделирование, которое дает возможность установить влияние амплитудно-зависимой скорости волны на параметры затухания волны в песчанике. Поведение затухания волны при совместном действии амплитудного фактора и девиации скорости волны имеет сложный характер. Изменение амплитуды деформации сдвигает пик затухания $1/Q_p(f)$ в координатах «затухание–частота». Максимальное изменение величины затухания в пике за счет амплитудного фактора и девиации скорости волны достигает 3–4 %. Открытая (незамкнутая) петля гистерезиса затухания волны обнаружена после действия замкнутого амплитудного цикла A1(+) --- A5(+) --- A1(−), где A1(+) = A1(−). Открытый гистерезис затухания имеет место как в случае постоянной, так и переменной скорости волны. Протяженность открытой части петли гистерезиса затухания по отношению к максимальной величине затухания составляет: для постоянной скорости волны 62,63 %, в режиме увеличения скорости волны – 91,58 % и в режиме уменьшения скорости волны – 47,01 %. Эффект незамкнутого гистерезиса затухания волны в песчанике может быть объяснен действием обнаруженной в ходе эксперимента микропластической деформации.

Ключевые слова

физика горных пород, амплитудно-зависимая скорость волны, открытый гистерезис затухания волны, микропластическая деформация, скачкообразная неупругость, упругий модуль, нанодеформация

Благодарности

Я выражаю благодарность Б.В. Пашкову и Г.В. Егорову за проведение экспериментов и дальнейшее обсуждение полученных результатов.

Для цитирования

Mashinsky E.I. Amplitude-initiated open hysteresis loop of *P*-wave attenuation in sandstone: experimental study. *Mining Science and Technology* (*Russia*). 2022;7(1):30–36. https://doi.org/10.17073/2500-0632-2022-1-30-36

Introduction and challenges

Fundamental new knowledge in physics of rock deformation can be used to improve the geological efficiency of seismic and acoustic survey methods. This requires an in-depth study of the deformation mechanism under conditions of elastic wave propagation and attenuation at the micro/nanoscale. The property of rock microplasticity, albeit exotic in geophysics, can manifest itself even at low strain. Seismic and acoustic methods use a range of low and very low dynamic strains. Dynamic processes at large and moderate strains are well understood. New knowledge about non-linearity has lead to a enhanced interest in the field of low strains in seismics [1-6].

A model has been proposed of mesoscopic elasticity to explain the mechanism of rock non-linearity. New tools, such as non-linear resonant ultrasound spectroscopy, are being used to reveal the complex behavior of rocks and other materials.

There is experimental evidence that visco-elastic-plastic models provide the most realistic representation of complex deformation in rocks when compared to traditional models. This is a significant advance in extending the range of applicability of the knowledge on inelastic processes and the prospect of practical application of the new knowledge [7, 8].

Theoretical and experimental studies in seismics and other fields of solid state physics and materials science have led to an improvement in the classical visco-elastic model of the standard linear body which describes well the dispersion, relaxation, and related inelastic processes [9–12]. The experimental findings were compared with wave velocity and attenuation predictions obtained using the Bio (jet flow) model and other models. However, these models do not take into account the effect of amplitude dependence of wave velocities and attenuation which were discovered in recent studies [13, 14]. Laboratory experiments on solid sediment samples extracted from great depths confirm the presence of amplitude effect. The behavior of dynamic parameters of seismic and acoustic waves during propagation in various media is complex and has been little studied so far.

With a change in the magnitude of the signal amplitude, both increases and decreases in the wave velocity and attenuation are observed. Decrease or increase in the elastic modulus took place in accordance with the stress-strain ratio slope of curve. Such non-standard behavior of various solids, including rock material, is caused by the joint action of elastic and microplastic deformation [15–19]. In the static stress mode, the strain amplitude effect is represented as a “stress-plateau” and “stress-descend” on the stress-strain diagram. In the dynamic mode (wave propagation), the influence of the amplitude effect can be seen in the waveform as short-term stress-plateaus and stress-descend. The microplasticity of rocks allows such an irregular short-term "inclusion" of the plasticity process with the simultaneous effect of elastic deformation which has been confirmed in theory [20, 21]. This paper presents the study results on the amplitude-dependent hysteresis of longitudinal wave attenuation in sandstone.

Research techniques and factual material

A specimen of fine-grained sandstone was prepared from a core taken from a depth of 2532 m. The sandstone density was 2.42 g/cm^3, the content of fine-grained sand fraction was 85 %, the siltstone fraction was 15 %, and the total porosity was 13 %. The experiment was conducted at a hydrostatic pressure of 20 MPa at room temperature. The cylindrical samples had the following dimensions: 40 mm in diameter; and 16 mm long. A standard three-layer model system (installation) was used in the experiment [22, 23]. The first and third layers provided identical wave reflection at the interfaces. The first layer acted as a delay line, and the third layer acted as an acoustic load. The rock sample was located in between these layers. Excitation and reception of acoustic signals was provided by piezoceramic sensors at frequency of ~ 1 MHz, which were polarized to longitudinal wave. The attenuation decrement $1/Q_p$ was calculated using standard relations [24, 25]. The wave attenuation decrement was measured in a closed amplitude cycle on the ascending and descending course, where $A_{\min} = A_1 \to A_2 \to \ldots \to A_5 = A_{\max} \to \ldots \to A_1 = A_{\min}$. In the Figures, the increase in amplitude is labeled (+) and its decrease is labeled (-). The pulse amplitude relative strain values were as follows: $\varepsilon_1 \approx 0.5 \times 10^{-6}$, $\varepsilon_2 \approx 1.0 \times 10^{-6}$, $\varepsilon_3 \approx 1.3 \times 10^{-6}$, $\varepsilon_4 \approx 1.7 \times 10^{-6}$ and $\varepsilon_5 \approx 2.0 \times 10^{-6}$. The longitudinal wave velocity in the solid sandstone was 4,330 m/sec. Increased noise immunity was provided by recording with signal accumulation.

Research Findings

The frequency dependence of *P*-wave attenuation for ascending and descending amplitude courses are shown in Figures 1 and 2 respectively. The wave attenuation at all amplitudes resembles a relaxation peak. As the signal amplitude increases, the attenuation decreases, and the peak shifts toward low frequencies, see Fig. 1. The nonlinear shift of the attenuation peak is shown by red arrows. On the descending amplitude course, the peak attenuation magnitude increases slightly, but does not return to the initial value (red arrows in Fig. 2). The amplitude dependence of longitudinal wave attenuation in sandstone at ascending and descending courses of strain amplitude is shown in Fig. 3. It represents a comparative picture of wave attenuation behavior for the three wave velocity cases. In all the cases, depending on the strain amplitude, the wave attenuation has the form of an open-type hysteresis loop. The first case took place in our experiment where the wave speed for all amplitudes was constant, 4,330 m/c. The other cases were the products of simple simulation. The second case showed a linear increase in the wave velocity at each amplitude: A1(+) = 4,350, 4,360, 4,370, 4,380, A5(+) = 4,390 m/s; and then reverse descending through the same velocity values, where(A1(−) = A1(+)). The third case showed a linear wave velocity descending from A1(−) to A5(−) (4,300, 4,290, 4,280, 4,270, 4,260 m/s) and the corresponding reverse return. The wave velocity magnitude change was linear and did not exceed the value of 0.92 %. At maximum signal amplitude, the wave attenuation decrease was as follows: for constant wave velocity, 2.83 %; for increasing wave velocity, 1.93 %; and for decreasing wave velocity, 3.77 %. At constant wave velocity, the share of the open part of the attenuation hysteresis loop is 62.63 %, at increasing wave velocity, 91.58 %, and at decreasing velocity, 47.01 %.

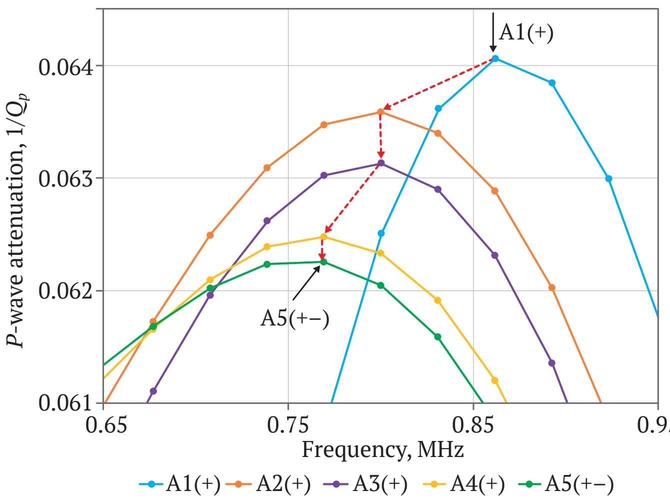

Fig. 1. Frequency dependence of the *P*-wave attenuation in sandstone at five ascending values of the strain amplitude

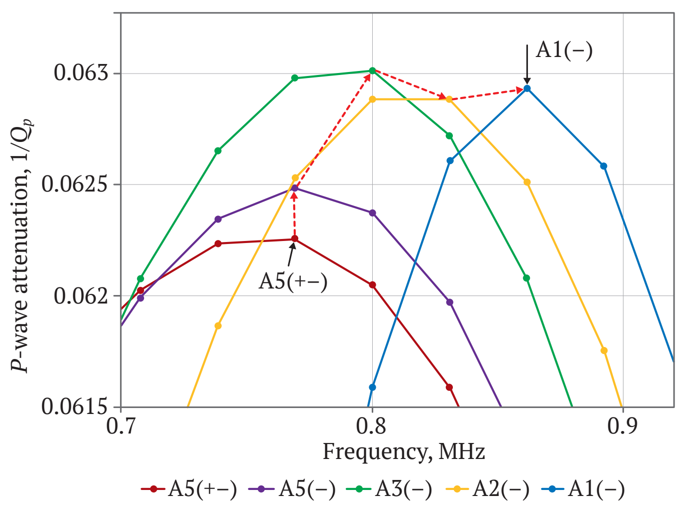

Fig. 2. Frequency dependence of *P*-wave attenuation in sandstone at five descending values of the strain amplitude

A large-scale image of fragments of the waveform at amplitudes A1(+), A1(−) and A2(+), A2(−) is shown in Fig. 4. This is the section of the wave front where the manifestations of non-standard behavior in the form of microplasticity can be seen. The Figure demonstrates the amplitude plateaus extending from one to several time quanta (tquantum), the amplitude local drop, and the effect of amplitude microhysteresis. The maximum of the wave front at amplitudes A1(+), A1(−) and A2(+), A2(−) coincide exactly in time at 31.3425 μs (red arrows in Figure 4). The lowest points on the wave front for the same two pairs of amplitudes are observed at the same time value of 31.765 μs (red dashed line in Fig. 4). At the pulse front there are local amplitude hysteresis loops of several quanta of time. Fragments of the waveform at amplitudes A3(+), A3(−), and A4(+), A4(−) are shown in Fig. 5. The signs of microplasticity described above are also present here. The peak and valley in the last phase of the pulse (31.3425 and 31.765 μs) are present at the same time as in the previous case.

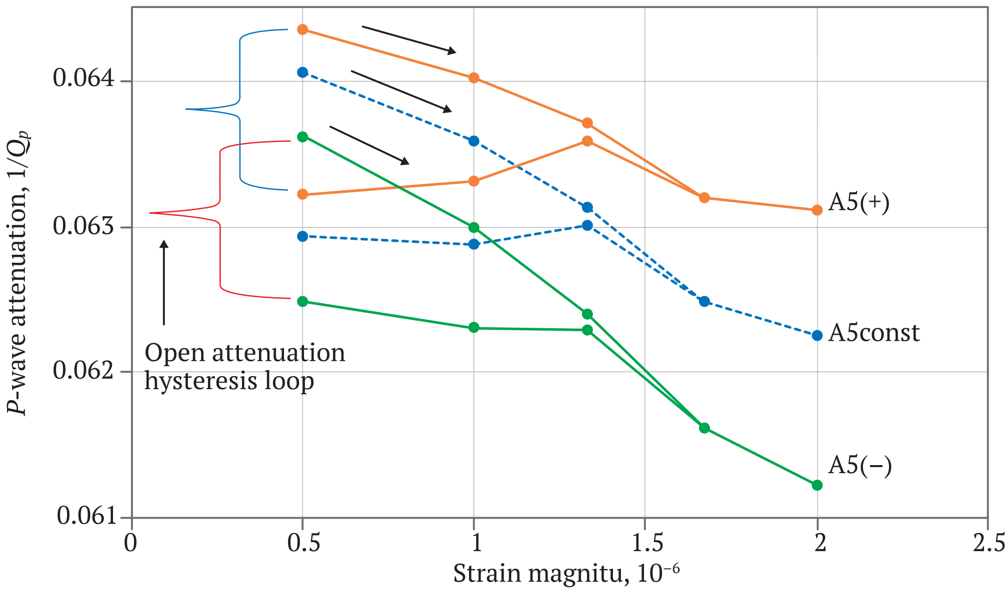

Fig. 3. Relationship between *P*-wave attenuation in sandstone and strain amplitude at the ascending and descending courses

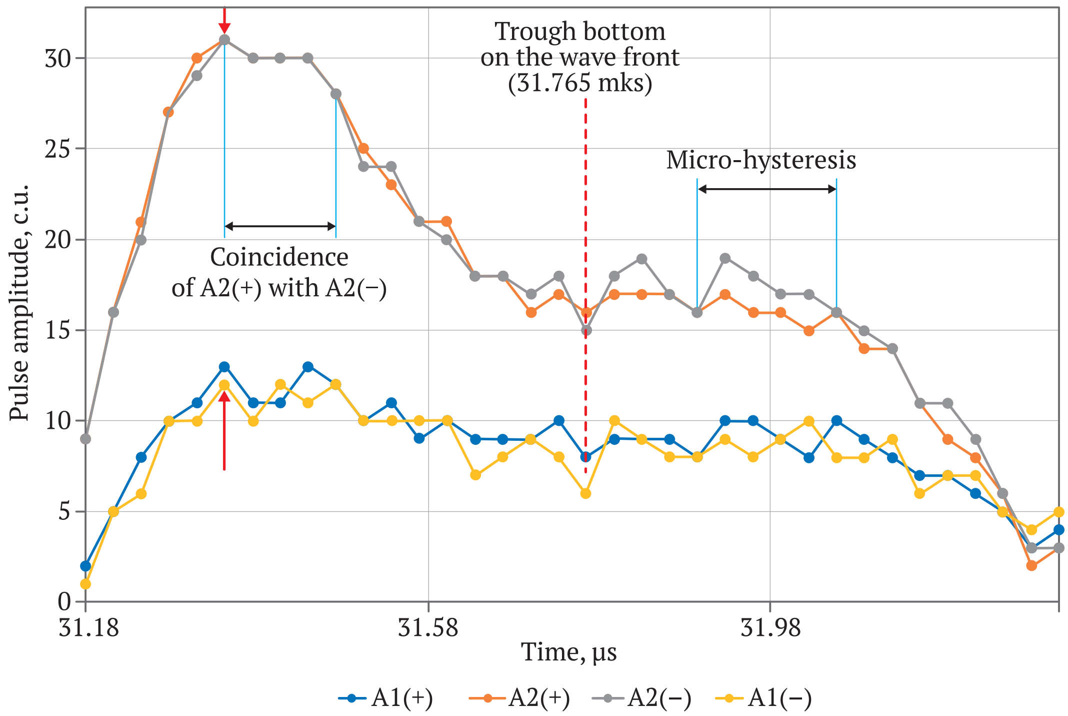

Fig. 4. Large-scale image of fragments of the waveform at amplitudes A1(+), A1(−) and A2(+), A2(−)

eISSN 2500-0632
https://mst.misis.ru/

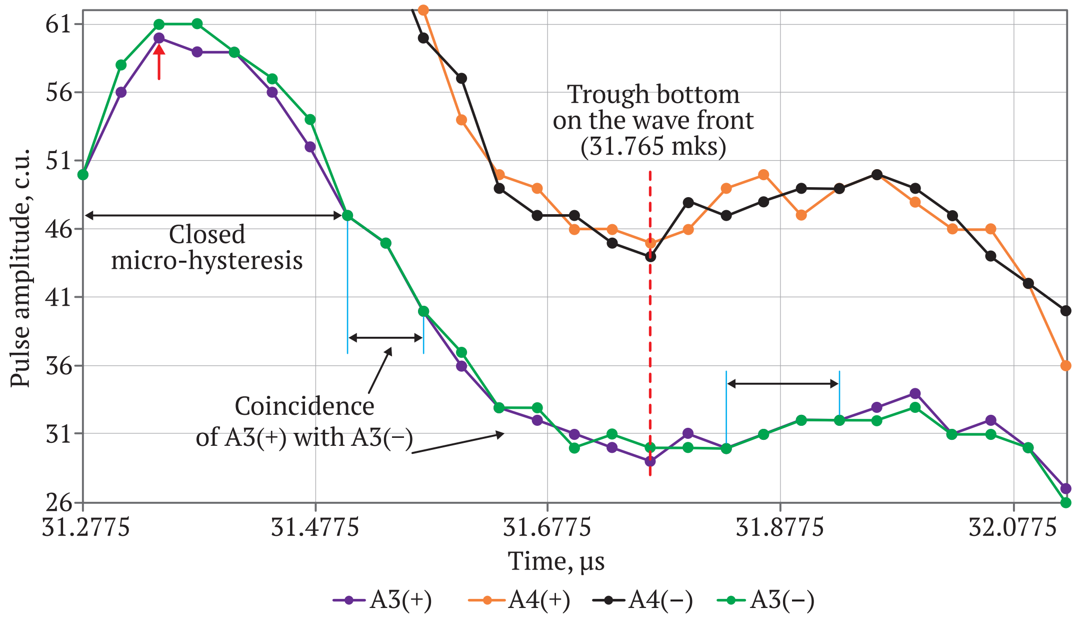

Fig. 5. Large-scale image of fragments of the waveform at amplitudes A3(+), A3(−) and A4(+), A4(−)

Discussion of Findings

The findings show that the effect of strain amplitude and wave velocity deviation on wave attenuation parameters in sandstone is unusual in character. When the amplitude value changes along the closed loop, the wave attenuation curve $1/Q_{peak}(A_{n-i})$ takes the form of open amplitude-dependent hysteresis. This requires an explanation of the deformation mechanism within the framework of rock deformation physics and solid-state physics. The open hysteresis for acoustic P-wave propagation indicates possible mechanism of non-standard inelasticity in sandstone. The most likely explanation for this effect is the mechanism of rock microplasticity. Microplastic strain depends in a complex way on the deformation leve l (the magnitude of the applied mechanical stress). The attenuation and velocity of the wave depend in a complex way on the level of dynamic deformation in the sandstone. A small change (from 0.23 to 0.9 %) in the longitudinal wave velocity in the amplitude cycle causes a greater change of 3 % in the attenuation. Novel studies conducted on rock specimens using high-precision laser Doppler interferometry showed that the change in wave velocity at the expense of amplitude reached 5 % [26, 27].

Conclusion

The experimental data analysis and the trial simulations showed the complex behavior of the wave attenuation depending on the magnitude of the amplitude and deviation of the wave velocity. In the frequency range of 0.5–1.4 MHz, wave attenuation takes the form of a relaxation peak. Changing the amplitude magnitude in a closed loop (ascending = descending) leads to shifting the attenuation peak in the “attenuation – frequency” coordinates. The maximum change in the peak attenuation value due to the amplitude factor (in the strain range of $(0.5–2.0)10^{-6}$) reaches 3 %. The combined effect of the amplitude factor and a small deviation of the wave velocity (in the range from 0.23 to 0.93 %) results in increased attenuation in the peak up to ~ 4 %. The open wave attenuation hysteresis loop detected in the experiment takes place both at constant wave velocity and at variable (amplitude-dependent) wave velocity. The relative magnitude of the open hysteresis depends significantly on the magnitude of the strain amplitude and the wave velocity deviation. The manifestations of microplasticity recorded in the experiment can be regarded as the cause of the open wave attenuation hysteresis effect in sandstone.

References

1. Gushchin V.V., Pavlenko O.V. Study of nonlinear elastic properties of rocks based on seismic data. In: *Modern Seismology, Achievements and Challenges*. Moscow; 1998. Vol. 13. (In Russ.)

2. Egorov G.V. Variations of nonlinear parameters of a consolidated porous water-saturated sample depending on the degree of gas saturation. *Fizicheskaia mezomekhanika*. 2007;10(1):107–110. (In Russ.)

3. Kondratyev O.K. *Seismic waves in Absorbing Media*. Moscow: Nedra Publ.; 1986. 176 p. (In Russ.)

4. Nikolaev A.V. *Problems of nonlinear seismic*. Moscow: Nauka Publ.; 1987. 288 p. (In Russ.)

5. McCall K.R., Guyer R.A. Equation of state and wave propagation in hysteretic nonlinear elastic materials. *Journal of Geophysical Research: Solid Earth*. 1994;99(B12):23887–23897.

6. Ostrovsky L.A., Johnson P.A. Dynamic nonlinear elasticity in geomaterials. *La Rivista del Nuovo Cimento*. 2001;24(4):1–46. https://doi.org/10.1007/BF03548898

7. Guyer R.A., Johnson P.A. Nonlinear mesoscopic elasticity: Evidence for a new class of materials. *Physics Today*. 1999;52(4):30–36. https://doi.org/10.1063/1.882648

8. Zhou Ch., Shen Zh.-J., Yin J.-H. Biot dynamic consolidation finite element analysis using a hypoplasticity model. In: *13th World Conference on Earthquake Engineering Vancouver, B.C.* August 1–6 2004. Canada; 2004. Paper No. 351. URL: https://www.iitk.ac.in/nicee/wcee/article/13_351.pdf

9. Diallo M.S., Prasad M., Appel E. Comparison between experimental results and theoretical predictions for P-wave velocity and attenuation at ultrasonic frequency. *Wave Motion*. 2003;37(1):1–16. https://doi.org/10.1016/S0165-2125(02)00018-5

10. Golovin I.S., Pavlova T.S., Golovina S.B. et al. Effect of severe plastic deformation of Fe–26 at. Al and titanium on internal friction. *Materials Science and Engineering A-structural Materials Properties Microstructure and Processing*. 2006;442(1–2):165–169. https://doi.org/10.1016/j.msea.2005.12.081

11. Sajeva A., Filograsso R., Capaccioli S. Including plastic behaviour in the Preisach-Mayergoyz space to find static and dynamic bulk moduli in granular media. In: *SEG Technical Program Expanded Abstracts*. 2018. Pp. 3517–3521. https://doi.org/10.1190/segam2018-2994837.1

12. Luoa Sh.-N., Swadenerb J.G., Ma Ch., Tschauner O. Examining crystallographic orientation dependence of hardness of silica stishovite. *Physica B: Condensed Matter*. 2007;399:138–142. https://doi.org/10.1016/j.physb.2007.06.011

13. Mashinskii E.I. Jump-like inelasticity in sandstone and its effect on the amplitude dependence of *P*-wave attenuation: An experimental study. *Wave Motion*. 2020;97:102585. https://doi.org/10.1016/j.wavemoti.2020.102585

14. Nishino Y., Kawaguchi R., Tamaoka S., Ide N. Amplitude-dependent internal friction study of fatigue deterioration in carbon fiber reinforced plastic laminates. *Materials Research*. 2018;21(2):e20170858. https://doi.org/10.1590/1980-5373-MR-2017-0858

15. Derlet P.M., Maaß R. Micro-plasticity and intermittent dislocation activity in a simplied micro structural model. *Modelling and Simulation in Materials Science and Engineering*. 2013;21(3):035007. https://doi.org/10.1088/0965-0393/21/3/035007

16. Duretz T., Souche A., Borst R., Le Pourhiet L. The benefits of using a consistent tangent operator for viscoelastoplastic computations in geodynamics. *Geochemistry, Geophysics, Geosystems*. 2018;19(12):4904–4924. https://doi.org/10.1029/2018GC007877

17. Huang J., Zhao M.,·Du X., Dai F., Ma Ch., Liu J. An elasto-plastic damage model for rocks based on a new nonlinear strength criterion. *Rock Mechanics and Rock Engineering*. 2018;51:1413–1429. https://doi.org/10.1007/s00603-018-1417-1

18. Mashinskii E.I. Difference between static and dynamic elastic moduli of rocks: Physical causes. *Russian Geology and Geophysics*. 2003:44(9):953–959. URL: https://repository.geologyscience.ru/bitstream/handle/123456789/32706/Mash_03.pdf?sequence=1&isAllowed=y

19. Mashinskii E.I. Seismo-micro-plasticity phenomenon in the rocks. *Natural Science*. 2010;2(3):155–159. https://doi.org/10.4236/ns.2010.23025

20. Vodenitcharova T., Zhang L.C. A new constitutive model for the phase transformations in monocrystalline silicon. *International Journal of Solids and Structures*. 2004;41(18–19):5411–5424. https://doi.org/10.1016/j.ijsolstr.2004.04.025

21. Liu Y., Dai F., Feng P., Xu N. Mechanical behavior of intermittent jointed rocks under random cyclic compression with different loading parameters. *Soil Dynamics and Earthquake Engineering*. 2018;113:12–24. https://doi.org/10.1016/j.soildyn.2018.05.030

22. Johnston D.H., Toksoz M.N. Thermal cracking and amplitude dependent attenuation. *Journal of Geophysical Research*. 1980;85(B2):937–942. https://doi.org/10.1029/JB085iB02p00937

23. Mashinskii E.I. Amplitude-frequency dependencies of wave attenuation in single-crystal quartz: Experimental study. *Journal of Geophysical Research: Solid Earth*. 2008;113(B11). https://doi.org/10.1029/2008JB005719

24. Jones S.M. Velocity and quality factors of sedimentary rocks at low and high effective pressures. *Geophysical Journal International*. 1995;123(3):774–780. https://doi.org/10.1111/j.1365-246X.1995.tb06889.x

25. Mavko G.M. Friction attenuation: an inherent amplitude dependence. *Journal of Geophysical Research: Solid Earth*. 1979;84(B9):4769–4775. https://doi.org/10.1029/JB084iB09p04769

26. Nourifard N., Lebedev M. Research note: the effect of strain amplitude produced by ultrasonic waves on its velocity. *Geophysical Prospecting*. 2019;67(4):715–722. https://doi.org/10.1111/1365-2478.12674

27. Nourifard N., Mashinskii E., Lebedev M. The effect of wave amplitude on S-wave velocity in porous media: an experimental study by Laser Doppler Interferometry. *Exploration Geophysics*. 2019;50(6):683–691. https://doi.org/10.1080/08123985.2019.1667228

Information about the author

Eduard I. Mashinskii – Dr. Sci. (Geol. and Min.), Trofimuk Institute of Petroleum Geology and Geophysics of Siberian Branch of Russian Academy of Sciences, Novosibirsk, Russian Federation; Scopus ID 8886240600; e-mail: MashinskiiEI@ipgg.sbras.ru

Received	03.12.2021
Revised	20.12.2021
Accepted	01.02.2022

 eISSN 2500-0632
https://mst.misis.ru/

SAFETY IN MINING AND PROCESSING INDUSTRY AND ENVIRONMENTAL PROTECTION

Research article

https://doi.org/10.17073/2500-0632-2022-1-37-48

Experimental study of transient thermal conditions in longwall faces

M. O. Perestoronin ✉, **A. B. Zaitsev**, **M. A. Semin**, **D. A. Borodavkin**
Mining Institute of the Ural Branch of the Russian Academy of Sciences (MI UB RAS), Perm, Russian Federation
✉ *per.maks1m.97@gmail.com*

Abstract
With limited mineral resources, existing mines are seeking to extract increasingly hard-to-reach and deep-seated mineral reserves. Increasing mining depth leads to problems connected with the provision of comfortable and safe working conditions. The main objective of creating favorable microclimate for miners is to provide acceptable values of air temperature in working areas at deep levels. Of particular interest are processes of formation of thermal conditions in longwall faces (longwalls), where high-performance hauling and mining equipment is used. We conducted a study to determine the formation of the thermal conditions in longwall faces. The study was based on experimental data obtained in the conditions of longwall face No. 1 of the first northern panel at the –440 m level of 4 RU mine of JSC "Belaruskali". The findings of the experimental study of the dynamic microclimatic air parameters allowed us to establish that the thermal conditions in longwall faces were variable. This is due to the fact that during mining operations in longwall faces, the mining process cycle includes mining and maintenance shifts, characterized by different levels of heat release. The influence of thermal inertia of the equipment during shutdown for the maintenance shift plays an important role in the formation of thermal conditions. The findings of the experimental study of transient thermal modes in a longwall face during transition from mining shifts to maintenance shifts will form a basis for developing a mathematical model to calculate the heat exchange processes in mine workings (longwall faces). These will take into account the non-stationary nature of the technogenic heat release sources. The mathematical model will allow the safest and most effective technical and economic process solutions to be implemented, in order to control longwall face ventilation.

Keywords
mine ventilation, longwall, air supply, experimental study, thermal conditions, mine microclimate, heat release, heat exchange, air heating

Acknowledgements
The research was carried out with financial support of the Russian Science Foundation under the project No. 19-77-30008.

For citation
Perestoronin M. O., Zaitsev A. B., Semin M. A., Borodavkin D. A. Experimental study of transient thermal conditions in longwall faces. *Mining Science and Technology* (*Russia*). 2022;7(1):37–48. https://doi.org/10.17073/2500-0632-2022-1-37-48

ТЕХНОЛОГИЧЕСКАЯ БЕЗОПАСНОСТЬ В МИНЕРАЛЬНО-СЫРЬЕВОМ КОМПЛЕКСЕ И ОХРАНА ОКРУЖАЮЩЕЙ СРЕДЫ

Научная статья

Экспериментальное исследование переходных тепловых режимов длинных очистных забоев

М. О. Пересторонин ✉, **А. В. Зайцев**, **М. А. Семин**, **Д. А. Бородавкин**
Горный институт Уральского отделения Российской академии наук (ГИ УрО РАН), г. Пермь, Российская Федерация
✉ *per.maks1m.97@gmail.com*

Аннотация
В условиях ограниченности минеральных ресурсов современные шахты и рудники стремятся к добыче все более труднодоступных и глубокозалегающих запасов полезных ископаемых. Увеличение глубины ведения горных работ приводит к возникновению проблем, связанных с обеспечением ком-

фортных и безопасных условий труда в горных выработках. Основной задачей создания благоприятного микроклимата для горнорабочих является обеспечение допустимых значений температуры воздуха в рабочих зонах глубоких горизонтов шахт и рудников. На сегодняшний день особый интерес вызывают процессы формирования теплового режима в длинных очистных забоях (лавах), в которых применяется высокопроизводительное транспортно-добычное оборудование. В связи с этим в работе проводится исследование, направленное на определение особенностей формирования теплового режима в длинных очистных забоях. Исследование основано на экспериментальных данных, полученных в условиях лавы № 1 первой северной панели горизонта –440 м рудника 4 РУ ОАО «Беларуськалий». Результаты экспериментального изучения динамических микроклиматических параметров воздуха позволили установить, что тепловой режим в лаве носит переменный характер. Это обусловлено тем, что при ведении горных работ в лаве технологический цикл отработки запасов полезных ископаемых включает добычные и ремонтные смены, характеризующиеся различными мощностями тепловыделений. При этом влияние тепловой инерции оборудования в период его остановки в ремонтную смену играет важную роль в формировании теплового режима. Предполагается, что результаты экспериментального исследования переходных тепловых режимов в лаве при переходе от добычных смен к ремонтным выступят основой при разработке математической модели теплообменных процессов в горных выработках, способной учитывать нестационарную природу техногенных источников тепловыделений. Разработанная математическая модель позволит принимать наиболее безопасные и эффективные технико-экономические технологические решения по управлению проветриванием лав.

Ключевые слова

рудничная вентиляция, лава, проветривание, экспериментальное исследование, тепловой режим, рудничный микроклимат, тепловыделение, теплообмен, нагрев воздуха

Благодарности

Исследование выполнено при финансовой поддержке РНФ в рамках проекта № 19-77-30008.

Для цитирования

Perestoronin M. O., Zaitsev A. B., Semin M. A., Borodavkin D. A. Experimental study of transient thermal conditions in longwall faces. *Mining Science and Technology* (*Russia*). 2022;7(1):37–48. https://doi.org/10.17073/2500-0632-2022-1-37-48

Introduction

Belaruskali OJSC is one of the largest producers of mineral fertilizers in the world. Mineral salts and their products are extracted at its mines at a large range of depths, ranging from 360 to 820 m. The depth of the mining operations continues to increase over time. Bearing in mind that the geothermal stage for the subsoil in the area of mining is from 50 to 65 m[1], at the lower elevations (levels) of the deposit the rock mass temperature can reach +26 °C. It should be noted that the mining operations at the Belaruskali's mines in most cases are performed by means of the pillar system based on shearer-based longwall set of equipment, characterized by high heat release. These factors considerably influence the thermal conditions of the mines [1, 2]. They also clearly promote the formation of an unfavourable microclimate for people in the working areas, with an air temperature above the permissible value of +26 °C[2].

According to the study [3], prolonged physical activity of a person in conditions of high ambient temperature leads to an increase in body temperature, dehydration of the body, slowed reactions, decreased mental and physical abilities. These processes, firstly, have an adverse impact on the functioning of human systems and organs, and secondly, contribute worker to fatigue and decreased his productivity [4].

In addition, high ambient temperatures have an adverse impact on the operation of a longwall equipment. If they heat is not removed quickly enough, this can lead to premature wear and tear. If it overheats, it is forced to shut down [5].

Considering the above, a study of the microclimate of underground working zones, the factors determining it, and the ways of its normalization are of particularly importance. An important question when studying the microclimate of longwall faces is the matter of air temperature distribution throughout its length – from the shearer's power train, which is the main source of heat release in the longwall, to the ventilation drifts.

At the present time, studies of heat exchange processes in underground workings are carried out, as a rule, with the use of mathematical models of heat, moisture and air distribution in the mine ventilation

[1] Instructions for calculating the amount of air required to ventilate the mines of the Starobin deposit. Soligorsk-Perm; 2018. 93 p.

[2] Industrial safety rules for underground mining of salt deposits of the Republic of Belarus (with amendments). Approved Decree of the Ministry for Emergency Situations of the Republic of Belarus on April 10, 2014, No. 10.

network [2, 6–8]. Existing models [9–11] are able to consider technogenic heat release sources (mining machinery and equipment) only in "operation" and "shutdown" modes. With regard to the first mode, heat release is assumed constant. In the case of the second mode, it is identically equal to zero. Thus, these models describe stationary heat release processes in the system of mine workings.

In actual practice, mining equipment has a finite heat capacity and experiences heating during operation (as well as the surrounding rock mass). After shutdown, prolonged heat releases from heated bodies takes place. This decreases over time from the maximum values corresponding to the normal mode of operation to zero (subject to a sufficiently long shutdown).

In other words, the equipment is characterized by thermal inertia [12]. This is important to consider for the correct modeling of heat release and exchange processes in mine ventilation networks.

In order to develop a correct model of heat exchange processes in mine workings, capable of taking into account the non-stationary nature of technogenic heat release sources, initial data is required. The data must reflect changes in microclimatic parameters of the mine air under different modes of ventilation and operation of hauling and mining equipment.

The studies [13] and [14] are of great value among the scientific studies of the features of microclimate formation in mines in Russia and neighboring countries. Important studies carried out in other countries include papers describing underground microclimate in mines of Canada [15], India [16, 17], and South Africa [18]. However, a review of the existing international reference sources shows that the available experience in research of microclimatic conditions of mines has an insufficiently detailed experimental and practical base suitable for mathematical modeling of heat exchange processes between hauling and mining equipment and mine air. This will require additional experimental studies aimed at determining the degree of effect of the parameters of the ventilation air supplied, and the effect of the equipment operation parameters on the air temperature in workings over time.

The purpose of this study was to investigate experimentally the transient thermal conditions of longwall faces. The study was carried out at longwall face No. 1 of the first northern panel at the –440 m level of 4 RU mine of JSC "Belaruskali". The following objectives were achieved:

1) the vertical air distribution in the longwall extraction pillar was determined;

2) the effect of the power train fan on the equipment cooling rate was determined;

3) the change in the air temperature near the equipment over time during its operation and shutdowns was determined;

4) the distribution of air temperature along the length of the longwall over time was determined.

Research subject

Extraction pillar of longwall No. 1 is extracted in reverse order and includes: three drifts (one conveyor and two ventilation (vent) drifts) and a longwall face. In order to ventilate the extraction pillar, a fresh air stream from the main haulage drift enters the conveyor drift and then to the longwall face. The return ventilation current (from the longwall) is removed through the ventilation drifts to the main ventilation drift of the mine. Schematics of longwall face No.1 ventilation is presented in Fig. 1.

The following equipmet is installed in longwall face No.1 working zone ventilation: main fan installation; VM-12 auxiliary fan, located at the base of the longwall pillar; and the shearer's power train fan.

The Korfmann fan of the shearer's power train ensures air distribution between the conveyor and transport drifts, increasing the amount of air in the longwall face. It switches on when the longwall set of equipment starts operation and switches off 5–10 minutes after the set has stopped operation. In turn, the main fan installations and the VM-12 fan are in permanent operation and do not depend on the operation mode of the longwall face.

The working area of the longwall face is understood as the longwall face itself, as well as adjacent to it part of the conveyor drift, in which power train of the longwall set of equipment is located, where the ore mining and equipment servicing personnel operate.

The longwall face equipment consists of: a shearer; a face scraper conveyor; a powered support; a face-end support; and a power train (a control station, pumping stations and a pumping unit). The equipment arrangement in longwall face No.1 is shown in Fig. 2.

At present, the standard working hours at Belaruskali mines consist of three daily mining shifts and one maintenance shift of 6 hours. A complete maintenance shift is often not required to maintain the longwall set of equipment between mining shifts. In such cases the maintenance shift is replaced by a short-term equipment shutdown for inspection for 2–3 hours.

Research techniques

The experimental study of longwall face No.1 was conducted during its transition from the mining shift to the maintenance shift for different modes of longwall face ventilation.

During the experiment, the VM-12 fan and the fan of the power train were unable to control the opera-

eISSN 2500-0632
https://mst.misis.ru/

tion parameters. In this case changes to the mode of the longwall face ventilation was carried out by means of controlling the fresh air losses through conveyor connection No. 4 by changing the parameters of the air brattice installation in it.

It was assumed that the main fan installations during the period of the study did not contribute to the change of the amount of air supplied to ventilate the longwall pillar over time.

During the experiment four longwall face ventilation modes were investigated:

1) mode No. 1 – air flow rate in the longwall face for mining and maintenance shifts is constant;

2) mode No.2 – air flow rate in the longwall face decreases immediately after completion of the mining shift and equipment shutdown;

3) mode No. 3 – air flow rate in the longwall face initially remains the same after the mining shift ends, but after some time it decreases significantly;

4) mode No. 4 – gradual decrease of air flow rate in the longwall face at the beginning of the maintenance shift.

The air temperature was measured continuously by means of Kestrel temperature and humidity sensors installed in the area of the 4th and 124th sections of the powered support. It was periodically inspected by manual instrumental measurements with a Fluke 971 temperature and humidity meter. These sections were selected due to the lack of direct impact of the heat flow from the power train while, at the same time, they provide characteristic measurements, ensuring understanding of how the air temperature changes when passing the longwall face. The sensors were installed on the powered support under the roof of the working at a height of 2.0–2.2 m. The position of the temperature and humidity sensors in the working face cross-section was selected, in order to ensure the safety of measuring instruments du-

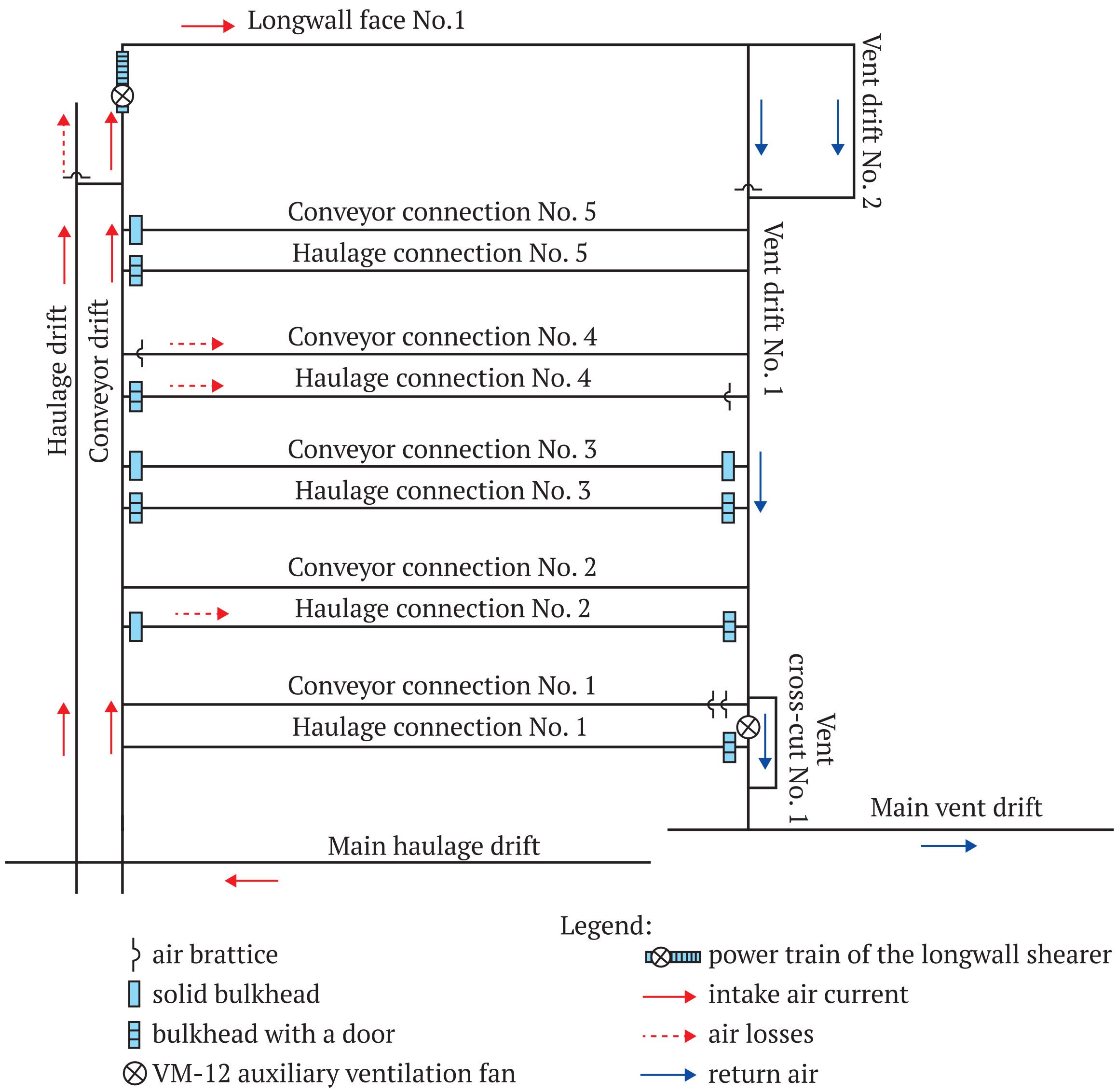

Fig. 1. Schematics of longwall face No. 1 ventilation

ring the mining operations in the longwall face. Fig. 3 shows a visual representation of the Kestrel temperature and humidity sensors arrangement in the longwall face cross-section.

The temperature of the face and surfaces of various components of the equipment located in the longwall face and the conveyor drift was also measured by means of the Fluke 568 infrared thermometer (pyrometer). The speed of the air current was measured by APR-2 anemometer. Measurement of the cross-section of mine workings was carried out by Leica Disto D3 laser rangefinder. Volumetric air flow rate was calculated as the product of the measured air speed and the cross-sectional area.

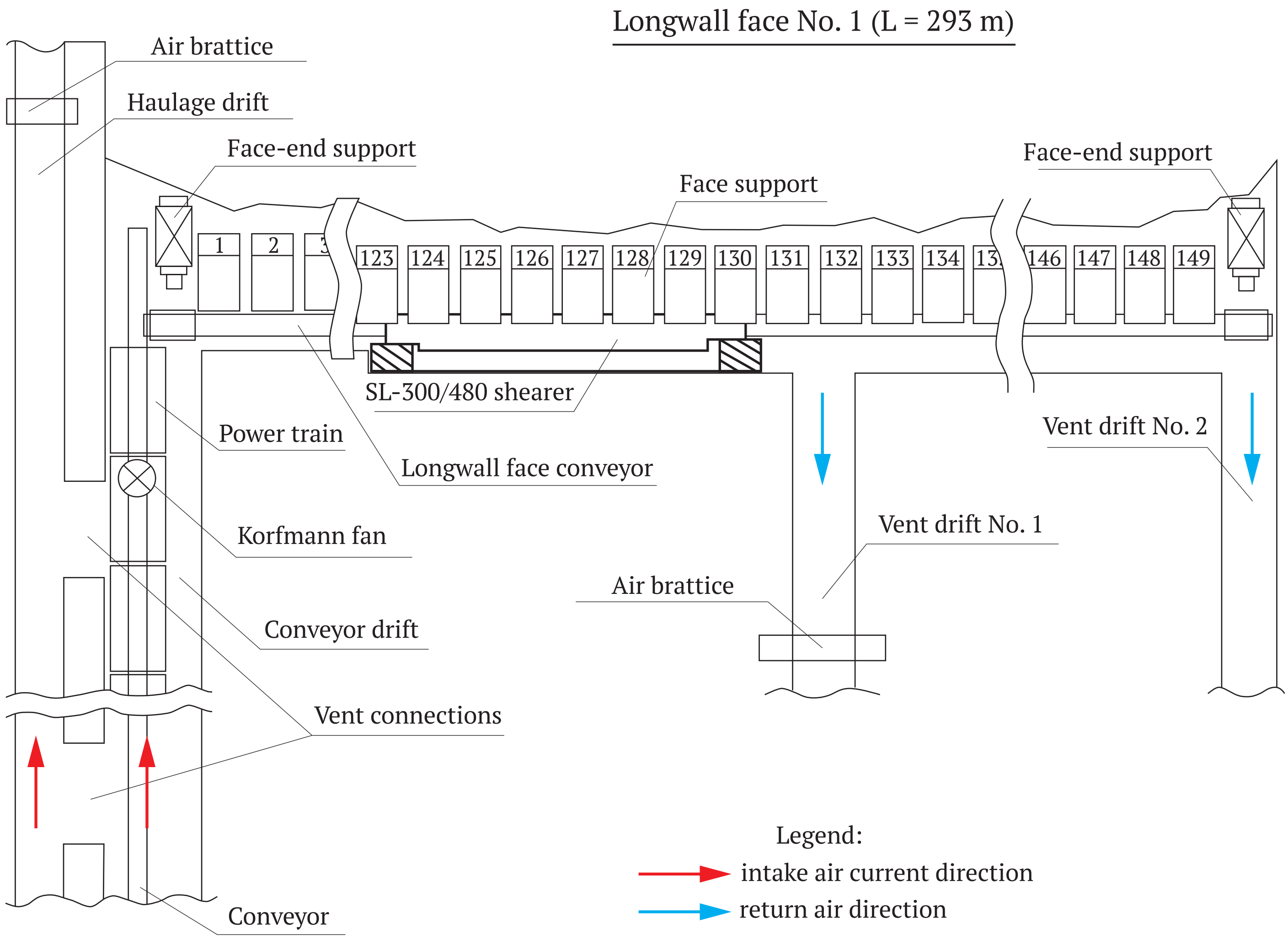

Fig. 2. Equipment arrangement in longwall face No. 1

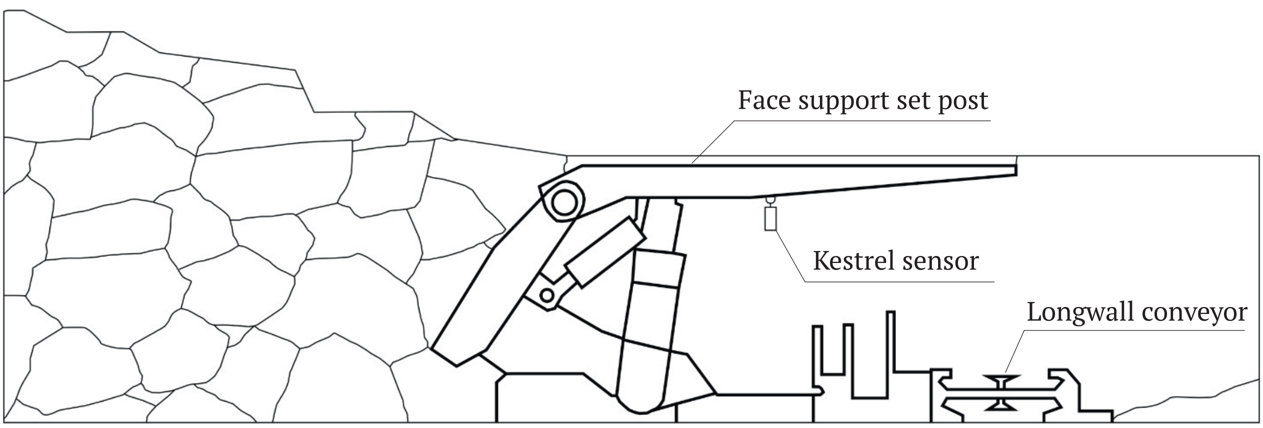

Fig. 3. Arrangement of Kestrel temperature and humidity sensors in the longwall face cross-section

The measuring instruments used in the experimental investigation of longwall face No. 1 showed the following measurement errors:

1) kestrel temperature and humidity sensor: temperature ±0,9 °C, humidity ±2,0 % RH;

2) Fluke 971 temperature and humidity meter: temperature ±0,5 °C, humidity ±2,5 % RH;

3) Fluke 568 pyrometer: temperature ±1,0 °C;

4) APR-2 anemometer: speed $\Delta = 0{,}2 + 0{,}05\nu$, m/s ($\nu$ – air flow speed, m/s);

5) Leica Disto D3 laser rangefinder: length $\Delta = 0{,}15l$ mm (l – measured length, m).

Research Findings

Taking into account air losses through the haulage and conveyor connections, calculation based on the experimental data on air flow rate in the longwall face No. 1 pillar showed that no more than 43 % of the total amount of air supplied to ventilate the pillar reach the longwall face. The return air from the longwall face to the longwall face ventilation drifts exceeds intake air (through the conveyor drift) by 15.6–22.4 %. This is due to the presence of air inflow from the worked-out space of the longwall, where it enters from the haulage drift.

When the VM-12 fan, located at the beginning of the longwall face, is switched on during the mining shift, the power train fan increases the amount of air, flowing through the power train of the longwall shearer, by about 12.4 %, which is an additional 0.82 m^3/sec. However, the flow rate of return air from the face through ventilation drifts Nos. 1 and 2 remains practically the same with the power train fan switched on or off. Thus, if there are other sources of ventilation at the panel, the power train fan has no effect on the general ventilation of the longwall face. However, it provides a local increase of air flow rate in the conveyor drift and increases the air flow which directly fans (i. e. cools) the power train equipment of the longwall shearer. This includes the heat exchanger of the shearer cooling system, which is the main source of heat release.

Study of the temperatures of the heated body surfaces in the longwall face showed that during the maintenance shift (1.5 h after switching off the equipment) the temperature of different parts of the shearer reaches 50 °C at the temperature of the intake fresh air stream of 25.6 °C. The temperature of the powered support in all sections of the longwall face practically coincides with the air temperature in the longwall, or insignificantly exceeds it.

At the connection of the conveyor drift and the longwall face, the temperature of the first sections of the support reaches 34.9 °C. This can be explained by its close location to the shearer's power train. In addition to the shearer equipment, the components with the highest level also include the face conveyor drive with temperature from 44 to 56 °C, and the face conveyor itself with temperature of 35.4 °C at the 4th section of the support.

The results of air temperature measurements in the working zone of longwall face No. 1 by the temperature and humidity sensors are shown in Fig. 4. Readings of the sensors were controlled by the temperature and humidity meter measuring.

Based on the air temperature measurements, we calculated the average powers of the heat releases, kW, from the longwall shearer power train and the longwall conveyor drive by means of the following formula [2]:

$$W = c\rho Q\Delta T, \qquad (1)$$

where c is mass heat capacity of air taken equal to 1.005 kJ/(kg·°C); ρ is air density taken equal to 1.25 kg/m^3;   is the heated air flow rate, m^3/s; is the difference in the air temperature before and after interaction with the source of heat release, °C.

The calculation of the power of heat release from the equipment was performed without taking into account the enthalpy of air. This due to the reason that there are no water occurrences in potash and salt mines and the moisture content of air moving in the longwall is approximately a constant value.

A summary of the results of longwall face No. 1 temperature survey at its connection with the conveyor drift is presented in Table 1.

During the long shutdown of mining equipment for complete maintenance shift with the mining ventilation mode of the longwall pillar, the air at the beginning of the longwall, according to the findings of the temperature survey of longwall face No.1 has time to cool down to the temperature of 29.1 °C. It then heats up to 38.5 °C during the mining shifts. In turn, during long shutdowns of mining equipment during complete maintenance with decreased air amount, supplied for the longwall face ventilation, the air at the beginning of the longwall is cooled only to a temperature of 30.0 °C.

In the area of the longwall face connection with the conveyor drift, the air temperature near the longwall roof is 1.3–1.5 °C higher than its temperature near the bottom. This can be explained by: uneven heating of the air flow from the equipment of the longwall shearer power train; the peculiarities of the air motion near the sharp turns, consisting in the division of the flow; the formation of turbulence zones; as well as the difference in the densities of different air masses entering the longwall face from heated equipment and from the mined-out space. Air temperature equalization in the plane of the longwall cross section occurs at a distance of 20 m from the longwall connection with the conveyor drift. The most unfavorable temperatures of air in the longwall face were recorded by the temperature sensor at the face at the beginning of the longwall near the 4th section of the powered support. The average temperature of air passing through this section of the longwall face, was lower than that measured. At the moment of the measurement it varied from 27.7 to 37.1 °C.

The change in air temperature in the longwall at the studied modes near ventilation drift No. 1 (at the 124th section of the support) ranged from 23.4 to 26.4 °C. As can be seen from the temperature trends shown in Fig. 4, the dynamics of the air temperature for the beginning (4th section of the support) and the end (124th section of the support) of the longwall are comparable with each other, taking into account the operation of the mining equipment.

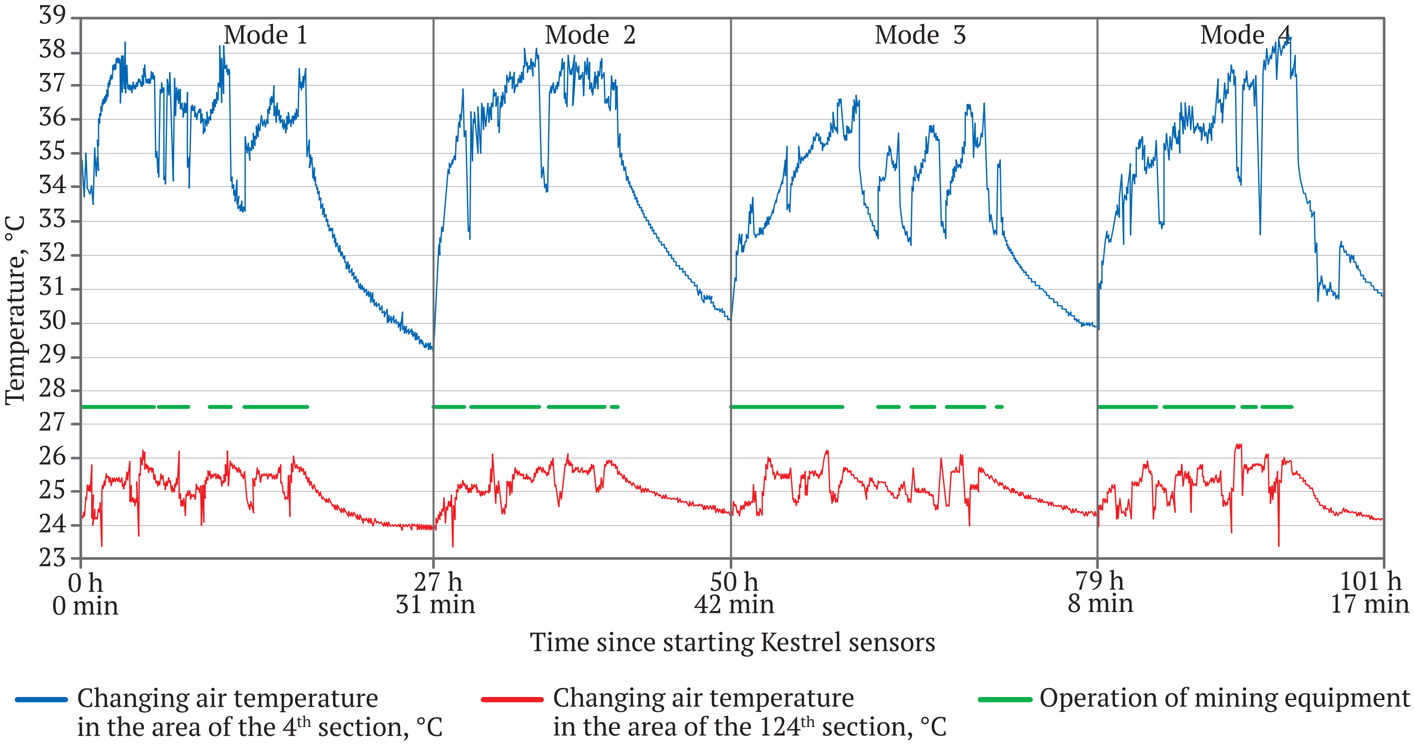

Fig. 4. Changes in the air temperature in longwall face No. 1, recorded by the temperature and humidity sensors

Table 1

The results of longwall face No. 1 temperature survey

		Power train fan	Q, м³/с	Duration	T_{max}, °C	T_{min}, °C	W_{cp}, кВт	dT/dt, °C/мин	
Mode 1	MINING	ON	7.46	17 h 29 min	38.3		98.2		
	MAINTENANCE	OFF	6.92	10 h 2 min	37.1	29.1	52.6	0.013	
Mode 2	MINING	ON	7.54	14 h 9 min	38.1		100.7		
	MAINTENANCE	OFF	5.05	9 h 2 min	37.2	30.0	41.4	0.012	
Mode 3	MINING	OFF	7.23	20 h 51 min	36.7		82.2		
	MAINTENANCE	OFF	6.45	1 h 25 min	34.8	31.7	54.3	0.037	0.012
	MAINTENANCE	OFF	4.97	6 h 10 min	31.7	29.8	31.2	0.005	
Mode 4	MINING	OFF	7.54	14 h 55 min	38.5		93.2		
	MAINTENANCE	OFF	6.68	1 h 0 min	38.2	33.8	85.7	0.075	
	MAINTENANCE	OFF	4.43	2 h 9 min	33.8	30.6	36.3	0.026	0.017
	MAINTENANCE	OFF	6.61	4 h 5 min	32.4	30.7	48.1	0.007	

Legend: MINING – mining shift, MAINTENANCE – maintenance shift, Q – flow rate of air fanning the power train, m³/s, T_{max} – maximum air temperature for the presented time period, °C, T_{min} – minimum air temperature for the presented time period, °C, W_{cp} – average heat release for the presented time period, kW, dT/dt – average air temperature decline rate for the maintenance shift, °C/min.

In order to estimate the intensity of thermal processes occurring in a longwall face, a one-dimensional model of convective heat transfer in a longwall face was developed, taking into account heat exchange with surrounding sources. Using the model, we obtained a formula linking the air temperature at the end of a mine working (longwall) with the air temperature at its beginning, as well as the rock mass temperature, flow rate and geometric parameters of the mine working (longwall) [19]. This formula is as follows:

$$T_e = T_r + \left(T_b - T_r\right) e^{-\frac{KPL}{c\rho Q}}, \qquad (2)$$

where T_e, T_b, T_r – air temperatures at the end and at the beginning of the mine working (longwall), temperature of intact rock mass, respectively, °C; K – non-stationary heat transfer coefficient, kW/(m^2 · °C); P, L – perimeter and length of the mine working (longwall), m; c – mass heat capacity of air, kJ/(kg · °C); ρ – air density, kg/m^3; Q – air flow rate in the mine working, m^3/s.

The average value of the non-stationary heat transfer coefficient for longwall face No. 1, determined by formula (2) on the basis of the experimental data, during the survey period was 4.21 W/(m^2·°C).This indicated a significant intensity of the heat exchange process between the mine air and rocks[3] [20].

Decreasing air temperature during the studied maintenance shifts can be conditionally divided into two stages (Fig. 5).

The first stage is characterized by a sharp decrease in air temperature due to fairly rapid decreasing heat release from the shearer power train. This is due to, firstly, shutdown of the shearer and, secondly, the continuation of the power train fan operation, concentrating the air flow on the heated equipment for 5–10 minutes. In this case, the air temperature decreases approximately according to the linear law. The second stage is characterized by a gradual decrease in temperature and obeys the exponential law, similar to dependence (2):

$$T = T_0 + \Delta T e^{-at}, \qquad (3)$$

where T_0 – temperature to which air at cooling tends (the minimum temperature to which air cools down), °C; ΔT – maximum difference between T and T_0, °C; a – exponent parameter, responsible for the rate of temperature decrease, h^{-1}; t – time, h.

Fig. 6 shows the approximating curves (3) for the empirical time dependence of the air temperature for the studied longwall face No. 1 ventilation modes.

Analysis of the Fig. 6 data showed that for modes 1–3 over the entire time interval, the experimental curves correspond well to the exponential law.

In order to estimate the rate of the equipment cooling, we introduced a characteristic time equal to the time interval, during which the excessive air temperature decreases 2.71 times (the value of the exponent). Thus, the characteristic time is determined by the following formula:

$$\tau = \frac{1}{a}. \qquad (4)$$

Table 2 shows the change in air temperature during maintenance shifts during the ventilation modes being studied here(conditions), as well as the values of the characteristic time of excessive air temperature decrease.

The cooling curves shown in Fig. 6 have a different character of cooling. Analysis of the first two investigated ventilation modes, as modes with constant air flow rate during the maintenance shift, showed that the decrease in the flow rate during transition

[3] Reference Manual to SNiP 2.01.55-85. Thermophysical calculations for national economic assets, positioned in mine workings. Moscow: Stroyizdat Publ., G.V. Plekhanov LGI, 1989, 76 p. (In Russ.)

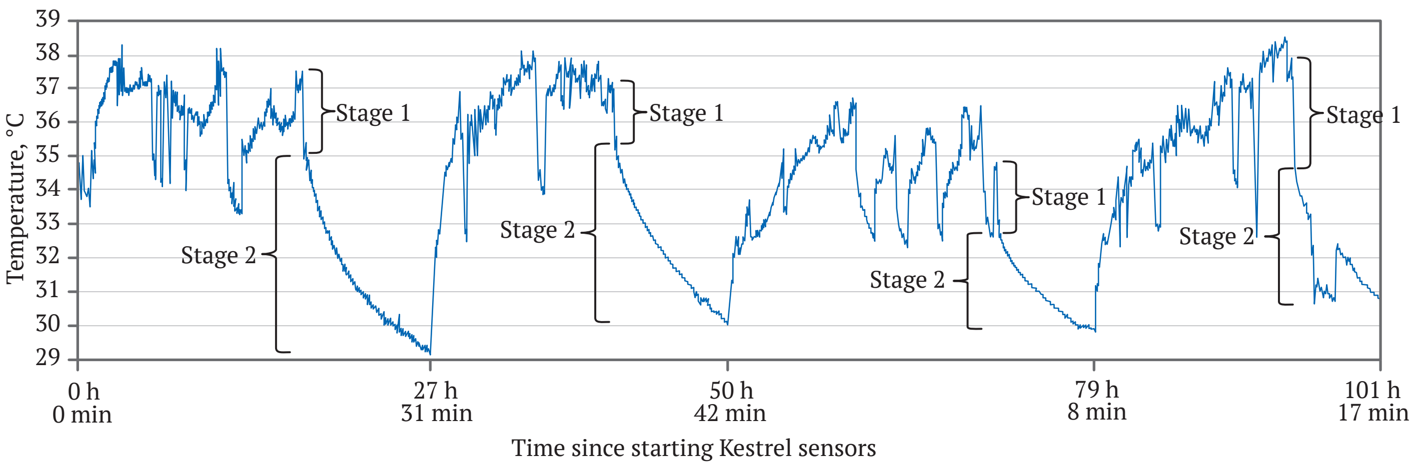

Fig. 5. Stages of air temperature decrease

eISSN 2500-0632
https://mst.misis.ru/

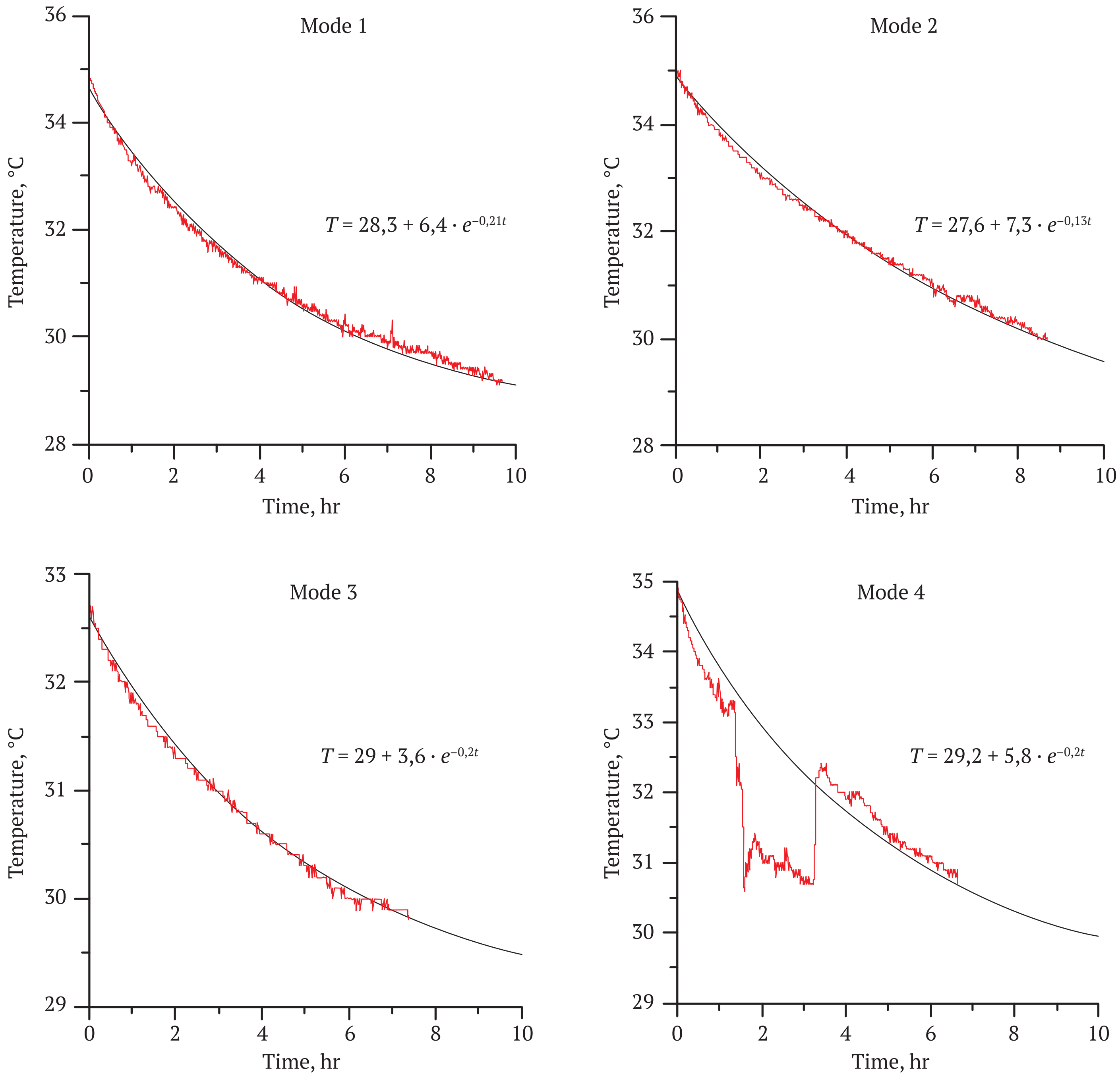

Fig. 6. Approximating curves of air cooling during the maintenance shift for the ventilation modes studied

Table 2

Changing air temperature during maintenance shifts at the modes being studied here

Air temperature at different modes	Mode 1	Mode 2	Mode 3	Mode 4
Air temperature in the beginning of maintenance shift, °C	37.5	37.1	36.4	37.9
Air temperature immediately after switching off the power train fan, °C	34.7	34.9	32.6	35.0
Minimum temperature to which the air cools down, °C	28.3	27.6	29.0	29.2
Typical time of decreasing the excessive air temperature	46 h 5 min	7 h 41 min	5 h 0 min	5 h 0 min

from the mining shift to the maintenance shift, significantly increased the rate of equipment cooling. For example, in the case of the first mode during transition from the mining shift to the maintenance shift and a 10.8 % decrease in the air flow rate caused by switching off the power train fan, the typical excessive air temperature decrease time was 4 hours 46 minutes. In the case of the second investigated mode with a 33 % decrease in the air flow rate, the typical excessive air temperature decrease time was 7 hours and 41 minutes.

The third investigated mode was characterized by relatively long regular equipment shutdowns during mining shifts and, thus low accumulated thermalpowers. The significant decrease in the air flow rate during the maintenance shift occurred 1 h 25 min after the end of the mining shift. During this time, a considerable part of the heat accumulated by the equipment was transferred to the air. This ventilation mode cannot be considered indicative from the viewpoint of evaluating the dependence of the temperature trends on the flow rate of air supplied during the maintenance shift.

Change in the the air flow rate during the maintenance shift in the 4th mode under study was performed in three stages:

– decrease in the flow rate by 11.5 % due to the power train fan shutdown and fixing it at 1h;

– 41.1 % decrease in the flow rate (relative to the flow rate during the mining shift) and fixing it at 2 hours and 9 minutes;

– decrease in the flow rate by 12.4 % (relative to the flow rate during the mining shift) and fixing it at 3 hours and 29 minutes.

As can be seen from the curve of air cooling during the maintenance shift in the 4th investigated mode, in the case of decreased air flow rate supplied for the longwall face ventilation by 41.1 %, a sharp decrease in the air temperature in the longwall face occurs. This is caused by a decrease in the heat flow amount from the heated equipment of the longwall power train. However, after the air flow rate increased, its temperature in the longwall face sharply increases to values higher than they would have been without flow rate reduction. This was caused by the fact that the rate of the equipment cooling decreased due to the decrease in the amount of air fanning it.

On the whole, it should be noted that the higher the heated equipment temperature at the end of the mining shift, the higher the cooling rate of air near the heated equipment during the maintenance shift. Furthermore, the air cooling rate depends on the speed of air movement, the temperature of the host rock mass, the area of the heat exchange surface determined by the workings geometry and configurations, and the energy intensity of the equipment.

Conclusion

Based on the findings of the experimental study of longwall face No. 1 of the first northern panel at the −440 m level of 4 RU mine of JSC "Belaruskali", the following conclusions can be made.

– The power train fan has no effect on the general ventilation of the longwall face. However, it provides a local increase of air flow rate in the conveyor drift and increases the air flow that directly fans (i. e. cools) the longwall shearer power train equipment.

– The main “accumulators” of heat in the longwall face during the mining shift are: the host rock mass; the longwall set of equipment (shearer+); and the powered support of the longwall face. After ore extraction shutdown, their long cooling and gradual transfer of accumulated heat to the mine's atmosphere occurs over a period of time that considerably exceeds the duration of the maintenance shift.

– At long shutdown of the mining equipment during the full-fledged maintenance shift, the air at the beginning of the longwall was able to cool down to a temperature of 29–30 °C only. It then experienced heating up to 38.5 °C during the mining shifts. The air temperature in the longwall face near the ventilation workings was within the allowable limits - from 23.4 to 26.4 °C. At the same time, the air temperature trends at the beginning and at the end of the longwall face were comparable with each other, when the mining equipment operation was taken into account.

– Decreasing air temperature in the longwall face at the equipment shutdown occurred in two stages: abrupt decline, close to linear (due to rather fast decreasing the heat release from the shearer's power train, caused by the shearer shutdown and continuation of the power train's fan operation for 5–10 minu-tes); and then gradual exponential decline. The decrease in air supply during the maintenance shift by 33 % resulted in increasing the characteristic time of the excessive air temperature decline by 61 %, from 4 h 46 min to 7 h 41 min.

Thus, the continuation of heat release from the heated components of equipment and rock mass determines the need for air supply to the longwall face during the maintenance shift at a volume equal to that supplied during the mining shift. This is necessary for removal of excessive heat from technogenic sources of heat release, which are turned off at the beginning of the maintenance shift, but with insufficient cooling time. This feature of the technogenic sources of heat releases should be taken into account when developing technical solutions to control the longwall face ventilation.

The findings of the experimental study could be used as initial data for developing a mathematical model for calculating the heat exchange processes in mine workings (longwall faces), taking into account the non-stationary nature of the technogenic heat release sources.

References

1. Gendler S.G. *Thermal conditions of underground structures*. Leningrad: G.V. Plekhanov LGI; 1987, 102 p. (In Russ.)

2. Zaytsev A.V. *Scientific bases of thermal management and calculations in underground mines*. doctoral thesis in engineering science. Perm; 2019. 247 p. (In Russ.)

3. Chebotarev A.G., Afanasieva R.F. Assessment of physiological and sanitary aspects of microclimate at workplaces in underground and opencast mines, and preventive measures against its adverse effect. *Russian Mining Industry*. 2012;(6):34–40. (In Russ.). URL: https://mining-media.ru/ru/article/prombez/3190-fiziologo-gigienicheskaya-otsenka-mikroklimata-na-rabochikh-mestakh-v-shakhtakh-i-karerakh-i-mery-profilaktiki-ego-neblagopriyatnogo-vozdejstviya.%20%D0%94%D0%B0%D1%82%D0%B0%20%D0%BE%D0%B1%D1%80%D0%B0%D1%89%D0%B5%D0%BD%D0%B8%D1%8F%2003.10.2018

4. Lapshin A.A. Influence of extraction chambers backfilling on microclimat of deep mines. *Eastern-European Journal of Enterprise Technologies*. 2014;(10):3–11. (In Russ.). URL: http://journals.uran.ua/eejet/article/view/22151/21021

5. Galushko V.N., Alferova T.V., Alferov A.A. Determination of reliability indicators of electrical systems taking into account changing operating conditions. *Vestnik Gomel'skogo Gosudarstvennogo Tekhnicheskogo Universiteta im. P. O. Sukhogo*. 2013;(3):80–87. (In Russ.)

6. Vengerov I.R. Vol. I. Paradigm analysis. In: *Thermophysics of Underground Mines and Open Pits. Mathematical Models*. Donetsk: Nord-Press Publ.; 2008. 632 p. (In Russ.). URL: https://www.geokniga.org/bookfiles/geokniga-teplofizika-shaht-i-rudnikov-matematicheskie-modeli-tom-1-analiz-paradigmy.pdf

7. Khokholov Yu.A., Kurilko A.S. Mathematical modelling of processes of heat mass exchange of ventilation air and rocks in the cryolithozone extensive mine workings. *Nauka i Obrazovanie*. 2015;(3):50–54. (In Russ.). URL: http://no.ysn.ru/attachments/article/1521/050-054_%D0%A5%D0%BE%D1%85%D0%BE%D0%BB%D0%BE%D0%B2.pdf

8. Lapshin A.A. Mathematical modeling of heat exchange processes at the movement of air in mine workings of ore mines. *Nachnyi Vestnik MSMU*. 2013;(12):93–101. (In Russ.). URL: https://readera.org/read/140215704

9. Levin L.Y., Semin M.A., Zaitsev A.V. Mathematical methods of forecasting microclimate conditions in an arbitrary layout network of underground excavations. *Journal of Mining Science*. 2014;50(2):371–378. https://doi.org/10.1134/S1062739114020203 (Orig. ver.: Levin L.Y., Semin M.A., Zaitsev A.V. Mathematical methods of forecasting microclimate conditions in an arbitrary layout network of underground excavations. *Fiziko-Texhnicheskiye Problemy Razrabbotki Poleznykh Iskopaemykh*. 2014;(2):154–161. (In Russ.))

10. McPherson M.J. The analysis and simulation of heat flow into underground airways. *International Journal of Mining and Geological Engineering*. 1986;4(3):165–195. https://doi.org/10.1007/BF01560715

11. Lapshin A.A. Mathematical simulation of microclimate normalisation processes in deep ore mines. *Naukovyi Visnyk Natsionalnoho Hirnychoho Universytetu*. 2014;(3):137–144. (In Russ.). URL: http://nvngu.in.ua/index.php/ru/component/jdownloads/finish/41-03/643-2014-3-lapshin/0

12. Minchev D.S., Gogorenko O.A. Effect of thermal on diesel engines transient performance. *Internal Combustion Engines*. 2020;(1):68–72. https://doi.org/10.20998/0419-8719.2020.1.09

13. Shuvalov Yu.V. *Thermal conditions control for underground mines and open pits in the North: Resource-saving systems*. Leningrad: Publishing House of Leningrad University; 1988. 196 p. (In Russ.)

14. Lugovsky S.I. *Ventilation of deep mines*. Gosgortekhizdat Publ.; 1962. 324 p. (In Russ.)

15. Rutherford J.G. Ventilation heat Exchanger at Inco's Greighton Mine. *Canadian Mining Journal*. 1958;79(10):97–100.

16. Barenbrug A.W. Deep level mining. Observations on the Kolar Field. *The South African Mining and Engineering Journal*. 1948:2886.

17. Caw J.M. The Colar Gold Field. *Mine and Quarry Engineering*. 1956;22(7):238–296.

18. McPherson M.J. The simulation of airflow and temperature in the stopes of S. African gold mines. In: *Proc. International Mine Ventilation Congress*. Johannesburg; 1975. Pp. 35–51.

19. Ozhegin M.A. Study of electric driven mining machines heat release in deep underground mining conditions and its effect on the thermal conditions at the 4th Mine Administration of JSC "Belaruskali". In: *Problems of Hydrocarbon and Ore Mineral Deposits Development. Proceedings of the XI All-Russian Research-to-Practice Conference*. Perm, November 7–9. 2018. Perm: Perm National Research Polytechnic University Publ.; 2018. Pp. 358–360 (In Russ.).URL: https://neftteh.ru/files/2018_1.pdf

20. Podvigin K.A. Analysis of heat release sources at deep levels of coal mines. Innovative prospects of Donbass. In: *Proceedings of the 6th International Research-to-Practice Conference*. Donetsk: May 26–28. 2020. Donetsk: Donetsk National Technical University Publ.; 2020. Pp. 60–75. (In Russ.). URL: http://ipd.donntu.org/dl/IPD2020/s1.pdf

Information about the authors

Maxim O. Perestoronin – Mining Engineer, Mining Thermal Physics Sector, Department of Aerology and Thermophysics, Mining Institute of the Ural Branch of the Russian Academy of Sciences, Perm, Russian Federation; e-mail per.maks1m.97@gmail.com

Artem V. Zaitsev – Dr. Sci. (Eng.), the Head of the Mining Thermal Physics Sector, Department of Aerology and Thermophysics, Mining Institute of the Ural Branch of the Russian Academy of Sciences, Perm, Russian Federation; Scopus ID 57213120380; e-mail aerolog.artem@gmail.com

Mikhail A. Semin – Cand. Sci. (Eng.), Researcher, Mining Thermal Physics Sector, Department of Aerology and Thermophysics, Mining Institute of the Ural Branch of the Russian Academy of Sciences, Perm, Russian Federation; ORCID 0000-0001-5200-7931, Scopus ID 56462570900, ResearcherID S-8980-2016; e-mail seminma@inbox.ru

Dmitry A. Borodavkin – Mining Engineer, Sector "Mining Thermal Physics", Department of Aerology and Thermophysics, Mining Institute of the Ural Branch of the Russian Academy of Sciences, Perm, Russian Federation; e-mail borodavkin.dmitriy@gmail.com

Received 18.10.2021
Revised 11.11.2021
Accepted 01.02.2022

eISSN 2500-0632
https://mst.misis.ru/

CONSTRUCTION OF MINING ENTERPRISES AND UNDERGROUND SPACE DEVELOPMENT

Research article

https://doi.org/10.17073/2500-0632-2022-1-49-56

Analysis of mechanized tunneling parameters to determine the overcutting characteristics

D.S. Konyukhov
JSC Mosinzhproekt, Moscow, Russian Federation
✉ *gidrotehnik@inbox.ru*

Abstract

Tunneling in urban conditions requires costly measures, in order to ensure the safety of existing buildings. On average, there are up to 17–20 buildings per 1 km of Moscow Subway Lines under construction. Analysis and comparison of geotechnical monitoring data and results of geotechnical estimations for underground construction using cut-and-cover and tunneling methods in conditions of high-density urban area shows an unsatisfactory correlation between estimated and actual data. This can be described in the following way: insufficient geotechnical survey data; discrepancy between the accepted estimation model and the actual behavior of soil under load; insufficient qualification of the construction workers; and overcutting. The study was aimed at solving the urgent scientific and engineering problem of determining the characteristics of overcutting during mechanized tunnel boring. At the first stage, the investigations were aimed at identifying the key reasons and factors which determine the quantitative parameters of overcutting in urban underground construction by tunneling. These factors include the following: mismatch between the cutting diameter and the outer lining diameter; displacement of the soil mass in front of the face; incomplete grouting of voids beyond the lining; incomplete filling of beyond-shield voids with clay mortar or slow-curing grouting mortar or no filling at all; and human factor (low qualifications of personnel). The overcutting coefficient was determined on the basis of the proposed empirical dependence of its values with regard to the depth of tunneling. The experimental data allowed the depth dependence of the overcutting coefficient for different tunneling depths to be defined, as well as for tunnel diameters from 4 to 10 meters in the case of mechanized tunnel boring machine (TBM) using the earth pressure balanced tunneling method. The practical importance of the studies consists in determining the range of the empirical overcutting coefficient variation from 0.5 % (for TBMs with nominal diameter of 10 m) up to 5 % (for TBMs with nominal diameter of 4 m). The development of organizational measures and justification of process solutions, aimed at ensuring the safety of the existing buildings in conjunction with the scientific and technical support of underground construction has led to a shortening of tunneling time between the Okskaya and Nizhegorodskaya stations of Nekrasovskaya Line of Moscow Subway by about six months. It has also provided savings of about 2.5 billion rubles.

Keywords

underground construction, tunneling, tunnel boring machine (TBM, blade shield), Herrenkneht, Robbins, geotechnical monitoring, overcutting, coefficient of overcutting

For citation

Konyukhov D.S. Analysis of mechanized tunneling parameters to determine the overcutting characteristics. *Mining Science and Technology* (*Russia*). 2022;7(1):49–56. https://doi.org/10.17073/2500-0632-2022-1-49-56

СТРОИТЕЛЬСТВО ГОРНЫХ ПРЕДПРИЯТИЙ И ОСВОЕНИЕ ПОДЗЕМНОГО ПРОСТРАНСТВА

Научная статья

Анализ параметров механизированной проходки тоннелей для определения характеристик перебора грунта

Д.С. Конюхов
АО «Мосинжпроект», г. Москва, Российская Федерация
✉ *gidrotehnik@inbox.ru*

Аннотация

Ведение горнопроходческих работ в условиях современного города требует проведения дорогостоящих мероприятий по обеспечению сохранности существующих зданий. В среднем на 1 км строящейся линии метрополитена Москвы приходится до 17–20 зданий. Анализ и сопоставление данных геотехнического мониторинга с результатами геотехнических расчетов для подземного строительства открытым и закрытым способами в условиях плотной городской застройки продемонстрировал неудовлетворительную сходимость расчетных и фактических данных. Основными факторами этого явления являются: недостаточность данных инженерно-геологических изысканий; несоответствие принимаемой расчетной модели реальному поведению грунта под нагрузкой; недостаточная квалификация исполнителей; перебор грунта. Публикация направлена на решение актуальной научно-технической задачи определения характеристик перебора грунта при механизированной проходке тоннелей. На первом этапе исследования были направлены на идентификацию ключевых причин и факторов, определяющих количественные параметры перебора грунта в условиях подземного строительства в городах при закрытом способе горностроительных работ. Среди таких факторов выделяются следующие: несоответствие диаметра резания наружному диаметру обделки, перемещения грунтового массива перед забоем, неполное заполнение тампонажным раствором заобделочного пространства, неполное заполнение пространства за оболочкой щита глинистым или медленно твердеющим тампонажным раствором или их отсутствие, человеческий фактор (низкая квалификация персонала). Коэффициент перебора устанавливается на основе предложенной эмпирической зависимости его значений от глубины заложения тоннеля. Экспериментальные данные позволили установить зависимости коэффициента перебора при разных глубинах заложения тоннеля, а также при диаметрах тоннелей от 4 до 10 м для тоннелепроходческого механизированного комплекса с активным пригрузом забоя. Практическое значение проведенных исследований состоит в установлении диапазона изменения значений эмпирического коэффициента – от 0,5 % (для щитов с условным диаметром 10 м) до 5 % (для щитов условным диаметром 4 м). Разработка организационных мероприятий и обоснование технологических решений по обеспечению сохранности существующих зданий в комплексе с научно-техническим сопровождением подземного строительства позволила примерно на 6 месяцев сократить срок проходки перегонов между станциями «Окская» и «Нижегородская» Некрасовской линии Московского метрополитена, а также и обеспечить экономию порядка 2,5 млрд руб.

Ключевые слова

подземное строительство, проходка, тоннели, щитовой комплекс, Herrenkneht, Robbins, геотехнический мониторинг, перебор грунта, коэффициент перебора грунта

Для цитирования

Konyukhov D.S. Analysis of mechanized tunneling parameters to determine the overcutting characteristics. *Mining Science and Technology* (*Russia*). 2022;7(1):49–56. https://doi.org/10.17073/2500-0632-2022-1-49-56

Introduction

Tunneling in urban conditions requires costly measures, in order to ensure the safety of existing buildings. On average there are up to 17–20 buildings per 1 km of Moscow Subway Lines under construction. Analysis and comparison of geotechnical monitoring data and results of geotechnical estimations for underground construction by cut-and-cover and tunneling methods in conditions of high-density urban area shows an unsatisfactory correlation between estimated and actual data. This can be described in the following way: insufficient geotechnical survey data; discrepancy between the accepted estimation model and the actual behavior of soil under load; insufficient qualification of construction workers; and overcutting.

Analysis of the geotechnical monitoring data and comparison with the results of estimates determining the effect of underground construction on buildings and structures in the surrounding area show that with regard to facilities of this kind constructed by cut-and-cover method (C&C) in excavations up to 9–12 m deep, the correlation between the estimated and actual data does not exceed 60 %. With regard to the construction of subway facilities in excavations up to 35 m deep, this correlation amounted to up to 32 %. In the case of tunneling using tunnel boring machines with a nominal diameter of 6 m, the figure is 70 %, while using tunnel boring machines with nominal diameter of 10 m – 7 %. This data testifies to the necessity of improving both the estimation methods and the geotechnical monitoring techniques [2–4]. The main reasons for unsatisfactory convergence of the geotechnical estimations and actual geotechnical monitoring data were identified in earlier studies [5–7].

When modeling the tunneling method of construction, an important parameter, depending on the construction techniques, is overcutting. This design parameter is set during the modeling of soil mass strains as a characteristic of tunneling. It is equal to the ratio of the excavated area within the limits of the tunnel contour to the tunnel cross-sectional area [8].

eISSN 2500-0632
https://mst.misis.ru/

It has been shown in historical studies that overcutting in the process of tunneling was caused by the following factors [9, 10]:

1. Cutting diameter mismatch with the lining outside diameter. In the case of using TBM with an external cutting tool (typical for majority of modern TBMs applying earth pressure balanced tunneling) rotor diameter is 3–5 % larger than the tunnel lining diameter on average.

2. Displacement of soil mass in front of the face. This factor is characteristic first of all for TBMs not performing earth pressure balanced tunneling, as well as in case of overcutting.

3. Overcutting may also occur due to human factor, i.e. insufficient personnel training.

4. Incomplete filling of beyond-shield voids with grouting mortar.

One more factor should be added to this list:

5. Lack of filling or incomplete filling of beyond-shield voids with clay mortar or slow-curing grouting mortar.

All the above factors indicate that overcutting leads to process strains of the surface [11].

Models for determining the overcutting coefficient in mechanized tunneling

The volume of soil loss (overcutting coefficient V_L) is commonly defined as the ratio of the surface subsidence area V_s to the cross-sectional area of the tunnel F_t:

$$V_L = \frac{V_s}{F_t} 100\%. \qquad (1)$$

The key points in predicting the overcutting coefficient were outlined in earlier studies [9]. It was shown later that V_L can be determined only on the basis of field observation data, while for weak soil the value of soil losses does not exceed 2 % [12]. In [13], data is given for the dependence of V_L on the tunnel diameter, its depth and geotechnical conditions of the construction of tunnels with diameter up to 4 m at a depth up to 8.1 m.

Other studies [14, 15] show that during driving by TBM (with soil face balance weight) 9.15 m in diameter in water-saturated sand overlain by marl, V_L does not exceed 0.3-0.5 %. The existing regulatory documents in Russia[1] regulate the values of overcutting coefficient for tunnel construction up to 4 m in diameter in the range of 1.5 to 5.5 % depending on the type of soil in the face. These values are significantly higher than V_L, values obtained by foreign researchers [12, 14, 15].

When constructing subway tunnels by mechanized tunneling method in conditions of high-density urban area the following needs to be taken into account:

– tunnel depth is generally no less than 1*d* (*d* is the tunnel diameter) with sand or clay soils in the tunnel crown;

– TBMs with soil face balance weight are used mainly in subway soft ground tunneling (among all the Moscow TBM fleet, there are 24 TBMs with soil face balance weight and one with bentonite face balance weight). This assumes squeezing grouting mortar through the tail part of the casing simultaneously with TBM (shield) advancement.

Thus, the review of data from earlier studies allows it to be concluded that the overcutting coefficient depends on the following factors when applying mechanized tunneling:

– relative depth of tunneling h/d;

– cohesion of soil;

– ratio of the clearance between the cutting tool and the tunnel lining to the tunnel diameter.

Digital estimation models of technological processes and the rock (soil) mass conditions for designing TBM tunneling in urban areas are performed in PLAXIS, GEOWALL, COMSOL and other software systems [16, 17]. Determining the overcutting parameters while tunneling is also of great importance for improving reliability of the digital models.

Findings of geotechnical monitoring during main line tunneling

Let us consider the findings of monitoring during the tunneling of the Nekrasovskaya Line and the Western segment of the Great Ring Line (GRL) of the Moscow Subway as an example.

The tunneling of Western segment of the GRL was performed by "ROBBINS" TBM with soil balance weight, with a shield blade (work tool) diameter d_r of 6.6 m and tunnel diameter *d* of 6.3 m.

ζ factor characterizing the ratio of the clearance between the cutting tool and the tunnel lining to the tunnel diameter

$$\zeta = \frac{d_r - d}{d} \qquad (2)$$

is equal to 0.048.

The tunneling was carried out in water-saturated fine/medium-grained sand.

[1] SP 249.1325800.2016 Underground utility systems. Design and construction by tunneling and C&C methods

eISSN 2500-0632
https://mst.misis.ru/

The empirical overcutting coefficient V_{le} was calculated by the backward analysis method on the basis of the following formula:

$$V_{le} = \frac{s_f i \sqrt{2\pi}}{S}, \tag{3}$$

where s_f is actual subsidence in the observation point located at the distance i from the axis of the tunnel; S is the face area.

The reduced (equivalent) overcutting coefficient V_{Lp} was calculated through the following expression:

$$V_{Lp} = \frac{\sum_{i=1}^{n} V_{lp_i} S_i}{S}, \tag{4}$$

where S_i is the face area with overcutting coefficient V_{lp_i}.

The results of the overcutting coefficient calculation in the form of characteristic curves

$$V_L = f\left(\frac{h}{d_r}, \xi\right) \tag{5}$$

are shown in Figures 1 and 2.

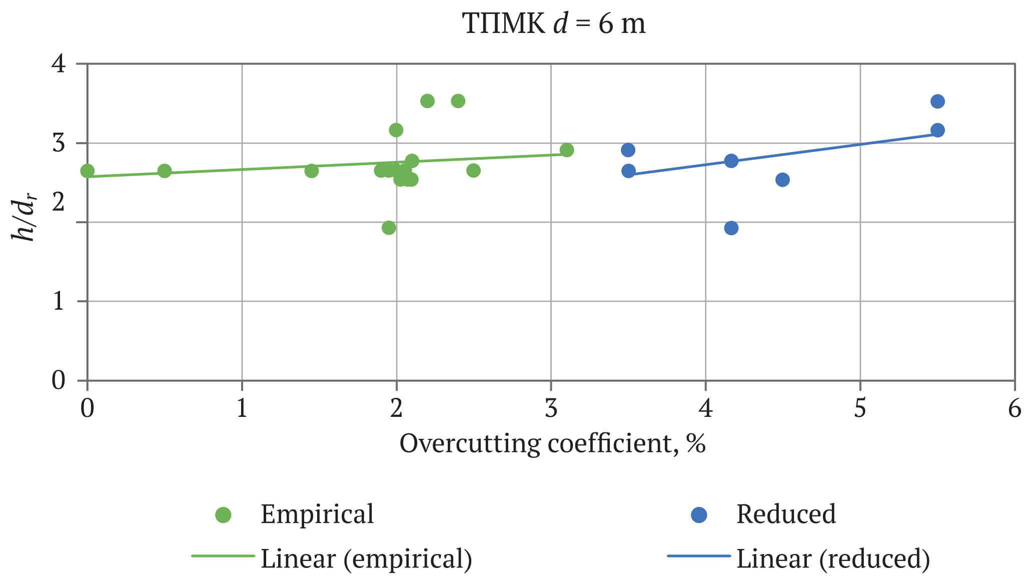

Fig. 1. Dependence of the empirical V_{le} and reduced V_{lp} overcutting coefficients on the relative depth of tunneling h/d_r with TBM with a nominal diameter of 6 m

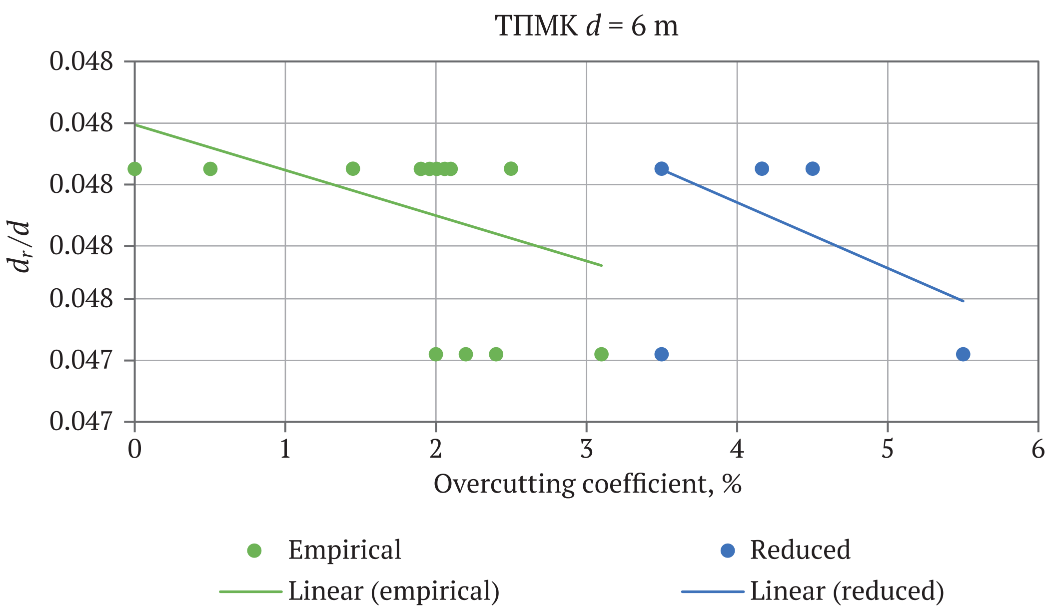

Fig. 2. Dependence of the empirical V_{le} and reduced V_{lp} overcutting coefficient on ζ factor for tunneling using TBM with nominal diameter of 6 m

During the construction of Nekrasovskaya Subway Line from Okskaya Ulitsa station to Stakhanovskaya Ulitsa station, a Herrenkneht TMB EPB with soil face balance weight and the work tool diameter d_r = 10.69 m was used. The diameter of the tunnel d = 10.3 m, and factor ζ = 0.038. The running (main line) tunnels are mainly located in Upper Jurassic clay, while the crown reveals Quaternary sediments almost throughout the whole length of the tunnels.

In the next segment from Kosino station to Yugo-vostochnaya station, tunneling was carried out using a Herrenkneht TMB EPB with soil face balance weight and work tool diameter d_r = 10.82 m. Diameter of the tunnel d = 10.5 m, and factor ζ = 0.03. The maximum additional subsidence of the building under whose foundations the TBM passed at a depth of 13 m, was 6.7 mm [18].

The values of empirical overcutting coefficient at these segments varied from 0.5 to 1.25 %, depending on the depth of tunneling and geotechnical conditions in the tunnel face.

Figs. 3 and 4 show generalized dependences (5) for tunnel boring machines with nominal diameter of 4–10 m.

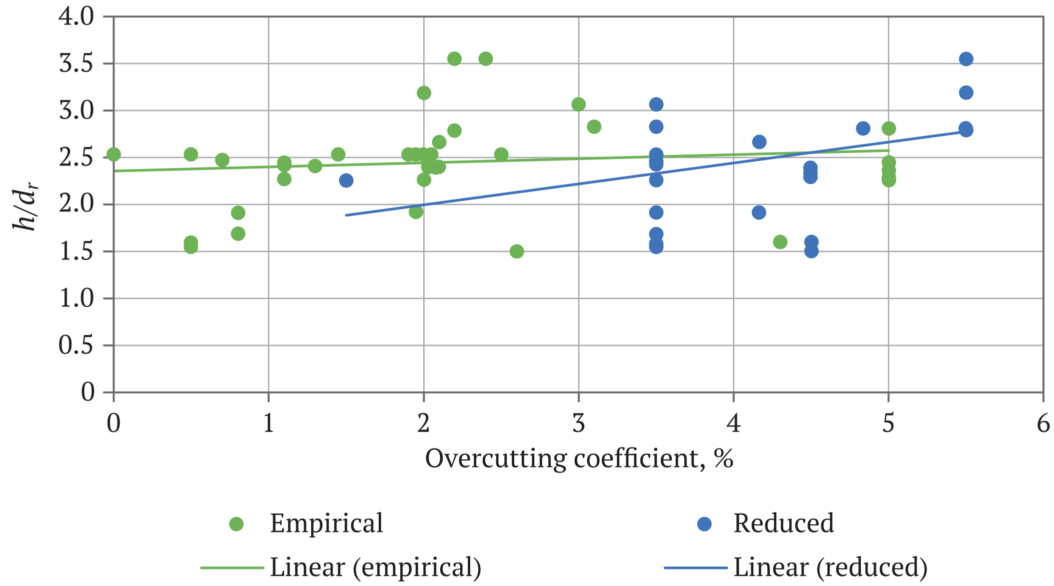

Fig. 3. Generalized dependence of the empirical V_{le} and reduced V_{lp} overcutting coefficients on the relative depth of tunneling h/d_r when tunneling at the diameter of 4–10 m using TBM with soil face balance weight

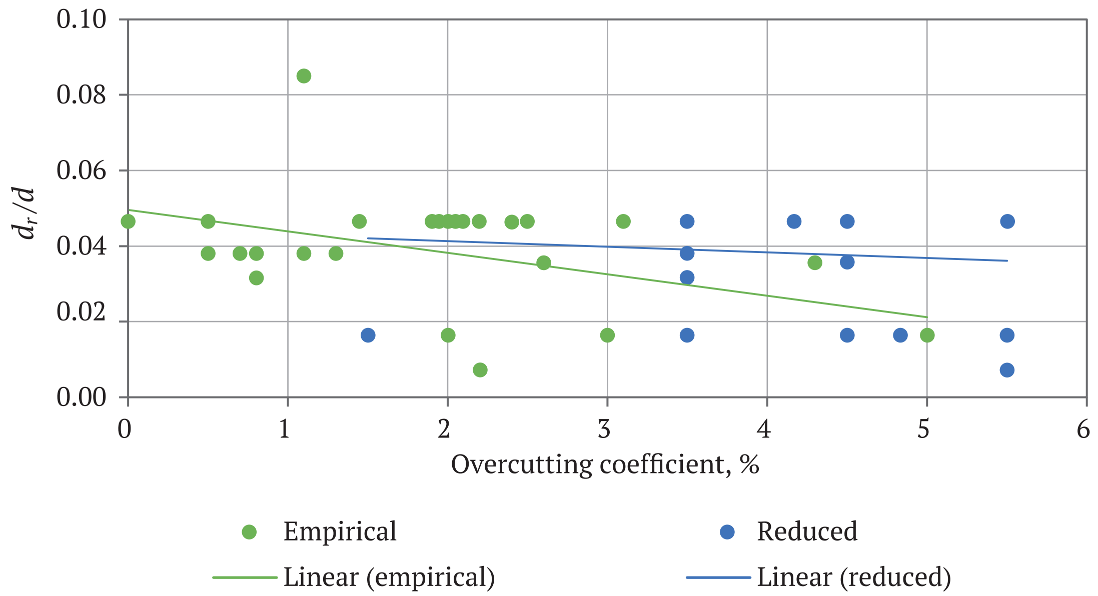

Fig. 4. Generalized dependence of the empirical V_{le} and reduced V_{lp} overcutting coefficients on ζ factor when tunneling at a diameter of 4–10 m using a TBM with soil face balance weight

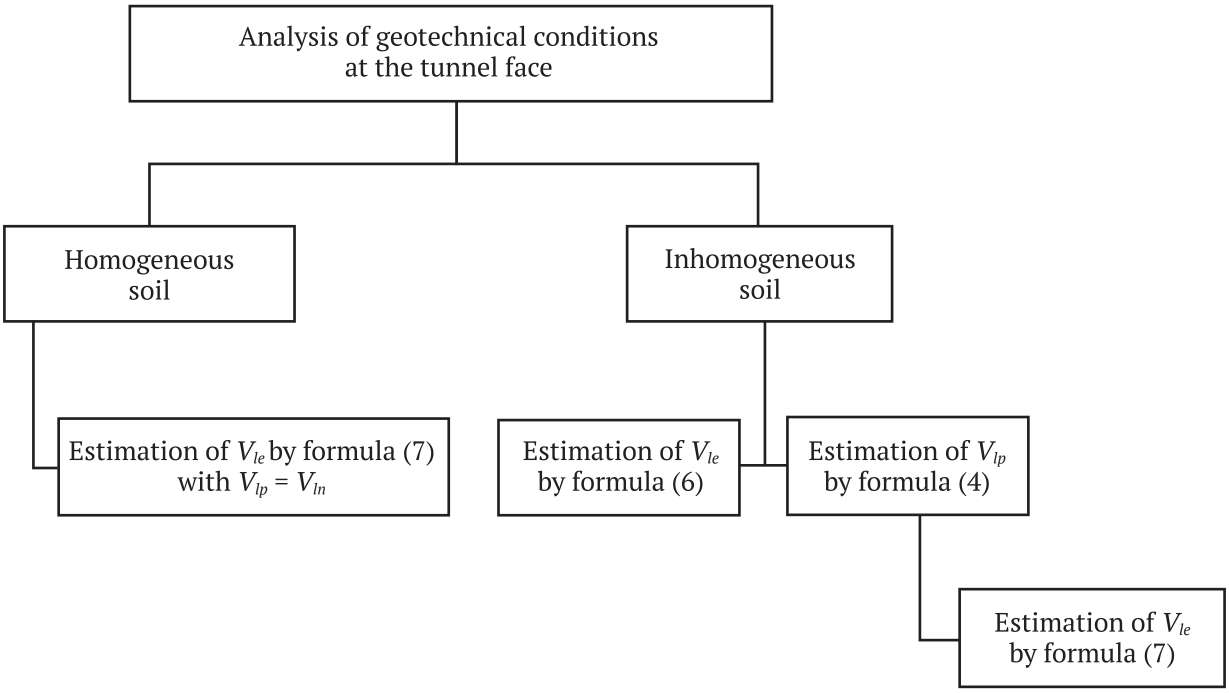

Fig. 5. Pattern of empirical overcutting coefficient V_{le} computation

It should be noted that the ζ factor is not a sufficiently reliable characteristic due to the constancy of ζ values for different types of TBMs. At the same time the value of overcutting coefficient depends on the TBM diameter.

The empirical values of the overcutting coefficient for TBMs with a nominal diameter of 4–10 m were determined by the backward analysis method. The empirical coefficient values vary in the range from 0.5 % (for TBM with nominal diameter of 10 m) to 5 % (for TBM with nominal diameter of 4 m). The characteristic curves shown in Fig. 3 allow overcutting coefficient to be calculated depending on the relative depth of tunneling (in mixed soils) according to the following empirical expression:

$$V_{le} = 0,49\frac{h}{d_r} + 0,96. \qquad (6)$$

A similar dependence between the empirical and reduced overcutting coefficients is as follows:

$$V_{le} = 0.69V_{lp} + 0.53 \qquad (7)$$

this allows, based on the normative values from SP 249.1325800.2016 “Underground utilities. Design and construction by tunneling and C&C” (Order of the Russian Ministry of Construction dated July 8, 2016 No. 485/pr), the empirical overcutting coefficient to be calculated, taking into account geotechnical conditions along the tunneling route.

Based on research findings, a pattern of the empirical overcutting coefficient V_{le} computation was proposed (as shown in Fig. 5). This pattern provides for computation of overcutting coefficient based on different dependencies. It takes into account the degree of soil homogeneity, determined on the basis of analysis of geotechnical conditions in the tunnel face.

Conclusion

The empirical values for overcutting coefficient in the case of TBMs with a nominal diameter of 4–10 m were determined by the backward analysis method. The empirical coefficient values vary in the range from 0.5 % (for TBMs with nominal diameter of 10 m) to 5 % (for TBMs with nominal diameter of 4 m). The computation pattern shown on Fig. 5 allows for the coefficient of overcutting at tunnel boring using TBMs with face balance weight to be determined, while taking into account the TBM diameter and the types of soil composing the tunnel face (homogenous/inhomogeneous).

The proposed method was successfully implemented during the construction of the Nekrasovskaya and Great Ring Lines of the Moscow Subway. Optimization of measures to ensure the safety of the existing buildings in conjunction with the scientific and technical support of underground construction allowed the time of tunneling between the Okskaya and Nizhegorodskaya stations of the Nekrasovskaya Line of the Moscow Subway to be shortened by about 6 months, as well as providing savings of about 2.5 billion rubles.

References

1. Potapova E.V. Typology of metro structures for the tasks of geotechnical risk classification. *Mining Science and Technology (Russia)*. 2021;6(1):52-60. (In Russ.) https://doi.org/10.17073/2500-0632-2021-1-52-60

2. Mangushev R.A., Sapin D.A., Kirillov V.M. Effect of finite element type on ultimate subsidence of neighboring building foundations in numerical modeling of shoring of excavation. In: *Soil Mechanics in Geotechnics and Foundation Engineering: Proceedings of the International Research-to-Practice Conference*. Novocherkassk. 2018. P. 708–718 (In Russ.)

3. Kulikova E.Yu. Methodical principles for improving the ecological and technological reliability of urban underground structures. *Mining Informational and Analytical Bulletin*. 2020;(6–1):176–185. (In Russ.) https://doi.org/10.25018/0236-1493-2020-61-0-176-185

4. Nikiforova N.S., Konnov A.V. Predicting deformations of the surrounding buildings foundations with regard to protective measures. *Soil Mechanics and Foundation Engineering*. 2020;(6):7–12. (In Russ.)

5. Gong Zh., Li Y., Liu M., Tang C. A case study for large excavation constructed by open cutting with under mining method in Xuzhou, China. In: *World Tunnel Digital Congress and Exhibition (WTC) 2020 and the 46th General Assembly*. 11–17 September 2020. Kuala Lumpur, Malaysia. 2020. Pp. 721–724.

6. Hewitt P., Suthagaran V. Dealing with the challenges of ground response on deep urban excavations adjacent to underground transport infrastructure in Australia. In: *World Tunnel Digital Congress and Exhibition (WTC) 2020 and the 46th General Assembly*. 11–17 September 2020. Kuala Lumpur, Malaysia. 2020. Pp. 801–806.

7. Konyukhov D.S., Polyankin A.G., Kazachenko S.A. An analysis of the factors which influence geotechnical calculations and monitoring data agreement. In: *Proceedings of International Tunneling Symposium in Turkey. Challenges of Tunneling*. Istanbul, Turkey. 2017. Pp. 51–63.

8. Ustinov D.V. Impact of the enclosing massif model selection over the results of subway tunnels excavation modelling. *Geotechnics*. 2018;(5–6):34–50. (In Russ.)

9. Lee Ch.-J., Wu B.-R., Chiou Sh.-Y. Soil Movements Around a Tunnel in Soft Soils. In: *Proceedings of the National Science Council, Republic of China (A)*. China. 1999;23(2):235-247.

10. Bourget A.P.F., Chiriotti E., Patrinieri E. Evolution of risk management during an underground project's life cycle. In: Peila D., Viggiani G., Celestino T. (eds.). *Tunnels and Underground Cities: Engineering and Innovation meet Archaeology, Architecture and Art.* London: Taylor & Francis Group; 2019. Pp. 4375–4385. https://doi.org/10.1201/9780429424441-463

11. Mangushev R.A., Nikiforova N.S. *Process subsidence of buildings and structures in the underground construction affected zone*. Moscow: ASV Publishing House; 2017. 168 p. (In Russ.)

12. Discussion sessions. Session 2: Bored tunnels: Construction. In: Bakker K.J., Bezuijen A., Broere W., Kwast E.A. (eds.) *Proc. of the 5th International symposium "Geotechnical Aspects of Underground Construction in Soft Ground"*. Netherlands, 2005. Pp. 945–950.

13. Tupikov M.M. *Peculiarities of straining soil mass and structures during construction of shallow utility tunnels in urban conditions*. [Ph.D. thesis in Engineering Science]. Moscow: MGUPS Publishing House; 2011. 24 p. (In Russ.)

14. Mahdi S., Gastebled O., Khodr S. Back analysis of ground settlements induced by TBM excavation for the north extension of Paris metro, line 12. In: Peila D., Viggiani G., Celestino T. (eds.). *Tunnels and Underground Cities: Engineering and Innovation meet Archaeology, Architecture and Art.* London: Taylor & Francis Group; 2019. Pp. 2606–2615. https://doi.org/10.4324/9781003031635-6

15. Mahdi S., Gastebled O., Ningre H., Senechal M. Grand Paris Express, Line 15 East – predictive damage analysis combining continuous settlement trough modelling, risk management, automated vulnerability checks and visualization in GIS. In: Peila D., Viggiani G., Celestino T. (eds.). *Tunnels and Underground Cities: Engineering and Innovation meet Archaeology, Architecture and Art.* London: Taylor & Francis Group; 2019. Pp. 5855–5864. https://doi.org/10.4324/9781003031871-9

16. El Houari N., Allal M.A., Abou Bekr N. Numerical simulation of the mechanical response of the tunnels in the saturated soils by Plaxis. *Jordan Journal of Civil Engineering*. 2011;5(1):9–31. URL: https://jjce.just.edu.jo/issues/show_paper.php?pid=171

17. Voznesensky A. S., Kidima-Mbombi L. K. Formation of synthetic structures and textures of rocks when simulating in COMSOL Multiphysics. *Mining Science and Technology (Russia)*. 2021;6(2):65–72. (In Russ.) https://doi.org/10.17073/2500-0632-2021-2-65-72

18. Ter-Martirosian A. Z., Kivliuk V. P., Isaev I. O., Shishkina V. V. Determination of the actual excess excavation ratio (section “Kosino” – “Yugo-Vostochnaya”). *Construction and Geotechnics*. 2021;12(2):5–14. https://doi.org/10.15593/2224-9826/2021.2.01

Information about the author

Dmitrii S. Konyukhov – Cand. Sci. (Eng.), Assoc. Professor, Head of the Department of Scientific Support for Construction, Mosinzhproekt JSC, Moscow, Russian Federation; ORCID 0000-0001-8635-232X, Scopus ID 6507981388; e-mail gidrotehnik@inbox.ru

Received 18.12.2021
Revised 05.01.2022
Accepted 01.02.2022

POWER ENGINEERING, AUTOMATION, AND ENERGY PERFORMANCE

Research article

https://doi.org/10.17073/2500-0632-2022-1-57-65

Automatic control system for walking dragline excavator digging

L.D. Pevzner SC ✉, **N.A. Kiselev**
Russian Technological University MIREA, Moscow, Russian Federation
✉ *lpevzner@msmu.ru*

Abstract
This paper presents the results of the development of automatic control systems for walking dragline excavator digging process. The process enables operational productivity to be enhanced through optimizing digging process. This also prevents extreme loads on machinery and hoist cable deflection. The paper also describes mathematical models of the electric drives of the main excavator machinery which form the bucket motion and the model of cable length change. Further the study will analyse the tructure of the control system and the automatic digging algorithm. Computer modeling findings are also described to confirm the operability of the automatic digging algorithm. Computer simulation of the processes in electric drives of main machinery of a walking dragline in digging operations was performed by means of SimInTech software. The automatic control system optimizes digging trajectory with very fast penetration with permissible overregulation following digging at a constant cut depth. The integrated system of dragline operation process control is practically independent due to the following factors: the automatic digging control system in combination with automatic systems for transporting the loaded bucket to dump and the empty bucket to the face; the automatic main machinery overload protection systems; and the system of control over safe bucket movement in the dragline working space

Keywords
mining machinery, walking dragline excavator, bucket, operation, digging, mathematical models, automation, electric drive, algorithm, control, controller

For citation
Pevzner L.D., Kiselev N.A. Automatic control system for walking dragline excavator digging. *Mining Science and Technology* (*Russia*). 2022;7(1):57–65. https://doi.org/10.17073/2500-0632-2022-1-57-65

ЭНЕРГЕТИКА, АВТОМАТИЗАЦИЯ И ЭНЕРГОЭФФЕКТИВНОСТЬ

Научная статья

Система автоматического управления процессом черпания шагающего экскаватора-драглайна

Л.Д. Певзнер SC ✉, **Н.А. Киселев**
Российский технологический университет – МИРЭА, г. Москва, Российская Федерация
✉ *lpevzner@msmu.ru*

Аннотация
Актуальность исследований, результаты которых составляют основу систем автоматического управления рабочей операцией черпания шагающего экскаватора-драглайна, обусловлена необходимостью повышения производительности машины и снижением предельных нагрузок на механизмы и канатные системы. Анализу подвергается система автоматического управления рабочей операцией черпания шагающего экскаватора-драглайна, позволяющая обеспечить повышение его эксплуатационной производительности за счет приближения процесса черпания к рациональному.
На основе методов математического моделирования систем электропривода основных механизмов экскаватора-драглайна составлены имитационные математические модели, которые описывают движение ковша и канатных систем. Результаты компьютерного модельного исследования, выпол-

ненные программными средствами SimInTech, подтвердили работоспособность предложенного алгоритма автоматического черпания.
Разработанная система автоматического управления операцией черпания позволяет приблизить траекторию черпания к оптимальной, обеспечивая предельно быстрое заглубление с допустимым перерегулированием и последующим равномерным черпанием с постоянной толщиной срезаемой стружки. Показатели качества управляемого процесса черпания в породах с удельным сопротивлением k_p = 1,45 ± 0,45 кг/см² и k_p = 3,35 ± 0,75 кг/см² практически совпадают: перерегулирование в первом случае 7,2 %, во втором – 10,4 %, время регулирования в первом случае 4 с, во втором – 3,5 с.
Разработанная система автоматического управления операцией черпания вместе с автоматическими системами транспортирования груженого ковша в отвал и порожнего ковша в забой, системами автоматической защиты от перегрузки главных механизмов, системой контроля безопасного движения ковша в рабочем пространстве драглайна позволяют повысить уровень автоматизации экскаватора-драглайна и его производительность

Ключевые слова

горная машина, шагающий экскаватор-драглайн, ковш, операция, черпание, автоматизация, математические модели, электропривод, алгоритм, управление, регулятор

Для цитирования

Pevzner L.D., Kiselev N.A. Automatic control system for walking dragline excavator digging. *Mining Science and Technology* (*Russia*). 2022;7(1):57–65. https://doi.org/10.17073/2500-0632-2022-1-57-65

Introduction

A walking dragline excavator is a highly effective mining machine with great technological capabilities. It is widely used in the mining industry for stripping via a non-transport process flow sheet applicable in open-cut mining of such minerals as: coal; shale; ores of ferrous and nonferrous metals; gold; and raw materials for chemical industry [1, 2].

The experience of operating these machines at coal mines in Russia over a long period shows that walking dragline efficiency does not exceed 70 %.

High efficiency of walking dragline excavator operation can be ensured by automating the following control processes: main working operations for transporting loaded buckets to the dump and empty bucket to the face; automation of digging process, through automatic limitation of dynamic loads in electromechanical systems; and providing safe control of excavation process [3–5].

Research aimed at the development of automatic control systems for walking dragline excavator digging process is relevant, since such systems will allow operational productivity to be enhanced through optimizing digging process, thus avoiding extreme loads on machinery and hoist cable deflection.

1. Mathematical model of digging operation

Mathematical modeling of walking dragline excavator processes is a first and important stage to resolving the question of creating algorithms and control systems for the individual devices/units and the machine as a whole [6, 7].

In order to compile a mathematical model of digging, it was assumed that drag cables are weightless and non-extensible, and that the rate of change in their length is constant. In the process of rock mass digging using a dragline excavator bucket, a resistance force F_c, arises. This can be represented as a sum of three forces F_1, F_2, F_3 – a bucket friction force on soil; cutting resistance force; and resistance force to movement of the rock mass dozing capacity. The bucket friction force on soil is defined by the expression $F_1 = \beta N$, where β – is the bucket friction on soil coefficient, and N is the normal support response. Cutting resistance force is determined by the expression $F_2 = k_p B_b h$, where k_p – specific resistance of rock mass to cutting, B_b – width of bucket, h – bucket depth of cut.

Figure 1 shows bucket and forces applied to it.

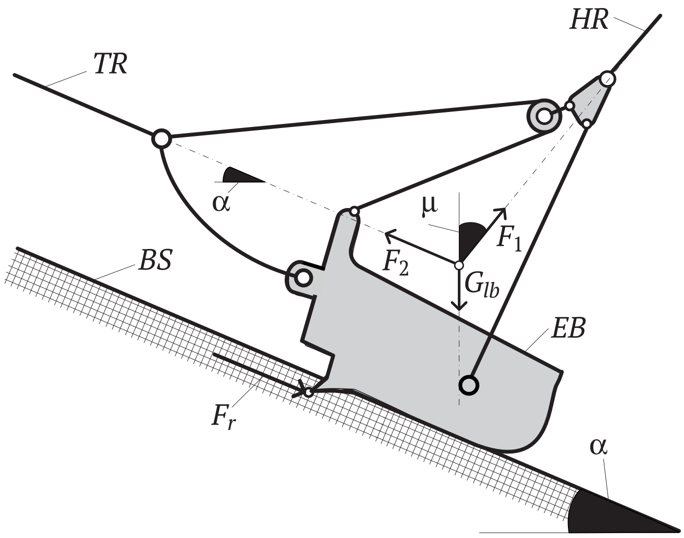

Fig. 1. Diagram of forces applied to the bucket:
HR – hoist cables; *TR* –drag cables; *BS* – face surface;
EB – excavator bucket; F_r – digging resistance forces;
F_1 – tension of hoist cables; F_2 – tension of drag cables;
G_{lb} – weight of loaded bucket; α – angle of face slope;
μ – deviation of drag cables from vertical direction

The diagram of forces applied to the bucket (Fig. 1) was used for further calculation. This was used to derive the equations of bucket movement dynamics in the axes of hoist and drag cables length $\{l_1, l_2\}$.

$$m_{lb}(t)\ddot{l}_1(t) = F_1(t) - G_{lb}(t)\cos\mu - (F_2(t) + F_r(t))\sin(\alpha - \mu),$$
$$m_{lb}(t)\ddot{l}_2(t) = F_2(t) - G_{lb}(t)\sin\alpha - (F_1(t) + F_r(t))\sin(\alpha - \mu), \quad (1)$$

where $m_{lb}(t)$ is the mass of the bucket together with the contained rock mass.

2. Mathematical model of electric drives of hoisting and traction mechanisms

The electric drives of the hoisting and traction mechanisms of ESh 20.90 walking excavator have the same structure [8, 13]: generator – motor (G-M) with thyristor excitation; and control system according to the diagram of double-loop slave regulation with power circuit current controller and generator voltage controller.

The mathematical model[1] of the hoisting mechanism–bucket–traction mechanism system was developed in accordance with the flowchart shown in Fig. 2, under the conditions of known assumptions [9, 14].

A system of equations presents the electric drive mathematical model for any of the mechanisms of hoisting or traction, the input of which is $U_t(t)$ – voltage of the command device for setting speed of changing length of the corresponding cable, and the output $\omega(t)$ – is the motor shaft speed (2).

$$\begin{aligned}
&u_{VR}(t) = \mathrm{sat}(U_t(t) - k_1 e(t);\, k_{VR},\, u^*_{VR}),\\
&u_{CR}(t) = \mathrm{sat}\left(u_{VR}(t) - k_4 I(t) + k_5\int_0^t (u_{VR}(t) - k_4 I(t))\,dt;\, k_{CR},\, u^*_{CR}\right),\\
&u_{MA}(t) = k_{MA} u_{CR}(t),\\
&T_{TC}\dot{u}_{TC}(t) + u_{TC}(t) = k_{TC}(t) u_{MA}(t),\\
&T_G \dot{u}_G(t) + u_G(t) = k_G u_{TC}(t),\\
&T_{AC}\dot{I}(t) + I(t) = k_{AC}(u_G(t) - C_E\omega(t)),\\
&J\dot{\omega}(t) = C_M I(t) - M_R.
\end{aligned} \quad (2)$$

[1] Technical documentation for ESH 20.90. URL: https://maxi-exkavator.ru /excapedia /technic/esh-2090_omz

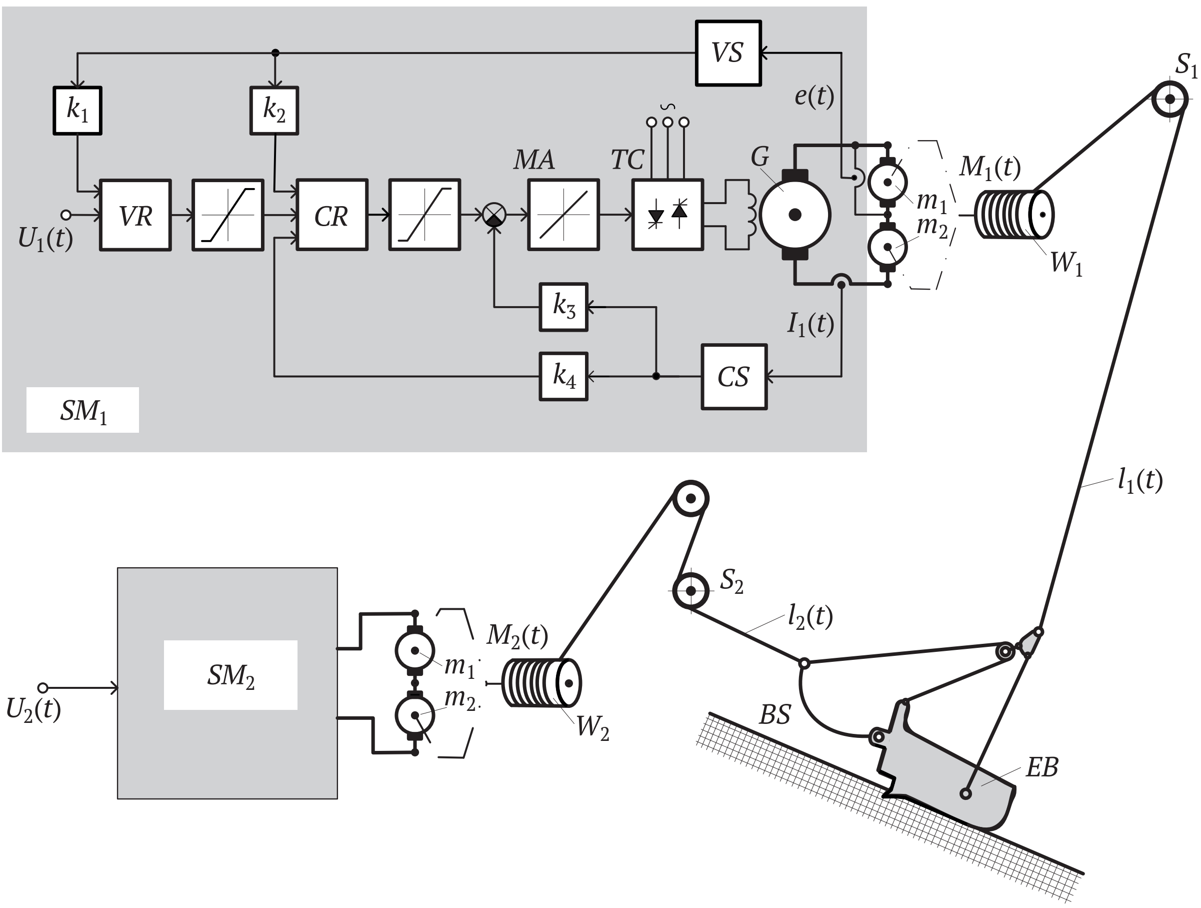

Fig. 2. Schematic diagram of the hoisting mechanism-bucket-traction mechanism system: S_1 – fairlead sheaves; S_2 – pointing units; l_1 – hoist cables; l_2 – drag cables; EB – excavator bucket; BS – face surface; W_1 – hoisting mechanism winch; W_2 – traction mechanism winch; SM_1, SM_2 – power control system for hoisting and traction motors, respectively; CS – hoisting drive current sensor; VS – generator voltage sensor; VR – voltage controller; CR – current controller; MA – matching amplifier; TC – thyristor converter; k_1, k_2, k_3, k_4 – loop gain blocks; m_1, m_2 – motors; M_1, M_2 – driving torques of hoisting and traction, respectively; U_1, U_2 – hoisting and traction motions assignments, respectively

eISSN 2500-0632
https://mst.misis.ru/

In these expressions:

$u_{VR}(t)$, $u_{CR}(t)$, $u_{MA}(t)$, $u_{TC}(t)$, $u_G(t)$ are the output signals of the voltage controller, current controller, matching amplifier, thyristor converter, and generator, respectively; u^*_{VR}, u^*_{CR} – threshold values of signals of voltage and current controllers; k_{VR}, k_{CR} – limiting controller transfer factors; T_{TC}, T_G, T_{AC} – response time of thyristor converter, generator, and armature circuit; k_1, k_4, k_5 – parameters of p-controller of voltage and PI-controller of current; k_{MA}, k_{TC}, k_G, k_{AC} – transfer factors of matching amplifier, thyristor converter, generator, and armature circuit; J – mass moment of inertia of mechanism, reduced to motor shaft; $I(t)$ – current of the motor armature circuits; C_E, C_M – design motor constants; M_R – resistance torque in drive, reduced to motor shaft.

We performed a synthesis procedure of the PI-controller for the inner circuit – current loop, by adjusting it to the modular optimum. The controller parameters and its transfer function

$$W_{CR}(s) = \frac{4.6s+1}{6.69s}.$$

were obtained using the ESH 20.90[2] excavator specifications.

The parameter of proportional (p) controller of voltage and its transfer function were defined according to the modular optimum synthesis procedure

$$W_{VR}(s) = 8.32.$$

[2] Some technical characteristics of walking dragline excavator ESh 20.90 used for obtaining transfer functions of its model driving media:

– transfer factor of thyristor excitation device $k_{TC} = 44{,}3V/V$;
– time response of thyristor excitation device $T_{TC} = 0{,}01s$;
– generator transfer factor $k_G = 14{,}0V/V$;
– generator time response $T_G = 4{,}6s$;
– motor armature circuit transfer factor $k_{AC} = 31{,}0\Omega^{-1}$;
– motor armature circuit time response $T_{AC} = 0{,}05s$;
– motor rotor and hoisting/traction system winch product of inertia reduced to motor shaft $J = 517Nm/A$;
– motor constructional constants $C_E = 8{,}64V/s$, $C_M = 8{,}64Nm/A$;
– current sensor transfer factor $k_{CS} = 0{,}0029V/A$;
– voltage sensor transfer factor $k_{VS} = 0{,}0081V/V$;
– thresholds of voltage and current controllers signals $10V$;
– stop motor armature current $I_{stop} = 3400A$;
– generator rated voltage $U^*_G = 1230V$; $U_{G_{nom}} = 1230$ V;
– nominal motor rotational rate $\omega^*_M = 70{,}6s^{-1}$;
– transfer ratio of hoisting/traction mechanism reducing gear $r = 22{,}53$;
– performance coefficient of hoisting/traction mechanism reducing gear $\eta = 0{,}9$;
– hoisting/traction mechanism winch barrel radius $r_W = 0{,}9m$;
– electromechanical time response of motor $T_M = 0{,}06s$;
– weight of empty bucket $G_b = 220$ kN;
– weight of loaded bucket (with rock mass) $G_{lb} = 480$ kN.

Technical documentation for ESh 20.90 https://maxi-exkavator.ru /excapedia /technic/esh-2090_omz

3. Digging operation modeling

The model of bucket movement in interaction with the face consists of the following: the model of traction and hoisting electric drives (2); the model of bucket movement while digging (1); and technical data of ESh 20.90 dragline excavator. The model structure is shown in Fig. 3.

3.1. Model studies of processes in electric drives of main machinery

SimInTech software was selected for computer simulation of key machinery (mechanisms') drives for a walking dragline excavator in the course of digging operations.

The modeling of processes of changing lengths of hoist and drag cables and processes in electric drives was performed on the basis of model representations (1), (2). The schematic diagrams of the computer models of the hoisting and traction electric drives and cable lengths changes are presented in Figs. 4 and 5.

The model parameters are taken from the specifications [11] for ESh 20.90 walking dragline excavator. The hoisting and traction electric drives use GPE-2500–750UZ generator with a rated voltage of 1200 V and MPE-1000-630UZ motors with the rated angular velocity of 70.6 s^{-1}.

Findings from the model studies shown in Fig. 6 show that the electric drive model run-up time amounted to 3 s. The steady-state rate of cable length change $v^{max} = 0.25$ ms^{-1} agrees with oscillograms of real curves of dragline electric drives run-up and braking, as presented in [12].

The model studies confirm the adequacy of the description of dynamic processes in electric drives and the kinematics of drag and hoist cables motion.

3.2. Modeling of digging process

The model studies of the digging process were performed according to schematic diagram in Fig. 3. The digging process is performed with a constant traction speed equal to 1ms^{-1}. The rational digging process is carried out either with maximum initial depth of cut or with a constant depth of cut.

In the first case, digging time is minimal, since maximum power of excavator traction and hoisting drives is used. However, this method can lead to locking of the traction drive and, just as importantly, to difficulties in subsequent digging due to the unevenness of the face profile.

In the second digging case, the face relief is processed evenly. The power of excavator drives is not used fully, the dynamic loads exclude the possibility of bucket locking.

The uniform bucket filling method was taken as a basis for the synthesis of the digging process control system, for which the adjustable value was the depth of cut.

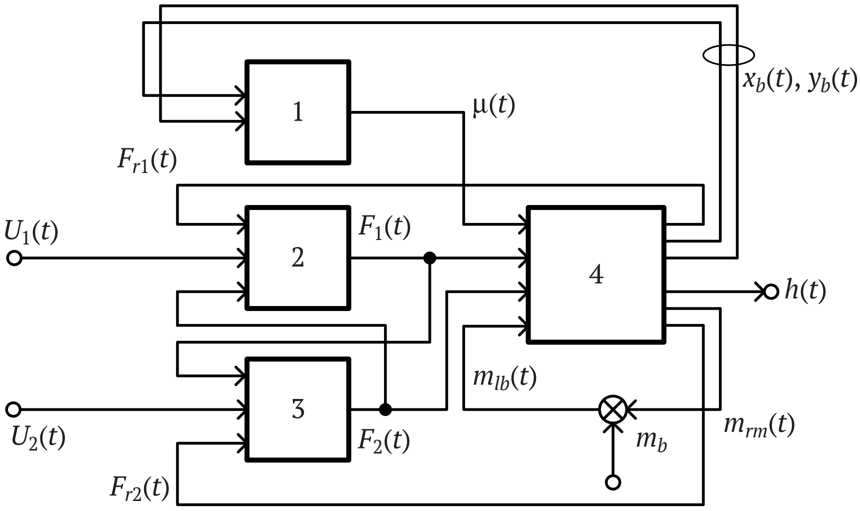

Fig. 3. The structure of model of bucket motion while digging:
block *1* – determination of angle μ; block *2* – model of hoisting mechanism; block *3* – model of traction mechanism; block *4* – model of face; $U_1(t)$, $U_2(t)$ – setting tensions of hoisting and traction drives; $x_b(t)$, $y_b(t)$ – current Cartesian coordinates of bucket position; μ – angle between hoist cables and *y*-axis; $h(t)$ – value of bucket penetration into the face; m_b, $m_{rm}(t)$, $m_{lb}(t)$ – mass of the empty bucket, rock mass in bucket, mass of loaded bucket, respectively; $F_1(t)$, $F_2(t)$ – force acting on bucket from traction and hoisting mechanisms, respectively; $F_{r2}(t)$ – force acting on bucket from the face along the axis of drag cable, including friction force, rock cutting resistance, resistance to movement of rock dozing capacity; $F_{rN}(t)$ – force normally acting on bucket from, including gravity force and rock cutting resistance

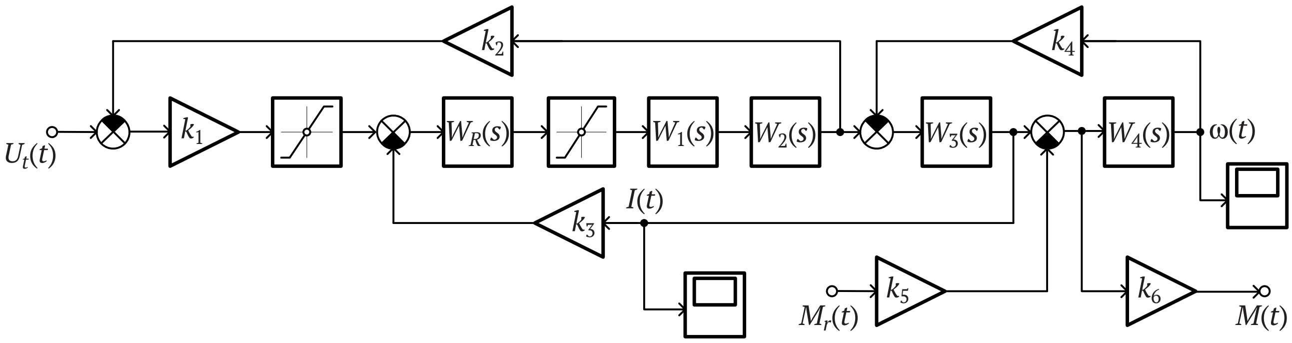

Fig. 4. Schematic diagram of electric drives model:
$U_t(t)$ – setting signal from master controller; coefficients: k_1 = 0.324, k_2 = 0.0081, k_3 = 0.0029, k_4 = 17.28, k_5 = 0.00231, k_6 = 389.769; transfer functions of link models: $W_1(s) = 44.3/(0.01s + 1)$, $W_2(s) = 14.0/(4.6s + 1)$, $W_3(s) = 31/(0.05s + 1)$, $W_4(s) = 0.032/s$; ω(t) – motor shaft speed; $M_r(t)$ – drag torque to motor shaft; $M(t)$ – hoisting/traction winch shaft torque

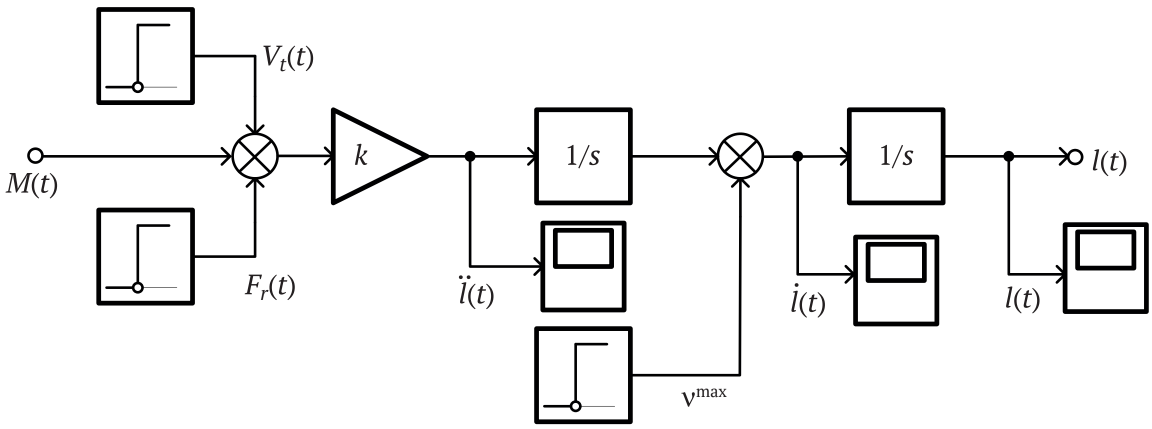

Fig. 5. Schematic diagram of the computer model of cable length change:
$V_t(t)$ – command signal for cable length change rate. For the maximum rate the command-apparatus signal is 10V; the maximum digging resistance force max $F_r(t)$ = 201,858.7234 кН; $M(t)$ – hoisting/traction winch shaft torque; factor $k = 3.2987e^{-06}$, v^{max} = 0.2497 мс$^{-1}$ (maximum cable length change rate); $\ddot{l}(t)$, $\dot{l}(t)$, $l(t)$ – current values of acceleration, rate, and length of hoist/drag cables, respectively

The automatic control system structure for the digging process is presented in Fig. 7.

The system investigated the possibility of using a PID-controller with parameters adjusted using the Ziegler-Nichols method: $k_P = 46$, $k_1 = 33.3$, $k_D = 15.19$. The setting of a small, 0.3 m, and significantly larger, 0.75 m depth of cuts was performed. The findings of the study are shown in Fig. 8. In both cases, unacceptable overregulation and long regulation time took place.

The use of the integral controller allowed a considerable decrease in overregulation. However, at the same time, the transition process became considerably longer.

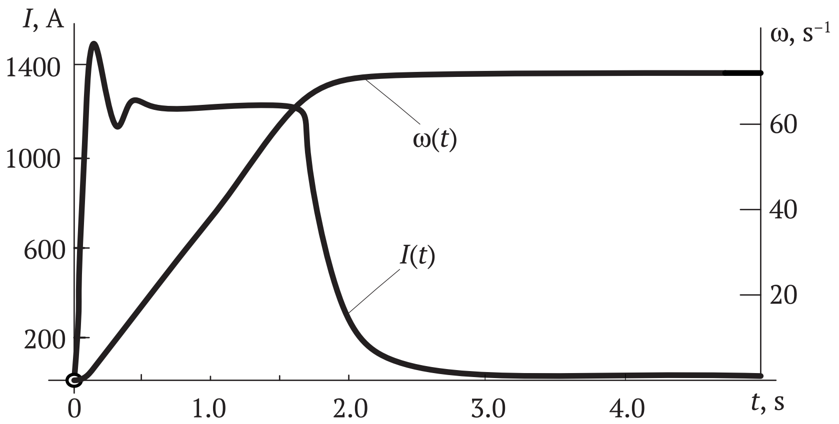

Fig. 6. Findings of simulation studies:
I – starting up to speed current, A; ω – motor shaft speed, s^{-1}

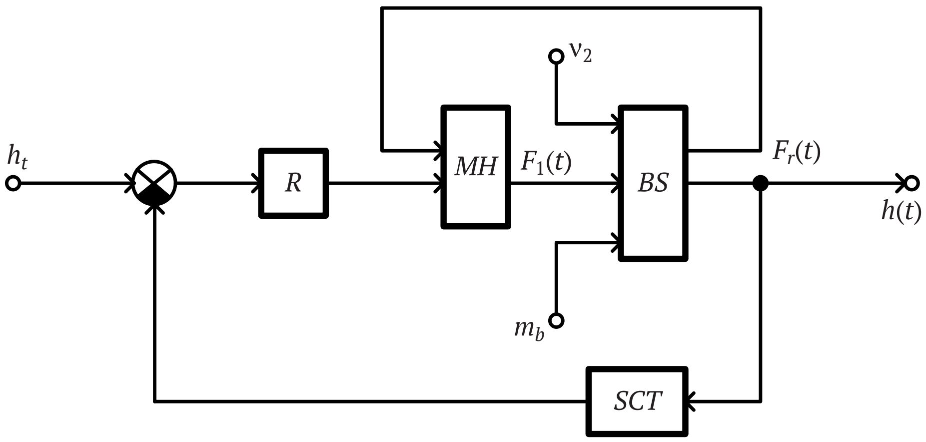

Fig. 7. Digging automatic control system structure:
block *R* – controller; block *MH*– model of hoisting mechanism; block *BS* – face model; $h(t)$ – current depth of cut; $F_r(t)$ – current resistance to rock mass (soil) cutting; *SCT* – depth of cut sensor; h_t – *assigned depth of cut*

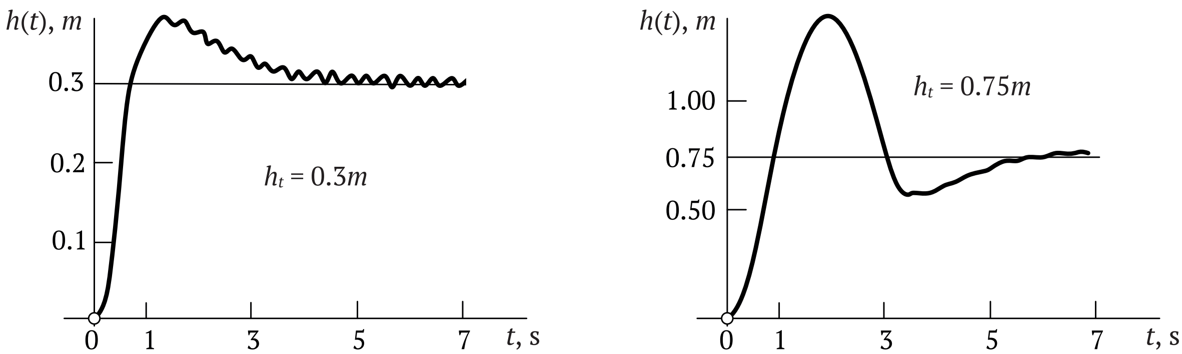

Fig. 8. Changing of cut depth at different parameters of three term controller (PID)

The studies showed inefficiency of linear controllers. Therefore, proceeding from the logic of real work of the operator, a two-step algorithm of forming control action on the traction drive is proposed.

The digging process is presented in two phases: digging, and movement of the bucket with constant cut depth. The second phase is provided by linear algorithm of three term controller, the first phase of digging is formed by non-linear algorithm

$$u(h;\ \mu)=\begin{cases}0, & \varepsilon \le h_0(\mu),\\ -10, & \varepsilon > h_0(\mu),\end{cases}$$

$$\varepsilon(t)=h_з-h(t).$$

In the expression, $h_0(\mu)$ – is the braking path when the bucket penetrates into soil. This depends on the hoist cable tension force, or more precisely, on the angle of inclination of the hoist cables.

The meaning of this algorithm is that the bucket's penetration into a rock (cutting) is performed with maximum force, and the movement should be terminated at the set depth. Thus, cut depth is a nonlinear function of time, while the rate of the depth of cut change is an almost linear function of time, as seen from Fig. 10.

Structural flowchart of automatic control system of walking dragline digging process is presented in Fig. 11.

Model research into the functionality of the digging process automatic control system process was carried out for the following case: weight of the empty bucket m_b = 22,000 kg; α = 30°; slope angle of the face; v_0 = 1 ms^{-1} – drag cable speed when digging; h_t = 0,85 m – assigned cut depth at specific resistance to digging k_p = 1.45±0.45 kg/cm^2; h_t = 0.45 m – assigned cut depth at specific resistance to digging k_p = 3.35±0.75 kg/cm^2.

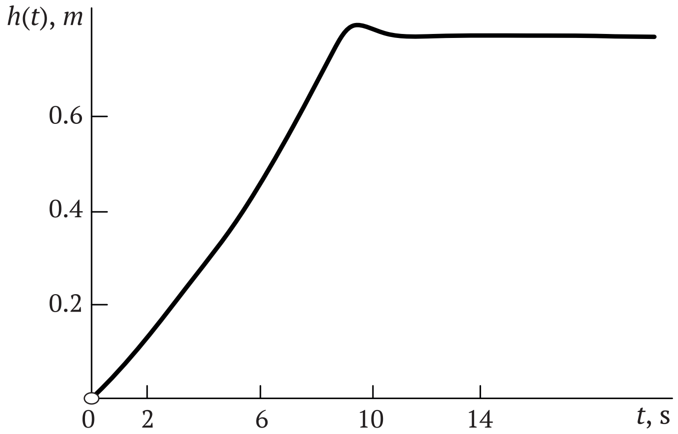

Fig. 9. Depth of cut changes with integral controller

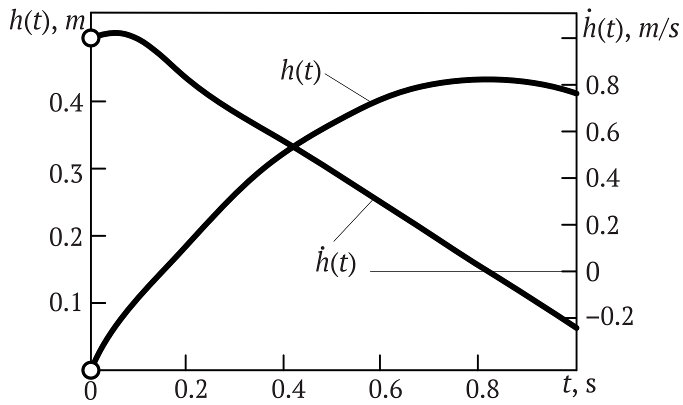

Fig. 10. Depth of cut change with non-linear controller: $h(t)$ – current cut depth; $\dot{h}(t)$ – rate of change in depth of cut

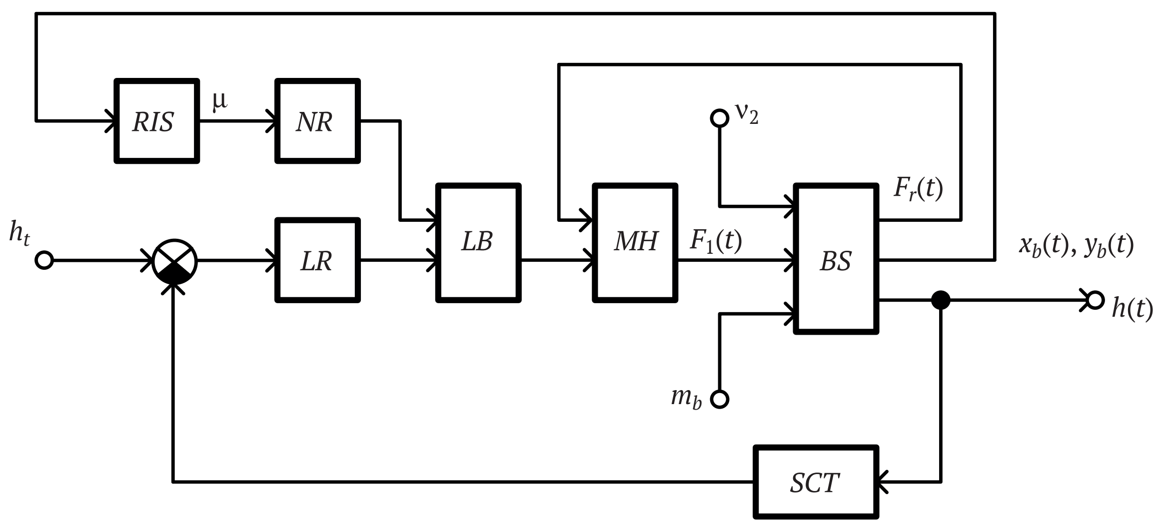

Fig. 11. Structural flowchart of automatic control system of walking dragline digging process: *LR* – linear controller; *NR* – non-linear controller; *LB* – logic block; *RIS* – hoist cables angle sensor; *MH* – hoisting mechanism model; *BS* – face model; *SCT* – depth of cut sensor; h_b – assigned depth of cut; $h(t)$ – current depth of cut; $x_b(t)$, $y_b(t)$ – current Cartesian coordinates of bucket; block $F_r(t)$ – current resistance to rock mass cutting

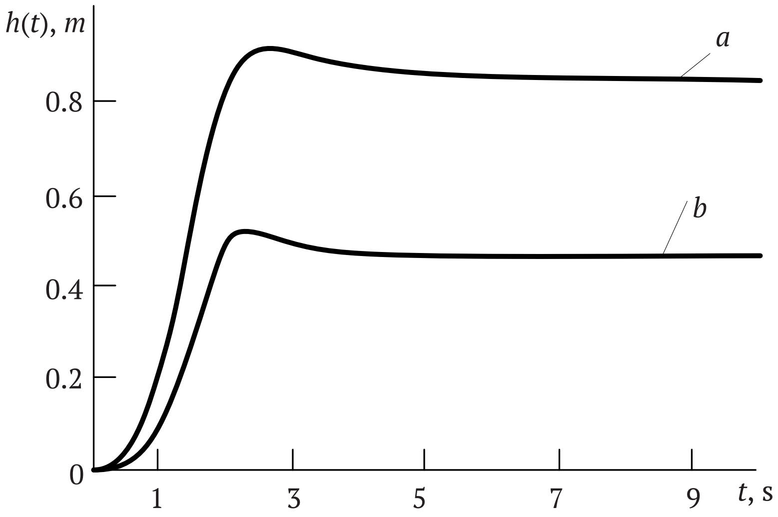

Fig. 12. Changing depth of cut in the process of automatic digging

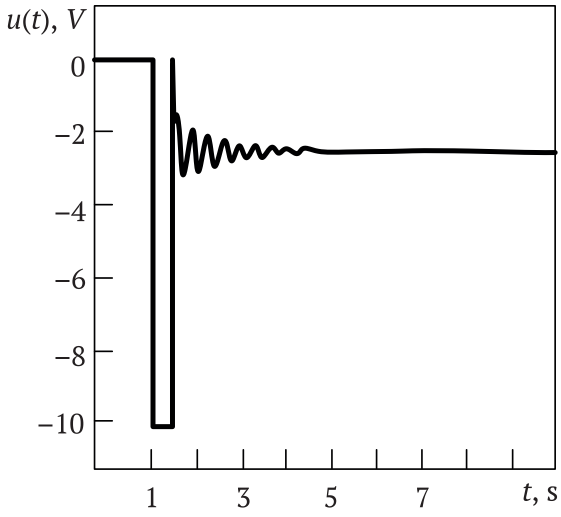

Fig. 13. Type of control action in the course of automatic digging

The simulation results are shown in the form of curves of depth of cut change in the process of automatic digging for the assignments *a*, *b*, respectively. They are presented below in Fig. 12. In addition, Fig. 13 shows a general view of the control action during automatic digging.

The quality indicators of the controllable digging process in rocks with specific resistance $k_p = 1.45 \pm 0.45$ kg/cm^2 and $k_p = 3.35 \pm 0.75$ kg/cm^2 are almost identical. Overregulation in the first case is 7.2 %. In the second it is 10.4 %. Control time in the first case is 4 s, in the second, 3.5 s.

Conclusion

The automatic digging operation control system allows the digging trajectory to be practically optimal. It ensures extremely quick penetration of no more than 3 sec with permissible overregulation of no more than 10%, with following even digging at a constant cut depth. Cut depth is set externally.

The automatic control system lead to decreased loads on the electromechanical equipment and allows for an increase in operational productivity of a walking dragline excavator.

The integrated system of the dragline work process control can be almost autonomous due to the following factors: automatic digging operation control; automatic systems of transporting loaded bucket to the dump and empty bucket to the face; systems of automatic protection against overload of the main mechanisms; and control system for safe movement of the bucket in the dragline working space.

References

1. Ponnusamy M., Maity T. Recent advancements in dragline control systems. *Journal of Mining Science*. 2016;52:160–168. https://doi.org/10.1134/S106273911601025X

2. Liu H., Kearney M., Austin K. Development of dragline excavation model for operation planning. In: *Australasian Conference on Robotics and Automation*, *ACRA*. 2016. Pp. 55–63. URL: https://www.araa.asn.au/acra/acra2016/papers/pap107s1.pdf

3. Corke P., Winstanley G., Dunbabin M., Roberts J. Dragline automation: experimental evaluation through productivity trial. In: Yuta S., Asama H., Prassler E., Tsubouchi T., Thrun S. (eds.) *Field and Service Robotics*. *Springer Tracts in Advanced Robotics*. Springer, Berlin, Heidelberg. 2006;24:459–468. https://doi.org/10.1007/10991459_44

4. Liu H., Kearney M.P., Austin K.J. Dragline operation modelling and task assignment based on mixed-integer linear programming. *Optimization and Engineering*. 2018;19:1005–1036. https://doi.org/10.1007/s11081-018-9386-5

5. Htay W.Z., Pevzner L.D., Temkin I.O. Algorithmic and hardware support for on-board information system of walking dragline excavator. *Mining Informational and Analytical Bulletin*. 2019;(2):190–196. https://doi.org/10.25018/0236-1493-2019-02-0-190-196

6. Gölbaşi O., Demirel N. Investigation of stress in an earthmover bucket using finite element analysis: A generic model for draglines. *Journal of the Southern African Institute of Mining and Metallurgy*. 2015;115(7):623–628. https://doi.org/10.17159/2411-9717/2015/v115n7a8

7. Kumar A., Nandikanti S., Batchu C. Analysis of stress distribution on the bucket of a dragline machine. *Journal of Mines, Metals and Fuels*. 2016;64(5-6):118–122.

8. Ha Q., Santos M., Nguyen Q., Rye D., Durrant-Whyte H. Robotic excavation in construction automation. In: *IEEE Robotics & Automation Magazine*. 2002;9:20–28. https://doi.org/10.1109/100.993151

9. Vul Yu. Ya., Kluchev V. I., Sedakov L. V. *Adjustment of electric drives of excavators*. Moscow: Nedra Publ.; 1975. (In Russ.)

10. Pevzner L. D. Automated control system for heavy cyclic excavators. *Russian Mining Industry*. 2011;(5):58. (In Russ.). URL: https://mining-media.ru/ru/article/karertekh/842-avtomatizirovannaya-sistema-upravleniya-tyazhelymi-ekskavatorami-tsiklicheskogo-dejstviya-2

11. Pevzner L. D. *Automated control of heavy-duty single-bucket excavators*. Moscow: Gornoe Delo Publ.; 2014 p. (In Russ.)

12. Winstanley G. J., Corke P. I., Roberts J. M. Dragline swing automation. In: *IEEE International Conference on Robotics and Automation*. Albuquerque, New Mexico, USA. 1997;3:1827–1832. https://doi.org/10.1109/ROBOT.1997.619053

13. Ridley P., Corke P. Dragline Automation. In: *Proceedings 2001 ICRA. IEEE International Conference on Robotics and Automation (Cat. No.01CH37164)*. Seoul, Korea (South). 2001;4:3742–3747. https://doi.org/10.1109/ROBOT.2001.933200

Information about the authors

Leonid D. Pevzner – Dr. Sci. (Eng.), Professor, Institute of Cybernetics, MIREA – Russian Technological University, Moscow, Russian Federation; Scopus ID 37093879700; e-mail: lpevzner@msmu.ru

Nikolay A. Kiselev – Undergraduate, Institute of Cybernetics, MIREA – Russian Technological University, Moscow, Russian Federation; e-mail: gost1996@gmail.com

Received	11.07.2021
Revised	17.09.2021
Accepted	01.02.2021

eISSN 2500-0632
https://mst.misis.ru/

POWER ENGINEERING, AUTOMATION, AND ENERGY PERFORMANCE

Research article

https://doi.org/10.17073/2500-0632-2022-1-66-77

Improvement of the electric energy quality in underground electric networks in highly productive coal mines

L.A. Plashchansky[1], **S.N. Reshetnyak**[2], **M.Y. Reshetnyak**[2]

[1] *National Research Technological University "Moscow Institute of Steel and Alloys" (NUST MISiS), Moscow, Russian Federation*

[2] *Institute for the Problems of Integrated Subsoil Development, Russian Academy of Sciences (IPKON RAS), Moscow, Russian Federation*

✉ *reshetniak@inbox.ru*

Abstract

One of the main factors for the effective functioning of the power supply system in highly productive coal mines is the uninterrupted power supply of underground consumers for the entire process cycle at sufficient amount of electric energy at a high level of quality and performance. The analysis of electric energy consumption in highly productive coal mine has shown that about 57 % of electric energy consumers are located in underground workings. Consumers can be divided into the following areas of basic technological process of coal production: production areas (13 %); conveyor transport areas (13 %); preparation areas (8 %), and areas of auxiliary processes of coal production: mine drainage (23 %). The increase in the share of controlled-velocity electric drives in the total power balance of fully-mechanized longwalls leads to factors previously atypical of underground power networks. Such factors include changes to the harmonic composition of the network, arising higher current and voltage harmonics, affecting the supplying network and causing heating of electrical equipment, power and electric energy losses. Therefore, the most pressing issues are to improve electric energy quality in underground electric networks of highly productive coal mines. The study has developed a technique for experimental investigations of quality indicators of electric energy (presented in the form of algorithm) in respect to specific conditions of highly productive coal mines. These include dangerous facilities in terms of sudden gas/dust outbursts. This technique was tested at a number of coal mines of JSC SUEK-Kuzbass. The study also presents the results of experimental investigations to determine the actual level of total harmonic distortion (factor) in underground electric networks of fully-mechanized longwalls of coal mines. Of greater importance is justification of higher harmonic filter parameters. To this end a calculation algorithm based on the developed technique has been proposed. Research has shown that application of forward and inverse Clarke transformations for calculating the harmonic filter parameters is applicable for all voltage levels. The simulation model of power supply system of a coal mine fully-mechanized longwall allows conditions of higher harmonics damping to be studied by means of a device for improvement of electric energy quality. Applying the proposed technical solutions to improve the quality of electric energy based on the simulation modeling allowed the successful damping of higher harmonics to be achieved. For example, the total harmonic components voltage (THD (U)) was reduced from 9.07 to 1.77 %.

Keywords

coal mine, power supply system, electric energy quality, harmonic components, energy efficiency, underground electric networks; simulation model, resistivity bridge harmonic filter

For citation

Plashchansky L.A., Reshetnyak S.N., Reshetnyak M.Y. Improvement of electric energy quality in underground electric networks of highly productive coal mines. *Mining Science and Technology* (*Russia*). 2022;7(1):66–77. https://doi.org/10.17073/2500-0632-2022-1-66-77

ЭНЕРГЕТИКА, АВТОМАТИЗАЦИЯ И ЭНЕРГОЭФФЕКТИВНОСТЬ

Научная статья

Повышение качества электрической энергии в подземных электрических сетях высокопроизводительных угольных шахт

Л. А. Плащанский[1], **С. Н. Решетняк**[2] ✉, **М. Ю. Решетняк**[2]

[1] *Национальный исследовательский технологический университет «Московский институт стали и сплавов» (НИТУ МИСиС), г. Москва, Российская Федерация*

[2] *Институт проблем комплексного освоения недр Российской академии наук (ИПКОН РАН), г. Москва, Российская Федерация*

✉ *reshetniak@inbox.ru*

Аннотация

Одним из основных факторов эффективного функционирования системы электроснабжения высокопроизводительных угольных шахт является бесперебойное питание электроэнергией подземных потребителей всего технологического цикла при достаточном количестве электроэнергии с обязательным соблюдением показателей ее качества. Анализ электропотребления высокопроизводительной угольной шахты показал, что порядка 57 % потребителей электрической энергии расположены в подземных выработках. Потребители можно разделить на участки основного технологического процесса добычи угля: добычные участки (13 %); участки конвейерного транспорта (13 %); подготовительные участки (8 %), и участки вспомогательных процессов добычи угля: водоотлив (23 %). Увеличение доли регулируемых электроприводов в общем балансе мощностей выемочных участков приводит к появлению факторов, не характерных ранее для подземных электрических сетей. К таким факторам относятся изменение гармонического состава сети, появление высших гармоник тока и напряжения, оказывающих влияние на питающую сеть, нагрев электрооборудования, потери мощности и электроэнергии. Поэтому вопросы повышения качества электрической энергии в подземных электрических сетях высокопроизводительных угольных шахт являются актуальными. В результате проведенных исследований разработана методика проведения экспериментальных исследований показателей качества электрической энергии (представленная в виде алгоритма) применительно к специфическим условиям высокопроизводительных угольных шахт, в том числе опасных по внезапным выбросам газа и пыли. Данная методика была апробирована на ряде угольных шахт компании АО «СУЭК-Кузбасс». Также представлены результаты проведенных экспериментальных исследований по определению фактического уровня суммарного коэффициента гармонических составляющих в подземных электрических сетях выемочных участков угольных шахт. Важное значение имеет обоснование параметров фильтра высших гармоник, представленный алгоритм расчета которого основывается на разработанной методике. Исследования показали, что применение прямого и обратного преобразований Clarke для расчета параметров фильтра высших гармоник применимы для всех уровней напряжений. Имитационная модель системы электроснабжения выемочного участка угольной шахты позволяет исследовать условия демпфирования высших гармоник с помощью устройства повышения качества электрической энергии. Использование предложенных технических решений по повышению качества электрической энергии на основе имитационного моделирования позволило сделать заключение об успешном демпфировании высших гармоник, в частности, снижении суммарного значения напряжения гармонических составляющих (THD (U)) с 9,07 до 1,77 %.

Ключевые слова

угольная шахта, система электроснабжения, качество электрической энергии, гармонические составляющие, энергоэффективность, подземные электрические сети; имитационная модель, активный фильтр высших гармоник

Для цитирования

Plashchansky L.A., Reshetnyak S.N., Reshetnyak M.Y. Improvement of electric energy quality in underground electric networks of highly productive coal mines. *Mining Science and Technology* (*Russia*). 2022;7(1):66–77. https://doi.org/10.17073/2500-0632-2022-1-66-77

Introduction

The stable operation of highly productive coal mines at a new technical and economic level forms the basis for the coal mining industry in Russia [1–3]. This is due to the current technological and geopolitical challenges that the Russian Federation is facing.

One of the main factors for the effective functioning of power supply system in highly productive coal mines is uninterrupted power supply for underground consumers of the entire process cycle at a sufficient amount of electric energy at a high level of quality and performance.

The technological processes in modern coal mines use power-intensive powerful stoping, tunneling, and transport complexes, digital telemetric control, protection, and blocking systems, as well as auxiliary devices. The high power intensity of the modern highly productive complexes is provided by various systems of electric drives, including controlled ones based on semiconductor devices, especially thyristor converters [4–6].

The use of these devices causes deviations in the electrical energy quality parameters from standard levels and leads to the inadmissible heating of electric motors, power transformers, cables, and other electrical equipment [7–9]. This poses a danger to the underground electric networks in highly productive coal mines with specific operating conditions and integrated technological process, on which the productivity of the whole enterprise depends. Therefore, it is of key important to monitor the quality of electrical energy in underground electric networks of high productivity coal mines.

Basic Framework

Analysis of electric energy consumption in highly productive coal mine has shown that about 57 % of electric energy consumers are located in underground workings. Such consumers can be divided into the areas of basic technological process of coal production: production areas (13 %); conveyor transport areas (13 %); preparation areas (8 %), and areas of auxiliary processes of coal production: mine drainage (23 %), etc. Fully-mechanized longwalls (stoping areas) are among the most energy-intensive consumers and the initial step of the entire technological process of coal production. Therefore, this stage requires specialattention.

In the historical studies [10, 11] the findings of the harmonic composition analysis in the electric networks of step-down substations (SDS) of the highly productive Polysaevskaya coal mine (JSC SUEK-Kuzbass) were presented. In particular, Total Harmonic Distortion Voltage (THD(U)) for the corresponding substations SDS-12 (48 %), SDS-910 (37.7 %), SDS-948 (41.75 %) was determined. These results were corrected and upgraded in the course of the further research. The finished (upgraded) values of Total Harmonic Distortion Voltage (THD(U)) for the corresponding substations were as follows: SDS-12, 13.48 %; SDS-910, 10.77 %; SDS-948, 11.8 %.

A fully-mechanized longwall includes the following equipment: coal shearer; powered support; longwall conveyor; loader; crusher. Examination of fully-mechanized longwalls has enabled the share of controlled power of the process electrical equipment to be identified in the highly productive fully-mechanized longwall of the coal mine.

For the network which is the subject of this study, the share of controlled power through using converters is about 15 % for the Eickhoff SL-300r coal shea-rer, but much higher, about 33 % for the FFC-9 scraper conveyor. This is due to the use of a soft starter that works for a short time. However, during repair work the number of starts can be large. The controlled power percentage of the FSL-9 loader is 100 %, and its electric motor is powered by a frequency converter. The FBL-10G crusher is directly connected to the power supply network [4, 5].

It should be noted that about 35 % of electric drive systems are connected to a power supply network through converters which are the source of higher harmonics [5, 11]. The increase in the share of controlled-velocity electric drives in the total power balance of stoping faces leads to factors previously atypical of underground power networks. Such factors include changes to the harmonic composition of the network, as well as higher current and voltage harmonics which can affect the supply network. They can also lead to the heating of electrical equipment, power and electric energy losses.

The research was carried out in the highly productive fully-mechanized longwalls in the JSC "SUEK-Kuzbass" mines. Experimental investigations were conducted using the method presented in the form of algorithm (Fig. 1). An Algodue Elettronica UPM 3080 recorder of parameters was used to analyze harmonic composition in the underground electric networks of the coal mines. The analyzer, in addition to measuring the basic parameters of electric energy, allows individual and total harmonic distortion (factor) (THD) to be measured for voltage and current up to the 40th harmonic.

Analysis of the results of the experimental studies (Fig. 2) showed the significant exceeding of normative values of the voltage harmonic distortion (factor) $U_{\text{ав}}$, (for the harmonic components). The 5th and 7th harmonics are particularly prominent.

Total Harmonic Distortion Voltage (*THD*(U)) was determined as:

$$THD(U) = \sqrt{\sum_{n=2}^{40} \frac{U_n^2}{U_1}} 100\%, \quad (1)$$

where U_n – voltage level of the n-th harmonic component; n – harmonic number; U_1 – voltage level of the 1st harmonic.

GOST 32144-2013 “Electric energy. Electromagnetic compatibility of technical means” introduces limits for the parameter (THD (U)) which may not exceed 5 % (voltage level of 6 kV).

The study allowed the actual total harmonic component of voltage in the electric network of the fully-mechanized longwall to be determined. This amounted to 10.72 %, exceeding the normative value (not more than 5 % according to GOST 32144-2013) by 2.14 times.

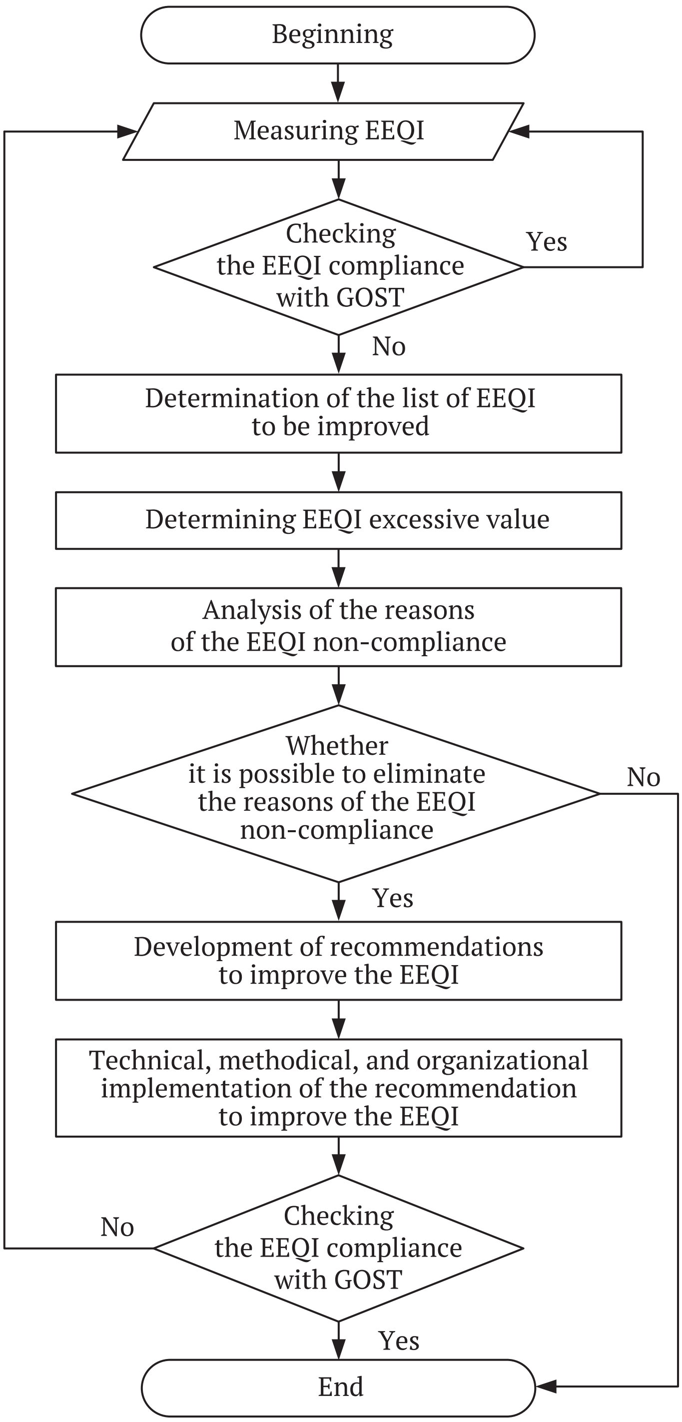

Fig. 1. Algorithm of experimental studies

The improvement of electric energy quality parameters in underground networks in highly productive coal mines may be achieved through the installation of resistivity bridge harmonic filters [12–14]. In order to select the optimal resistivity bridge harmonic filter, an algorithm was developed (Fig. 3). Selection of the resistivity bridge harmonic filter based on this algorithm was carried out through determining the power factor. If the power factor requires upward correction, then a resistivity bridge harmonic filter is proposed for installation. If no correction is required, then a number of passive narrow-band (higher) harmonic filters or a passive broad-band (higher) harmonic filter can be installed [15–17]. The experimental study showed a low power factor cos φ = 0.77 at the fully-mechanized longwall. Thus a resistivity bridge harmonic filter was adopted as a higher harmonic filter. Examination of the existing resistivity bridge harmonic filters shows that the most common connection diagram for resistivity bridge harmonic filter connection is the diagram with its parallel connection to the network with capacitive storage. This is due to the simplicity of the filter implementation [18, 19].

The general operation principle of a resistivity bridge harmonic filter consists of the following: active generation of compensating current (I_{AHF}) in antiphase with the load-affected current harmonic distortion (I_{load}), mutual compensation of these currents; and obtaining a sinusoidal current as a result (I_{grid}).

The theoretical basis for the creation of resistivity bridge harmonic filters is the instantaneous power theory (p-q Theory) presented in [19, 20]. According to this theory the instantaneous power is determined in the time domain through transformation of the voltage and currents from an *abc* reference frame to components in a stationary αβ0 reference frame. This is known as the Clarke transform.

In the case of underground electric networks of coal mines, where there is no zero protective conductor (insulated neutral mode), the matrices of Clarke transforms will be as follows:

– forward Clarke transformation for voltages in underground coal mine networks:

$$\begin{bmatrix} u_\alpha \\ u_\beta \end{bmatrix} = \sqrt{\frac{2}{3}} \begin{bmatrix} 1 & -\frac{1}{2} & -\frac{1}{2} \\ 0 & \frac{\sqrt{3}}{2} & -\frac{\sqrt{3}}{2} \end{bmatrix} \begin{bmatrix} u_a \\ u_b \\ u_c \end{bmatrix}, \tag{2}$$

where u_α – projection of voltage vector on α axis; u_β – projection of voltage vector on β axis; u_a – voltage of *A*-phase; u_b – voltage of *B*-phase; u_c – voltage of *C*-phase;

– inverse Clarke transform for voltages in underground coal mine networks:

$$\begin{bmatrix} u_a \\ u_b \\ u_c \end{bmatrix} = \sqrt{\frac{2}{3}} \begin{bmatrix} 1 & 0 \\ -\frac{1}{2} & \frac{\sqrt{3}}{2} \\ -\frac{1}{2} & -\frac{\sqrt{3}}{2} \end{bmatrix} \begin{bmatrix} u_\alpha \\ u_\beta \end{bmatrix}; \tag{3}$$

– forward Clarke transform for current in underground coal mine networks:

$$\begin{bmatrix} i_\alpha \\ i_\beta \end{bmatrix} = \sqrt{\frac{2}{3}} \begin{bmatrix} 1 & -\frac{1}{2} & -\frac{1}{2} \\ 0 & \frac{\sqrt{3}}{2} & -\frac{\sqrt{3}}{2} \end{bmatrix} \begin{bmatrix} i_a \\ i_b \\ i_c \end{bmatrix}, \tag{4}$$

where i_α – projection of current vector on α axis; i_β – projection of current vector on β axis; i_a – current of A-phase; i_b – current of B-phase; i_c – current of C-phase;

– inverse Clarke transform for current in underground coal mine networks:

$$\begin{bmatrix} i_a \\ i_b \\ i_c \end{bmatrix} = \sqrt{\frac{2}{3}} \begin{bmatrix} 1 & 0 \\ -\frac{1}{2} & \frac{\sqrt{3}}{2} \\ -\frac{1}{2} & -\frac{\sqrt{3}}{2} \end{bmatrix} \begin{bmatrix} i_\alpha \\ i_\beta \end{bmatrix}. \tag{5}$$

Instantaneous total power in complex form:

$$\begin{gathered} s = \overline{u}\,\overline{i}^{*} = (u_\alpha + ju_\beta)(i_\alpha - ji_\beta) = \\ = (u_\alpha i_\alpha + u_\beta i_\beta) + j(u_\beta i_\alpha - u_\alpha i_\beta); \\ p = u_\alpha i_\alpha + u_\beta i_\beta = \bar{p} + \tilde{p}; \\ q = u_\beta i_\alpha - u_\alpha i_\beta = \bar{q} - \tilde{q}, \end{gathered} \tag{6}$$

where p – instantaneous actual (active) power; q – instantaneous fictitious (reactive) power; $\bar{p}$ – average value of active power; $\tilde{p}$ – pulsed active power (average value is equal to 0); $\bar{q}$ – average value of reactive power; $\tilde{q}$ – pulsed (oscillating) part of reactive power.

The levels of currents in matrix form in coordinates α and β are defined as:

$$\begin{bmatrix} i_\alpha \\ i_\beta \end{bmatrix} = \frac{1}{u_\alpha^2 + u_\beta^2} \begin{bmatrix} u_\alpha & u_\beta \\ u_\alpha & -u_\beta \end{bmatrix} \begin{bmatrix} p \\ q \end{bmatrix}. \tag{7}$$

The levels of currents in α and β coordinates are defined as:

$$\begin{gathered} i_\alpha = \frac{u_\alpha}{u_\alpha^2 + u_\beta^2}\bar{p} + \frac{u_\alpha}{u_\alpha^2 + u_\beta^2}\tilde{p} + \frac{u_\alpha}{u_\alpha^2 + u_\beta^2}\bar{q} + \frac{u_\alpha}{u_\alpha^2 + u_\beta^2}\tilde{q}; \\ i_\beta = \frac{u_\beta}{u_\alpha^2 + u_\beta^2}\bar{p} + \frac{u_\beta}{u_\alpha^2 + u_\beta^2}\tilde{p} - \frac{u_\beta}{u_\alpha^2 + u_\beta^2}\bar{q} - \frac{u_\beta}{u_\alpha^2 + u_\beta^2}\tilde{q}. \end{gathered} \tag{8}$$

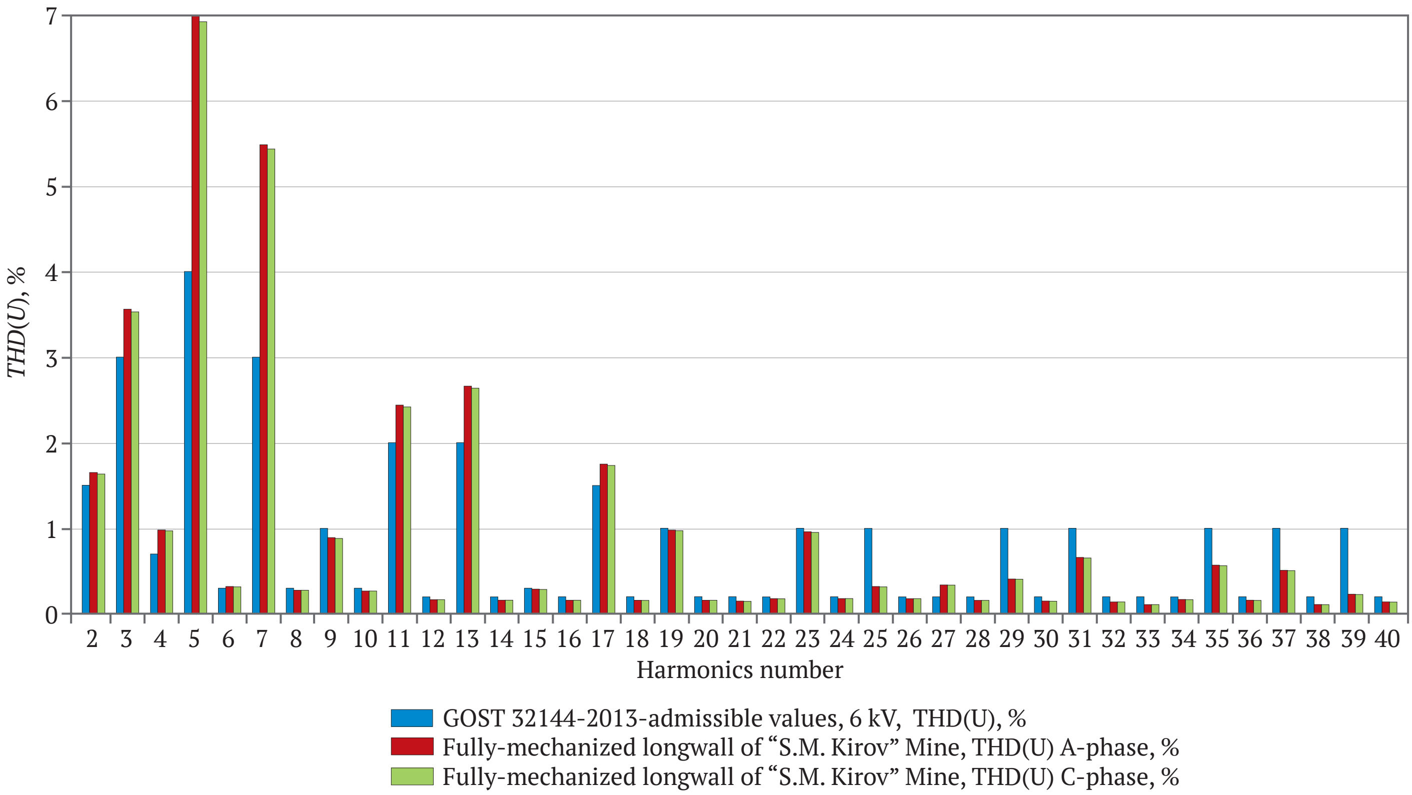

Fig. 2. Harmonic composition at the feeder cubicle of the fully-mechanized longwall of "S.M. Kirov" Mine (JSC "SUEK-Kuzbass")

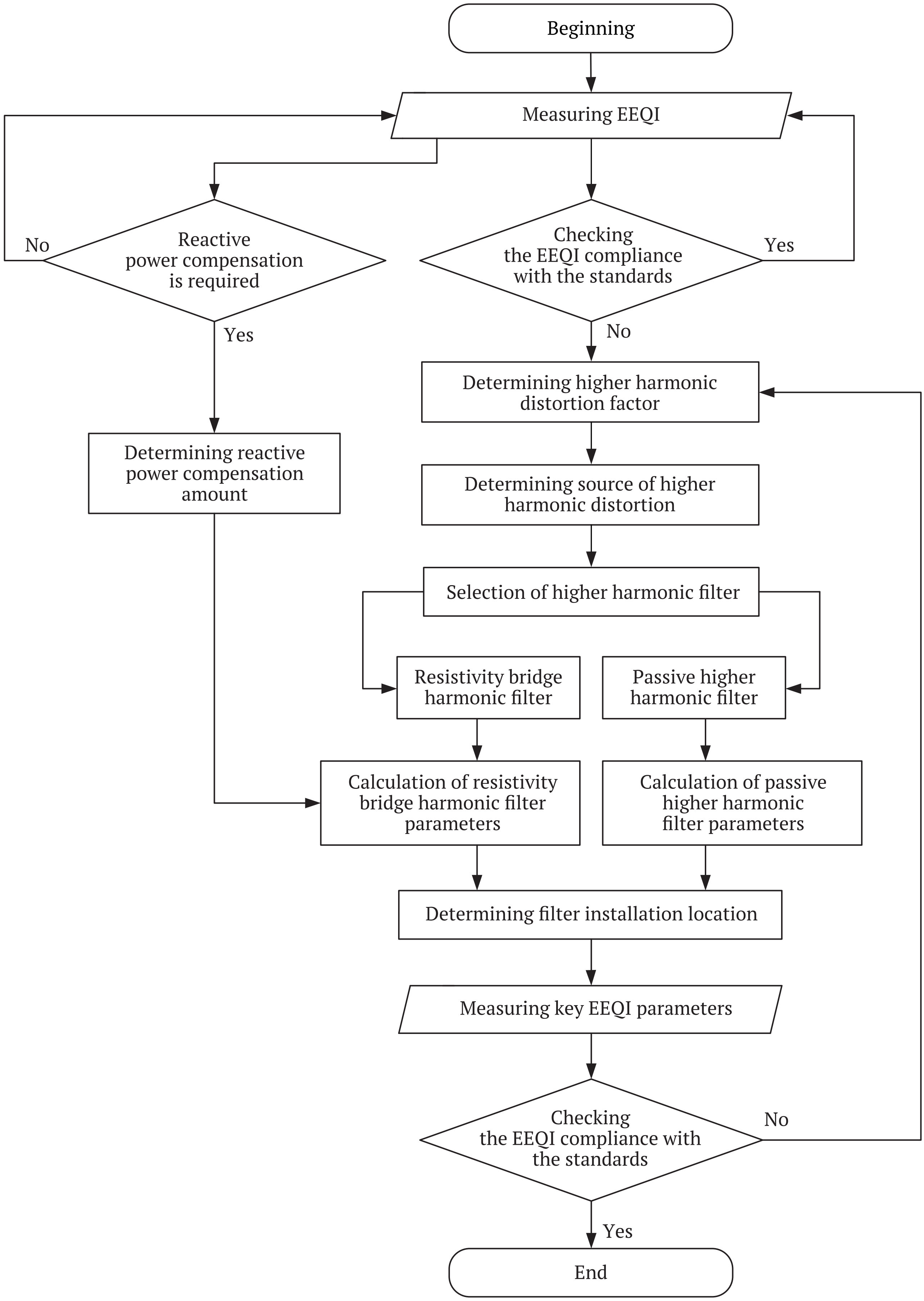

Fig. 3. Algorithm for selecting resistivity bridge harmonic filters for highly productive coal mines

The capacitance of the storage capacitor of the resistivity bridge harmonic filter according to [16] can be defined as:

$$C = 2\frac{\int_0^{T/12}(T_u + P_A)dt}{\Delta U_{dC}(\Delta U_{dC} + 2U_{dC})}, \qquad (9)$$

where C – capacitance of storage capacitor, μF; T – supply-line voltage period; T_u – capacitor distortion power (rectified voltage), VA; P_A – IGBT losses power, VA; ΔU_{dC} – magnitude of rectified voltage variation, V; U_{dC} – magnitude of rectified voltage, V.

In order to determine the capacitance of storage capacitor of a resistivity bridge harmonic filter we take the following assumptions:

$$T_u = \sqrt{3}U\sum_{n=2}^{40} I_n;$$

$$T_u = \sqrt{3}I\sum_{n=2}^{40} U_n; \qquad (10)$$

$$P_A = P_{cond} + P_{sw} = i_c u_{ce} + \frac{1}{2}U_{CE_{\max}} I_{C_{\max}};$$

$$\Delta U_{dc} = 0{,}05U_{dc},$$

where U – first harmonic rms voltage, V; I_n – nth harmonic component current, A; I – first harmonic rms current, A; U_n – nth harmonic component voltage, V; P_{cond} – IGBT static losses power, VA; P_{sw} – IGBT dynamic losses power, VA; i_c – instantaneous IGBT collector current, A; u_{ce} – instantaneous IGBT emitter-collector voltage, V; $U_{CE_{\max}}$ – maximum IGBT emitter-collector voltage, V; $I_{C_{\max}}$ – maximum IGBT collector current, A. In this case, the resulting formula for calculating the storage capacity of a resistivity bridge harmonic filter for voltage levels of distribution networks of highly productive coal mines has the following form:

$$C = 2\frac{\int_0^{T/12}\left(\frac{S}{\sqrt{3}U_1}\sum_{n=2}^{40}U_n + \left(i_c u_{ce} + \frac{1}{2}U_{CE_{\max}} I_{C_{\max}}\right)\right)dt}{\Delta U_{dC}(\Delta U_{dC} + 2U_{dC})}. \qquad (11)$$

Results of calculating storage capacity of resistivity bridge harmonic filter at different voltage levels of underground mine distribution networks are shown in Fig. 4.

The calculation of the input choke inductance of the resistivity bridge harmonic filter is as follows:

$$\Delta U = 2\pi fLI \text{ or } L = \frac{\Delta U}{2\pi fI}, \qquad (12)$$

where ΔU – is choke voltage losses, V; f – is power frequency, Hz; I – current, A; L – inductance, H.

The value of the input choke inductance of the resistivity bridge harmonic filter is calculated based on the total power of the circuit $S = \sqrt{3}UI$ and (12):

$$L = \frac{\sqrt{3}U\Delta U}{2\pi fS}. \qquad (13)$$

The results of calculating the inductance of the input choke of resistivity bridge harmonic filter for voltage levels of underground mine distribution networks are shown in Fig. 5.

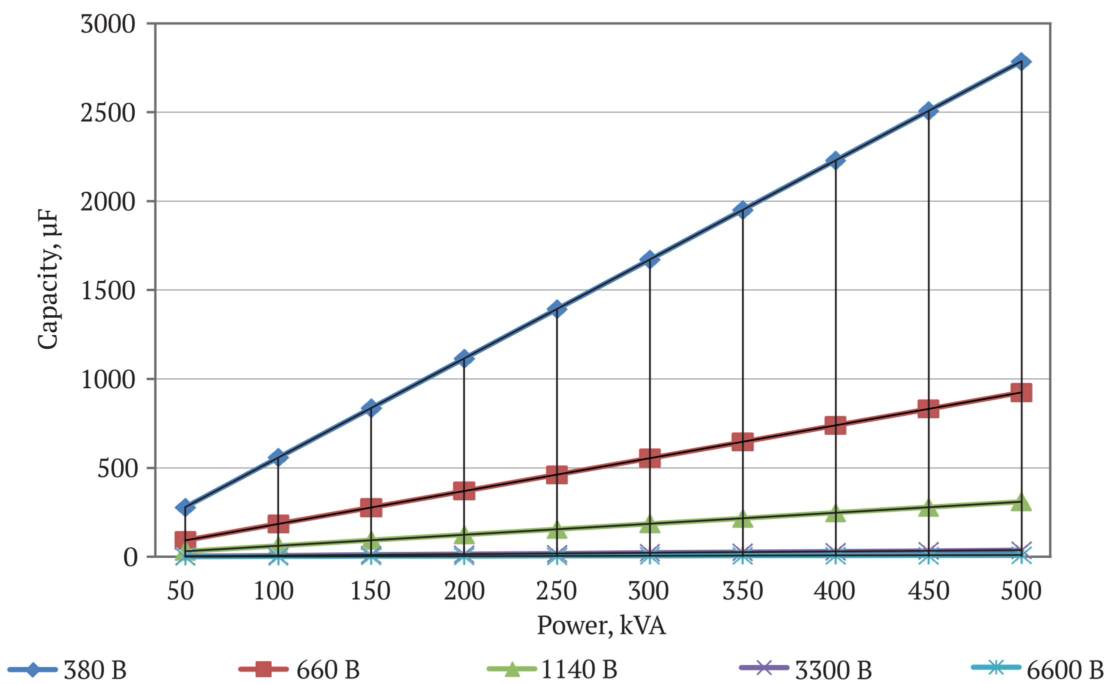

Fig. 4. Parameters of storage capacity of resistivity bridge harmonic filter

eISSN 2500-0632
https://mst.misis.ru/

Practical implementation of research findings

The study allowed for a device for automated monitoring of electric energy quality parameters to be developed.

The device is installed in the power train of fully-mechanized longwall of a mine. When current flows through the device, the analyzer determines the main parameters of electric energy quality (power factor, harmonic composition, etc.).

The research findings regarding the possibilities of higher harmonics dampening in underground networks of coal mines using the proposed device allowed a simulation model of the power supply system to be built (Fig. 6) This model establishes the possibility of reducing higher harmonics effect on the supply network. The model included a three-phase universal meter which allows the waveform at the voltage source to be estimated when the higher harmonic components compensation system is OFF and when is ON. An oscillograph is used as the output device of the three-phase universal meter.

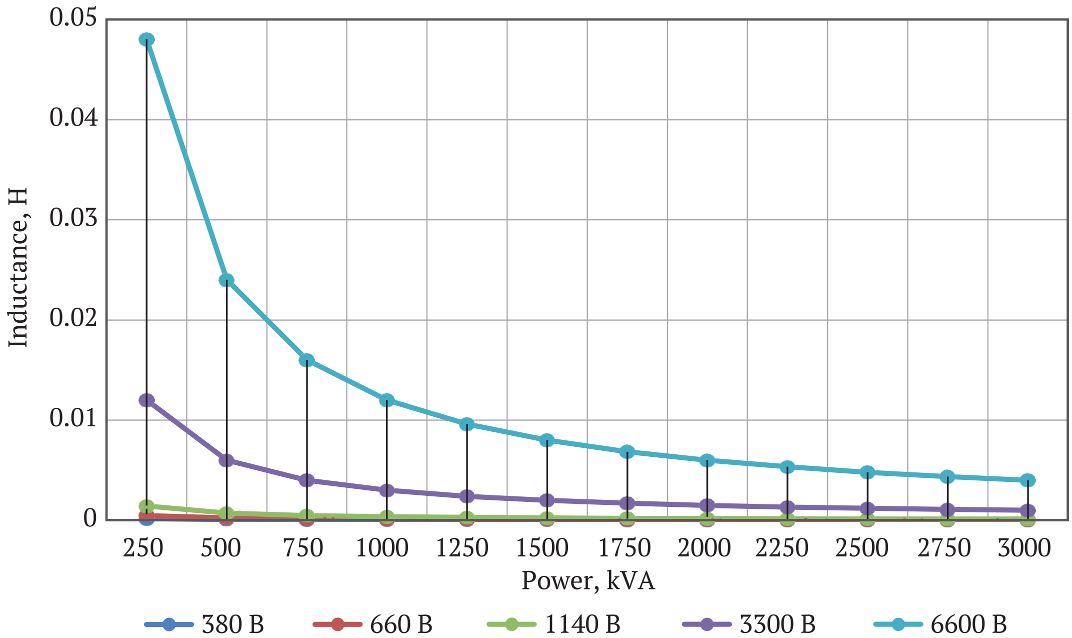

Fig. 5. Parameters of input (prefilter) choke of resistivity bridge harmonic filter

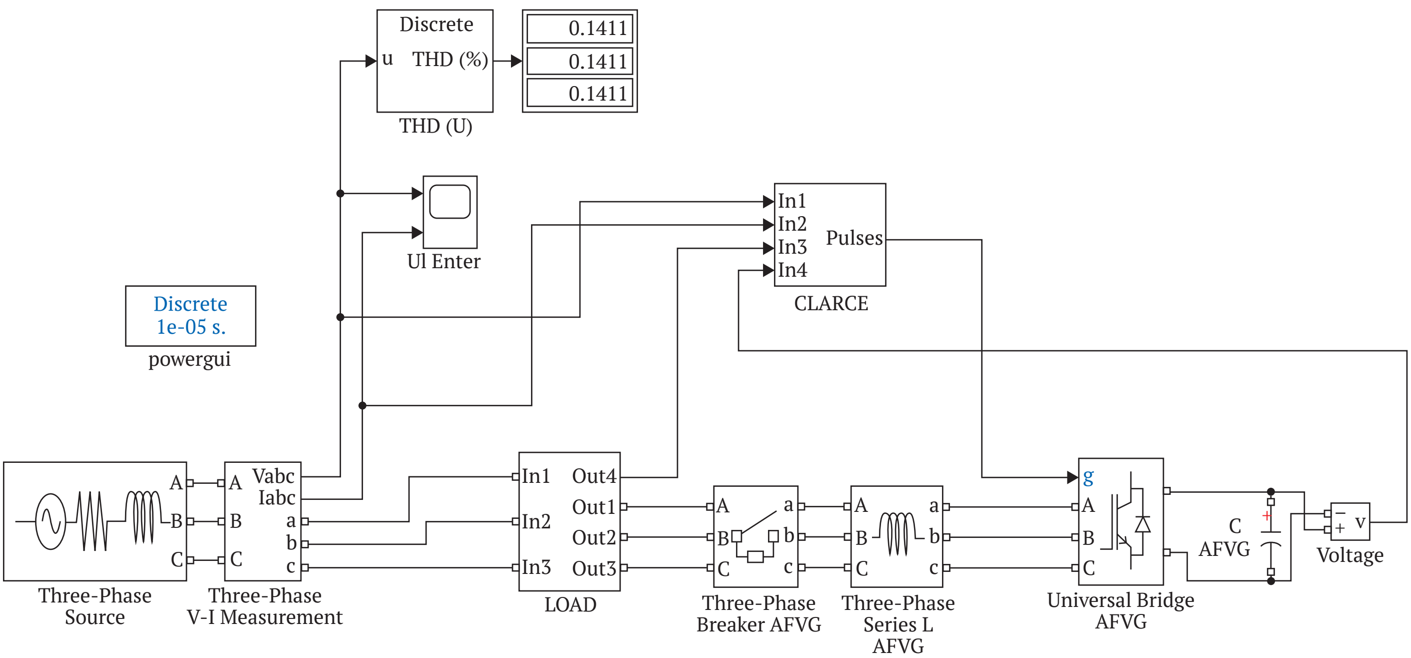

Fig. 6. Simulation model of power supply system for a coal mine fully-mechanized longwall with the basic process equipment and the resistivity bridge harmonic filter

The model also includes a resistivity bridge harmonic filter, connected to the power supply system of the fully-mechanized longwall. The resistivity bridge harmonic filter includes: an input reactor; a three-phase active bridge rectifier based on high-voltage IGBTs; a capacitive storage of the resistivity bridge harmonic filter C; and the filter control system. The simulation model includes several subsystems: LOAD (load (Fig. 7)); CLARKE resistivity bridge harmonic filter control system (Fig. 8).

The LOAD subsystem of the simulation model includes three step-down substations (TEC 1324, TEC 1534, TEC 1324) of the fully-mechanized longwall power train and a number of subsystems which simulate the load of the electric networks of the longwall: EickoffSL-300, FBL-10Glinik, FSL-9 Glinik, FFC-9 Glinik.

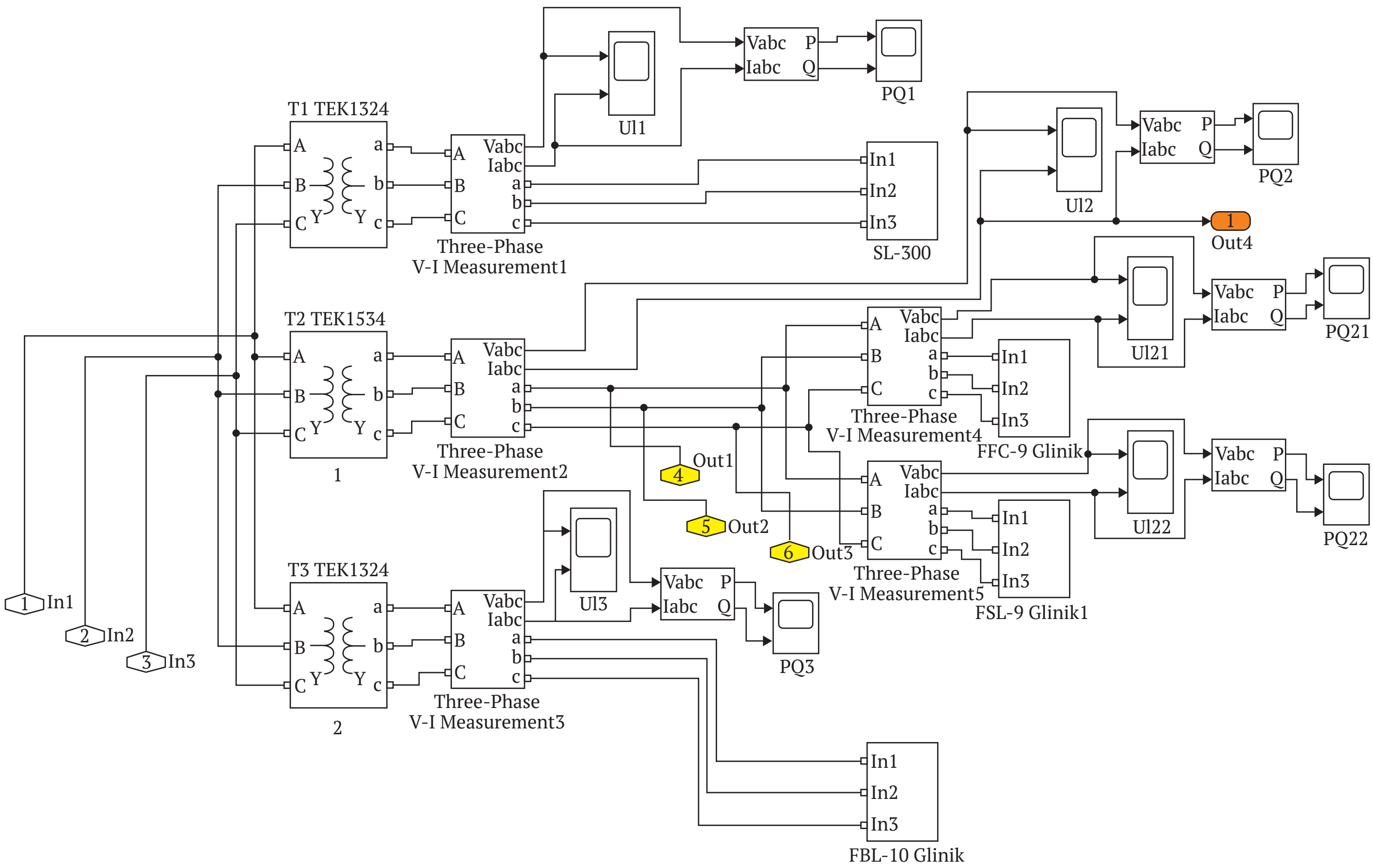

Fig. 7. LOAD (load) subsystem of the simulation model

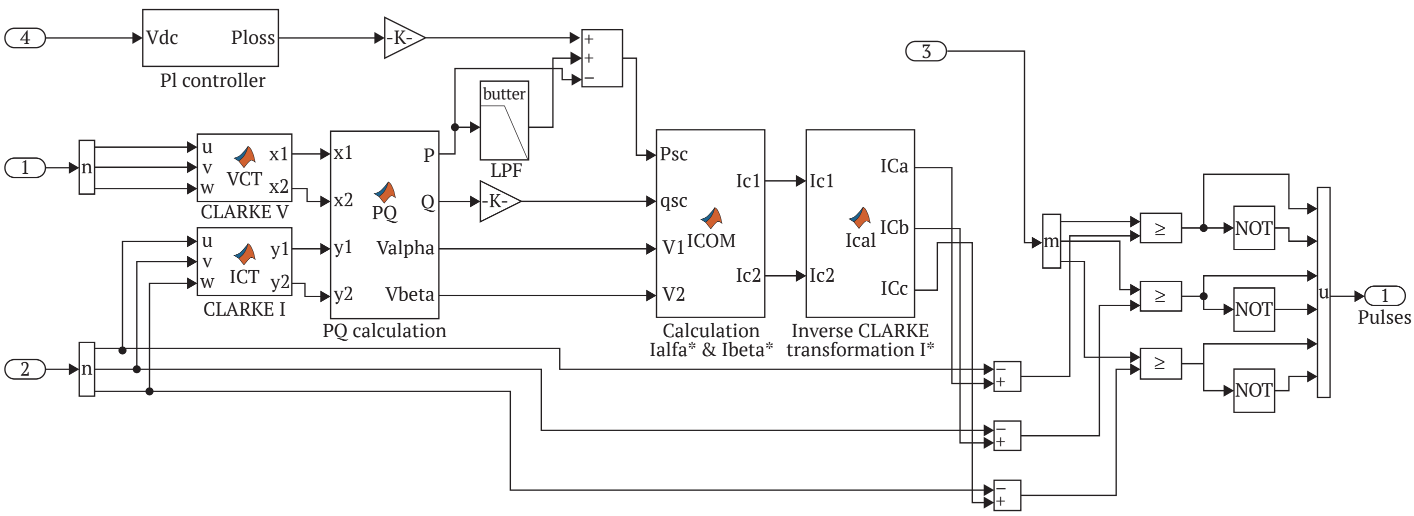

Fig. 8. CLARKE simulation model subsystem (resistivity bridge harmonic filter control system)

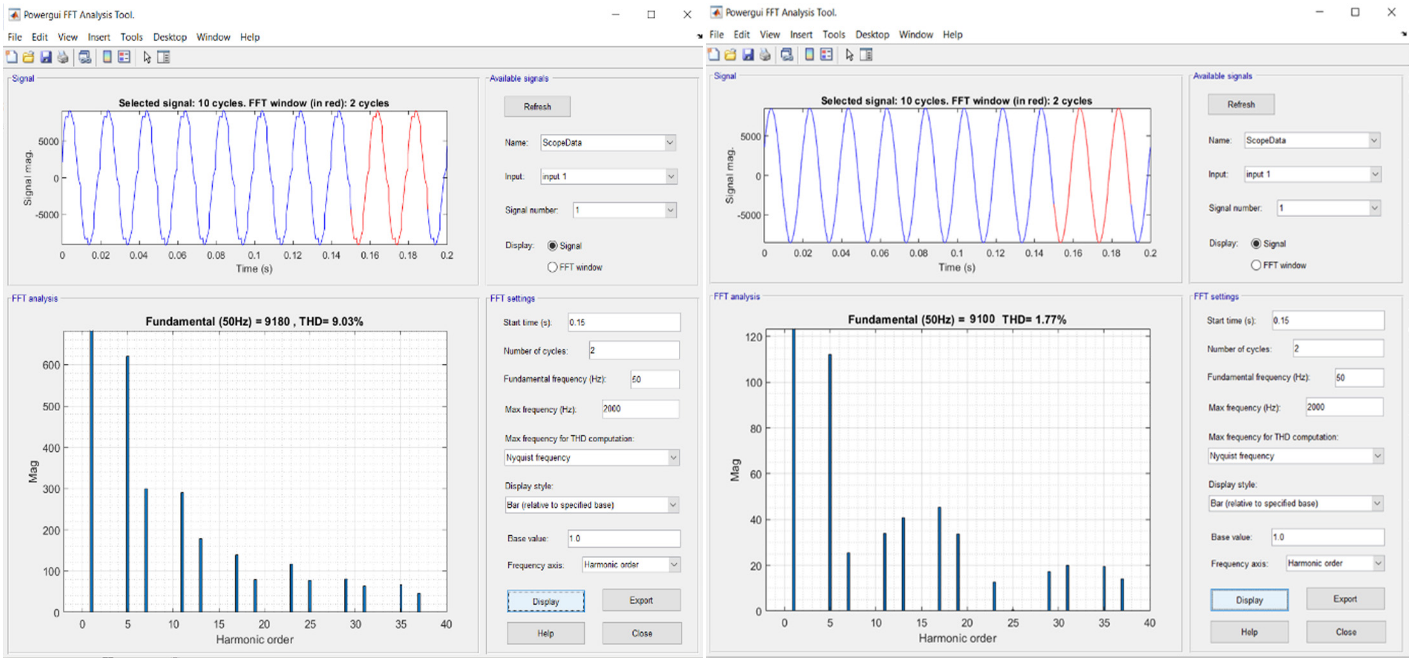

Fig. 9. Results of the simulation modeling of power supply system for a coal mine fully-mechanized longwall with basic process equipment and a resistivity bridge harmonic filter

The simulation modeling of power supply system for a coal mine fully-mechanized longwall with basic process equipment and a resistivity bridge harmonic filter (Fig. 9) showed significant reduction of the total voltage of harmonic components (THD (U)). This confirms the effectiveness of the resistivity bridge harmonic filter in underground electric networks of coal mines.

Conclusion

The study presents the results of the first experimental investigations to determine a number of electrical energy quality indicators in specific conditions in coal mines with highly productive fully-mechanized longwalls using the technique herein developed. For example the results of determining the total harmonic components voltages (THD (U)) and power factor cos φ are given. Furthermore, the study also substantiated the effective application of devices aimed at improving the quality of electrical energy in underground electric networks of highly productive coal mines, the selection of which was carried out using the proposed technique. The parameters of the device were adjusted using the proposed technique. This allowed the analytical dependences to be obtained. It also allowed the parameters of the resistivity bridge harmonic filter for the specific conditions of the underground electric networks to be determined depending on the harmonic composition, voltage levels, and power of consumers of the fully-mechanized longwalls.

A simulation model of a power supply system of a fully-mechanized longwall aimed at investigating the conditions of higher harmonics dampening using the device for improvement of electric energy quality was constructed. Application of the proposed technical solutions, in order to improve the quality of electric energy based on the simulation modeling allowed successful damping of higher harmonics to be achieved, for example, a reduction of the total harmonic components voltage (THD (U)) from 9.07 to 1.77 %.

References

1. Ruban A.D., Artemyev V.B., Zaburdyaev V.S., Zaburdyaev G.S., Rudenko Y.F. *Problems of providing high productivity of stoping faces in methane-abundant mines*. Moscow: Moscow Publishing House LLC Publ.; 2009. 396 p. (In Russ.)

2. Sidorenko A.A., Dmitriyev P.N., Yaroshenko V.V. Integrated justification of technological structure for coal mine. *Mining Informational and Analytical Bulletin*. 2021;(8):5–22. (In Russ.) https://doi.org/10.25018/0236_1493_2021_8_0_5

3. Kazanin O.I., Sidorenko A.A., Meshkov A.A., Sidorenko S.A. Reproduction of the longwall panels: modern requirements for the technology and organization of the development operations at coal mines. *Eurasian Mining*. 2020;(2):15–30. https://doi.org/10.17580/em.2020.02.05

4. Kopylov K.N., Kubrin S.S., Reshetnyak S.N. Improvement of energy efficiency and safety in coal longwalls. *Gornyi Zhurnal*. 2019;(4):85–89. (In Russ.) https://doi.org/10.17580/gzh.2019.04.19

5. Plashyansky L., Reshetnyak M. High-performance coal mining shearer loader electromechanical systems. *Energy Safety and Energy Economy*. 2019;(3):17–21. (In Russ.) https://doi.org/10.18635/2071-2219-2019-3-17-21

6. Kopylov K.N., Kubrin S.S., Reshetnyak S.N. The importance of improving energy efficiency and safety of coal mine extraction area. *Ugol'*. 2018;(10):66–71. (In Russ.) https://doi.org/10.18796/0041-5790-2018-10-66-67

7. Pivnyak G.G., Zaika V.T., Samoilenko V.V. Scientific and methodical grounds of efficient usage of electric power at coal mines in the Ukraine. *Gornyi Zhurnal*. 2010;(7):92–96. (In Russ.)

8. Babokin G.I., Shprekher D.M. Enhancement of energy efficiency in fully mechanized longwall mining. *Mining Informational and Analytical Bulletin*. 2021;(9):122–134. (In Russ.) https://doi.org/10.25018/0236_1493_2021_9_0_122

9. Kosareva-Volod'ko O.V. Review of the current approaches and systems of oil transformer diagnostics. *Mining Informational and Analytical Bulletin*. 2019;(2):129–135. (In Russ.) https://doi.org/10.25018/0236-1493-2019-02-0-129-135

10. Reshetnyak M.Yu. Study of harmonic composition in the electrical networks of the surface complex of high-performance coal mines. *Electrical and Information Systems and Complexes*. 2019;(4):61–67. (In Russ.) https://doi.org/10.17122/1999–5458-2019-15-4-61-67

11. Plashchanskiy L.A., Reshetnyak M. Yu. Analysis of harmonic composition in electrical networks of step-down substations in coal mines. *Gornyi Zhurnal*. 2020;(5):63–67. (In Russ.) https://doi.org/10.17580/gzh.2020.05.11

12. Shevyrev Yu.V., Shevyreva N.Yu. Improvement of voltagewaveform in power supply systems with dynamic rectifier in mineral mining and processing industry. *Gornyi Zhurnal*. 2019;(1):66–69. (In Russ.) https://doi.org/10.17580/gzh.2019.01.14

13. Do T.L. Research, assessment and proposals on resolving power quality problem for the power supply system of Lam Dong alumina refinery, Vietnam. *Mining Science and Technology* (*Russia*). 2021;6(2):121–127. (In Russ.) https://doi.org/10.17073/2500-0632-2021-2-121-127

14. Limongi L.R., da Silva Filho L.R., Genu L.G.B., Bradaschia F., Cavalcanti M.C. Transformerless hybrid power filter based on a six-switch two-leg inverter for improved harmonic compensation performance. In: *IEEE Transactions on Industrial Electronics*. 2015;62(1):40–51. https://doi.org/10.1109/TIE.2014.2327571

15. Bebikhov Y.V., Egorov A.N., Semenov A.S. How higher harmonics affect the electrical facilities in mining power systems. In: *2020 International Conference on Industrial Engineering, Applications and Manufacturing (ICIEAM)*. 2020. Pp. 1–7. https://doi.org/10.1109/ICIEAM48468.2020.9111965

16. Cheng M., Yanbin L. Research on application of active power filter in harmonic wave suppression of coal mine. *Journal of Chongqing University of Technology* (*Natural Science*). 2014;28(11):107–110.

17. Meshcheryakov V.N., Evseev A.M., Boikov A.I. The active energy filter for compensation of harmonic distortion in motor soft starter. In: *IEEE 58th International Scientific Conference on Power and Electrical Engineering of Riga Technical University (RTUCON)*. 2017. Pp. 1–6. https://doi.org/10.1109/RTUCON.2017.8124786

18. Semenov A.S., Kuznetsov N.M. An analysis of the results of monitoring the quality of electric power in an underground mine. *Measurement Techniques*. 2014;57(4):417–420. https://doi.org/10.1007/s11018-014-0470-8

19. Shevyrev Yu.V., Shevyrev N.Yu., Plekhov A.S., Titov D.Yu. *Computer models application for selecting power quality regulators for electric drives with semiconductor converters*. Nizhniy Novgorod: R.E. Alekseyev Nizhniy Novgorod State Technical University; 2018. 180 p. (In Russ.)

20. German-Galkin S.G. *Virtual semiconductor systems laboratories in Matlab-Simulink environment*. St. Petersburg: Lan' Publishing House; 2013. 448 p. (In Russ.)

Information about the authors

Leonid A. Plashchanskiy – Cand. Sci. (Eng.), Professor of the Department of Energy and Energy Efficiency of the Mining Industry, National University of Science and Technology "MISiS" (NUST "MISiS"), Moscow, Russian Federation; Scopus ID 57193312566; e-mail pla3768@yandex.ru

Sergey N. Reshetnyak – Cand. Sci. (Eng.), Senior Researcher, Laboratory 2.3 "Geotechnological Risks in the Development of Gas-Bearing Coal and Ore Deposits", Research Institute of Comprehensive Exploitation of Mineral Resources of the Russian Academy of Sciences, Moscow, Russian Federation; ORCID 0000-0002-6982-5583, Scopus ID 57117619500; e-mail reshetniak@inbox.ru

Maria Yu. Reshetnyak – Researcher of Laboratory 2.3 "Geotechnological risks in the development of gas-bearing coal and ore deposits", Research Institute of Comprehensive Exploitation of Mineral Resources of the Russian Academy of Sciences, Moscow, Russian Federation; Scopus ID 57210212672; e-mail maria_reshetnyak@mail.ru

Received 25.05.2021
Revised 02.01.2022
Accepted 01.02.2022

POWER ENGINEERING, AUTOMATION, AND ENERGY PERFORMANCE

Research article

https://doi.org/10.17073/2500-0632-2022-1-78-88

Behaviour of electric drive of roller-bit drilling rig swivel head with fuzzy control

N.M. Kuznetsov[1] ✉, **I.N. Morozov**[2]

[1] *Kola Scientific Center of the Russian Academy of Sciences, Apatity, Russia*

[2] *Murmansk Arctic State University, Murmansk, Russia*

✉ *n.kuznetsov@ksc.ru*

Abstract

The efficient consumption of electric power in mining is an important task in power consumption optimization. The use of high-performance drilling rigs requires special attention to the development of energy-saving electric drive for open-cut mining operations. The increase of the efficiency factor and energy performance of a drilling rig is achieved through controlling the electric drive which allows the specific resonance frequency and limiting the current and velocity amplitudes to be regulated. The main idea of the study lies in the application of fuzzy controllers in the systems of automatic control of processes and equipment modes in mining production. The use of fuzzy controllers is aimed at improving the characteristics of PI and PID controllers. The calculations and simulation of transients based on simulation models in the MatLab 7.11 Simulink software package allowed reliable analysis of modes of a swivel head electric drive operation to be carried out. In the course of simulating the transients of swivel head velocity varying with the use of a fuzzy controller, fuzzy variables including mismatch of rotation velocity, mismatch change speed, velocity setting voltage were justified. The analysis allowed for the term-sets of fuzzy variables and the membership functions for each term-set of fuzzy variable to be defined. The simulation results showed that the control time (response) of transients of the swivel head motor torque and current change when using the swivel head velocity control by a fuzzy controller with increasing load depending on the rock hardness decreased by a factor of 2. Implementation of a system of automatic control of swivel head velocity with the application of a fuzzy controller allows drilling rig vibration to be reduced and provided effective protection of the swivel head electric (motor) drive from overload, thus increasing reliability of the equipment, and increasing drilling productivity.

Keywords

minerals, mining, power consumption, energy performance, drilling rig, swivel head, electric drive, automatic control, controllers, transients, fuzzy controller

For citation

Kuznetsov N. M., Morozov I. N. Behaviour of electric drive of roller-bit drilling rig swivel head with fuzzy control. *Mining Science and Technology* (*Russia*). 2022;7(1):78–88. https://doi.org/10.17073/2500-0632-2022-1-78-88

ЭНЕРГЕТИКА, АВТОМАТИЗАЦИЯ И ЭНЕРГОЭФФЕКТИВНОСТЬ

Научная статья

Исследование динамики электропривода вращателя бурового станка шарошечного бурения с нечетким управлением

Н.М. Кузнецов[1] ✉, **И.Н. Морозов**[2]

[1] *Кольский научный центр РАН, г. Апатиты, Российская Федерация*

[2] *Мурманский арктический государственный университет, г. Мурманск, Российская Федерация*

✉ *n.kuznetsov@ksc.ru*

Аннотация

Применение высокопроизводительных буровых станков требует особого внимания к разработке энергосберегающего электропривода при добыче полезных ископаемых открытым способом. Повышение коэффициента полезного действия и энергоэффективности бурового станка достигается при управлении электроприводом, позволяющим регулировать удельную резонансную частоту и ограничивать амплитуды тока и скорости. Основная идея работы заключается в применении нечетких регуляторов в системах автоматического регулирования режимами работы электропривода вращателя бурового станка шарошечного бурения. Использование нечетких регуляторов направлено на улучшение характеристик ПИ- и ПИД-регуляторов. Расчеты и моделирование переходных процессов с применением имитационных моделей в программном комплексе MatLab 7.11 Simulink позволили проводить достоверный анализ режимов работы электропривода вращателя бурового станка. При моделировании переходных процессов изменения скорости вращателя бурового станка с применением нечеткого регулятора обоснованы нечеткие переменные: рассогласование скорости вращения, скорость изменения рассогласования, напряжение задания по скорости. Проведенный анализ позволил установить терм-множества нечетких переменных и функции принадлежности каждому терм-множеству нечеткой переменной. Результаты выполненного моделирования показывают, что время регулирования переходных процессов изменения момента и тока двигателя вращателя при применении регулирования скорости вращателя нечетким регулятором с увеличением нагрузки в зависимости от крепости породы уменьшается в 2 раза. Внедрение системы автоматического регулирования скорости вращателя бурового станка с применением нечеткого регулятора позволяет снизить вибрацию бурового станка, обеспечить эффективную защиту двигателя вращателя от перегрузки, повысить надежность работы оборудования и производительность при бурении.

Ключевые слова

полезные ископаемые, горное дело, электропотребление, энергоэффективность, буровой станок, механизм вращателя, электропривод, автоматическое управление, регуляторы, переходные процессы, нечеткий регулятор

Для цитирования

Kuznetsov N. M., Morozov I. N. Behaviour of electric drive of roller-bit drilling rig swivel head with fuzzy control. *Mining Science and Technology* (*Russia*). 2022;7(1):78–88. https://doi.org/10.17073/2500-0632-2022-1-78-88

Introduction

In order to create intelligent systems for predicting electricity consumption at mining enterprises, energy and technological indicators must be monitored and the effect of the indicators on electricity consumption analysed. Modes of process facility operation also need to be simulated

When developing mathematical models of power consumption process, methods and approaches of predictive modeling of power consumption must be applied which take into account the specific features of organizing, planning, and conducting mining [1, 2]. Analysis of geological, technological, and organizational factors which influence mining operations in coal mines [3, 4] allows for dynamic and predictive models of power consumption to be developed while taking into account the basic temporal tendencies and additive components within the limits providing stable level of power consumption. The model for determining the processing plant's ball mill power consumption [5] for intelligent predicting system allows the efficiency of electricity consumption by the mill electric drive to be assessed. It also allows for the control system quality indicators to be determined, including controlling the load schedule, predicting production cycles and power consumption peaks, redistributing loads and analyzing changes in the mill operating mode. The implementation of automated systems of monitoring and control of production processes of mining enterprises with the use of frequency-controlled electric drives allows for a significant reduction in power consumption, as well as equipment maintenance and repairing costs [6]. Efficient power consumption in minerals mining and processing sector is an key objective in power consumption optimization [7]. The application of high-performance drilling rigs requires special attention with regard to the development of energy-saving frequency-controlled electric drive for open-cut mining operations. The increase in the efficiency factor, power quality, and energy performance of a drilling rig is achieved through controlling the electric drive. This allows the specific resonance frequency and restricting the current and velocity amplitudes to be regulated using simulation of transients with a PID controller [8, 9]. Frequency-controlled electric drive used for swivel head velocity control provides for high-quality mechanical characteristics in the entire range of electric motor velocity controlling.

Effect of the key process parameters in unstable drill bit rotation mode on the energy performance is shown in [10].

The application of common harmonic filters [11, 12] and resistivity bridge harmonic filters [13] allows the quality of electric power to be improved. The use of fuzzy controllers in automatic process control systems of mining enterprises is expanded [14]. Libraries of fuzzy control in modern programming systems have convenient graphical interface and allows for correction of the type of fuzzy output membership function that greatly simplifies the setting up of fuzzy controllers automatic control systems and improves the characteristics of PI and PID controllers [15]. The computation and simulation of dynamic drilling processes is a complex task which makes it difficult to automate drilling process and requires the use of human resources to control and manage the process. Therefore, the development of drilling process control systems with the use of fuzzy control seems urgent.

Description of swivel head electric drive

The velocity control of swivel head drive (of self-propelled rotary drilling rigs (BSSh-1M, BSSh-2M, 2SBSH-200) was achieved by changing the generator excitation in the generator-motor system with the use of generator voltage feedback and rotating magnetic amplifier [16]. The swivel head electric drive of BASh-320 self-propelled roller-bit drilling rig was powered by a three-phase power magnetic amplifier. The swivel head electric motor drive of SBSh-250 MN self-propelled roller-bit drilling rig is provided by the thyristor converter, a direct current motor system with automatic bit velocity control, when changing drilling parameters. A voltage and velocity sensor is used in the swivel head motor control and excitation circuit. After applying voltage to the control and excitation circuit of the swivel head motor drive, the velocity and feed force are set depending on rock hardness. The required axial force applied to the bottom hole is set with the control knob of the pressure controller.

Model parameters

Parameters of the main drive links of the swivel head electric motor drive control system were determined pursuant to the traditional method and are shown in Table 1.

Table 1

Parameters of swivel head electric motor drive control system with different types of standard controllers

Parameter, model element	Function	Value
	Current elements	
Transfer function $W(p)$	$W(p)=\dfrac{\beta}{1+T_e p}$	$\dfrac{42.07}{1+0.066p}$
Modulus of rigidity of linearized mechanical characteristic of electric motor, β	$\beta=\dfrac{2M_k}{\omega_{0_{nom}}}s_{cr}$	42.07
Breakdown torque M_c, Nm	–	309
Critical slip, s_{cr}	–	0.144
Angular rated motor velocity $\omega_{0_{nom}}$, c^{-1}	$\omega_{0_{nom}}=\dfrac{2\pi n_n}{60}$	102
Equivalent electromagnetic time constant of motor stator and rotor circuits T_e, c	$T_e=\dfrac{1}{\omega_{0_{el.nom}} s_{cr}}$	0.066
Angular velocity of electric motor electromagnetic field $\omega_{0_{el.nom}}$, rad/s	$\omega_{0_{el.nom}}=\dfrac{2\pi f}{p}$	104.7
Supply frequency f, Hz	–	50
Number of pole pairs, p	–	3
	Mechanics	
Transfer function $W(p)$	$W(p)=\dfrac{1}{\beta T_m p}$	$\dfrac{1}{0.13p}$
Electromechanical time constant of motor, T_m	$T_m=\dfrac{J}{\beta}$	0.003
Mass moment of inertia reduced to motor shaft, J, kg · m^2	0.126	

End of Table 1

Parameter, model element	Function	Value
Frequency transformer (pole zone $f_1 \le f_{1_{nom}}$ = 50 Hz)		
Transfer function $W_{pr}(p)$	$W_{pr}(p) = \frac{k_{pr}}{1+T_{pr}p}$	$\frac{0.3}{1+0.001p}$
Transfer factor k_{pr}	$k_{pr} = \frac{\Delta\omega_0}{\Delta U_{pc}} = \frac{2\pi\Delta f_1}{p\Delta U_{pc}}$	0.3
Integration constant T_m, s	$T_m = T_{02} + T_{pr}$	0.021
PI controller of velocity		
Transfer function $W_{pc}(p)$	$W_{pc}(p) = \frac{\Delta U_{pc}}{\Delta U_y} = k_{pc} + \frac{1}{T_{pc}p}$	$\frac{0.008p+1}{0.09p}$
Integration constant T_{pc}, c	$T_{pc} = k_{f.c}k_{pm}k_{pr}a_m T_m$	0.09
Transfer factor k_{pc}	$k_{pc} = \frac{T_{01}}{T_{pc}}$	0.09
PI controller of current		
Transfer function $W_{pm}(p)$	$W_{pm}(p) = \frac{\Delta U_{pm}}{\Delta U_y} = k_{pm} + \frac{1}{T_{pm}p}$	$\frac{0.06p+1}{0.03p}$
Integration constant T_{pm}, c	$T_{pm} = k_{o.t}k_{pr}a_m T_m$	0.3
Transfer factor k_{pm}	$k_{pm} = \frac{T_{01}}{T_{pm}}$	0.2
Feedback circuit		
Transfer function $W_{f.c}(p)$	$W_{f.c}(p) = \frac{\Delta U_{f.c}}{\Delta\omega} = k_{f.c}$	
Velocity feedback factor k_y	$k_y = \frac{u_{f.c_{nom}}}{\omega_{nom}}$	3.7
Current feedback factor k_c	$k_c = \frac{u_{f.c_{nom}}}{I_{nom}}$	0.03
Rated control signal $u_{f.c_{nom}}$, V	–	380
Rated velocity ω_{nom}, rad/s	–	102
Asynchronous motor		
Transfer function $W_d(p)$	$W_d(p) = \frac{\Delta\omega}{\Delta\omega_0} = \frac{1}{T_e T_m p^2 + T_m p + 1}$	
at $T_m \ge 4T_e$	$W_d(p) = \frac{1}{(T_{01}p+1)(T_{02}p+1)}$	$\frac{1}{(0.008p+1)(0.02p+1)}$
Small uncompensated constant T_{01}, s	$\frac{1}{T_{01}} = \frac{1}{2T_e}\left(1+\sqrt{1-\frac{4T_e}{T_m}}\right)$	0.008
Small uncompensated constant T_{02}, s	$\frac{1}{T_{02}} = \frac{1}{2T_e}\left(1-\sqrt{1-\frac{4T_e}{T_m}}\right)$	0.02

Simulation of transients with PI controller

Transient design and calculation was carried out using MatLab 7.11 software by means of simulating the system in Simulink program (Fig. 1).

The simulation was performed for the following modes of the swivel head velocity change: start-up; velocity change according to the setpoint at the 5th second; velocity change at the 10th second, introducing variable load at the 15th second. The load application mode is a sharp change in static torque on the motor shaft. The simulation results are shown in Fig. 2.

Simulation of transients with PID controller

When performing the system control with a PID-controller. In MatLab 7.11, it is possible to automatically determine PID controller parameters for a given system using the tune (tune, adjust) button available in the PID controller parameters. Entering the tune block allows for the parameters to be adjusted manually. By comparing the characteristics obtained by automatic tuning and manual tuning, we select the most favorable PID controller control for the given system. The control of the PID controller parameters is shown in Fig. 3.

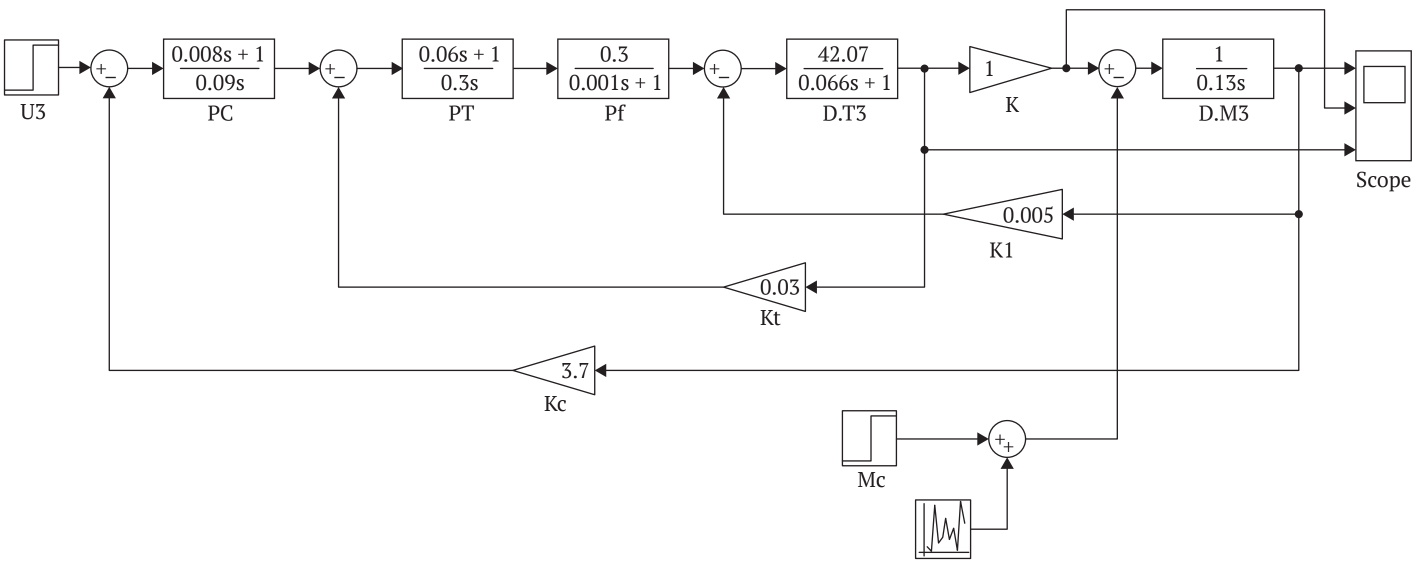

Fig. 1. The system model in the MatLab environment

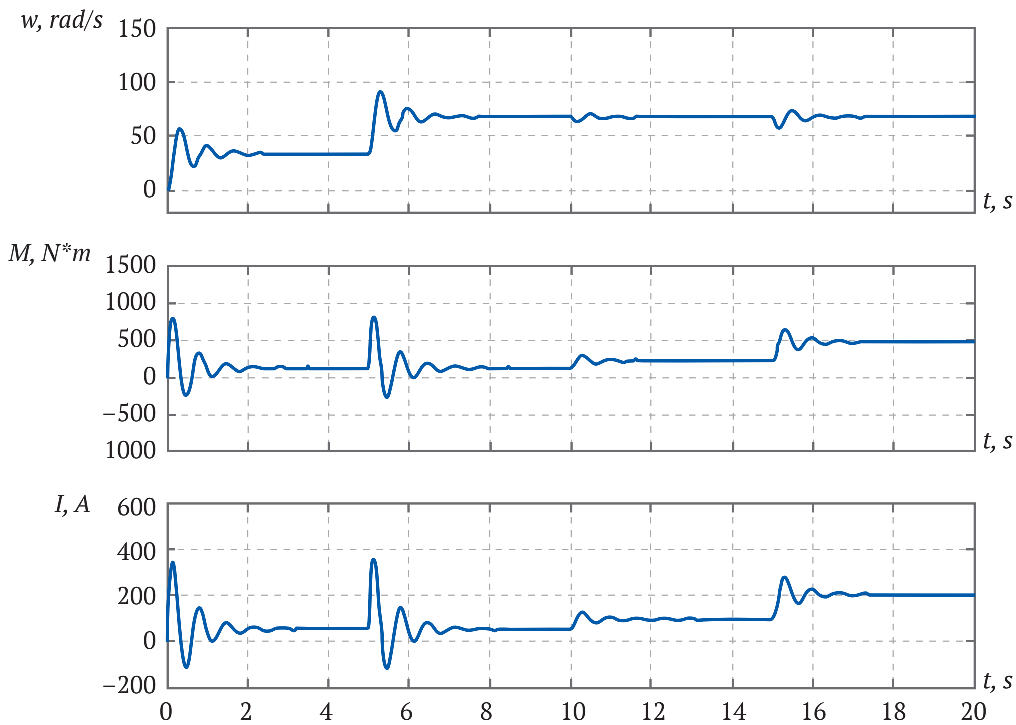

Fig. 2. Plots of transients with PI controller

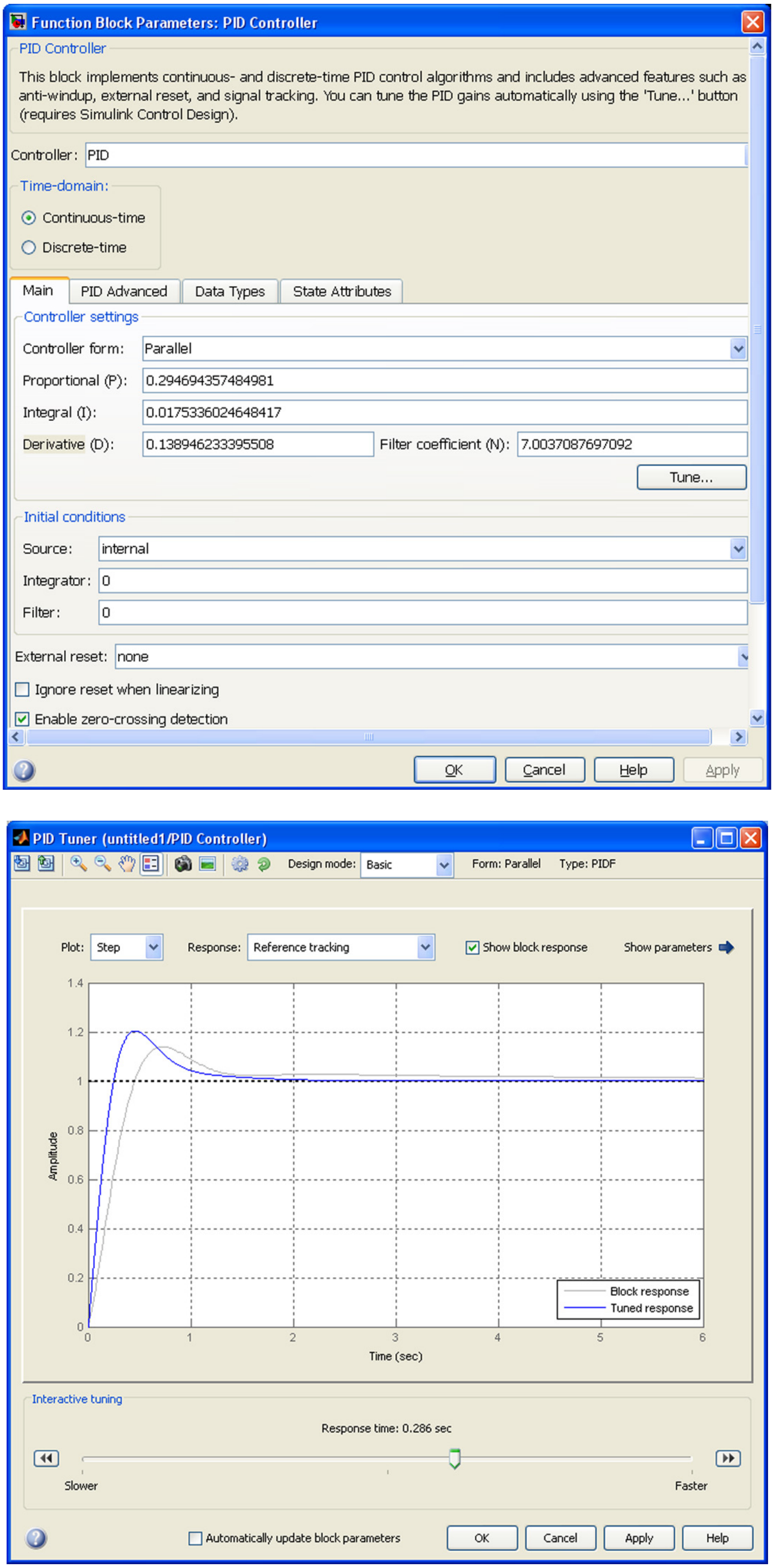

Fig. 3. PID controller parameters control

The simulation was performed for the following modes of the swivel head velocity change: startup, velocity change according to the setpoint at the 5th second, load change at the 10th second, introducing variable load at the 15th second (Fig. 4).

The load application mode is represented by a sharp change in static torque on the motor shaft. The simulation results are presented in Fig. 5.

The graphs of transients when using PID controller show the change in swivel head velocity, change in torque, change in current at the preset values. The graphs show that the use of a PID velocity controller has a much better effect on the change in velocity, torque, and current characteristics. The control time (response or transient period) decreases. The use of such a controller is most advantageous for this system.

Synthesis of fuzzy controller for automatic control of swivel head velocity

In order to simulate the transients of a swivel head velocity varying with the use of a fuzzy controller, the fuzzy variables were set, including mismatch of rotation velocity, mismatch change rate, velocity setting voltage. The term-sets of fuzzy variables were determined, and the membership functions were set for each term-set of fuzzy variable. All these membership functions were implemented in the MatLab function editor (Fig. 6).

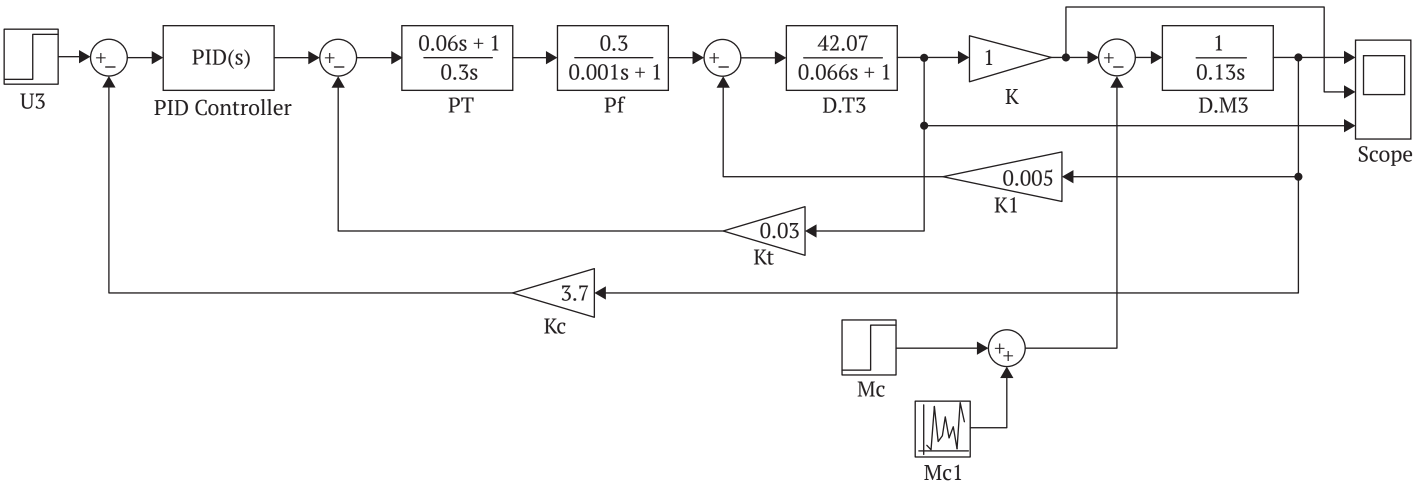

Fig. 4. System model in MatLab

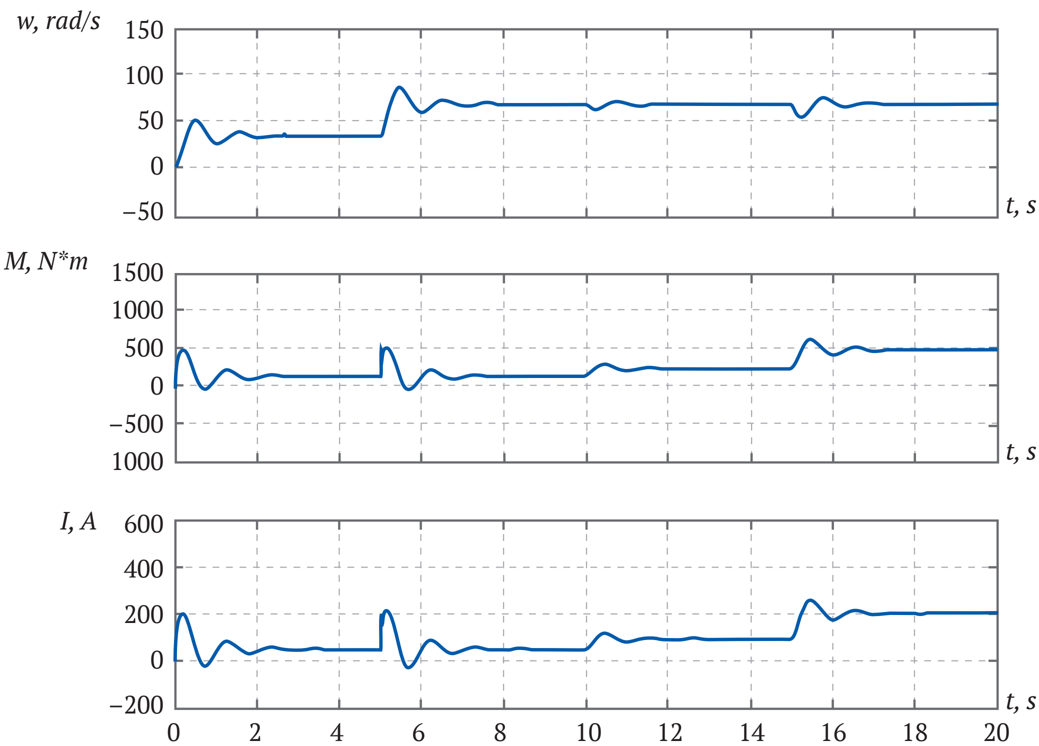

Fig. 5. Graphs of transients with PID controller

eISSN 2500-0632
https://mst.misis.ru/

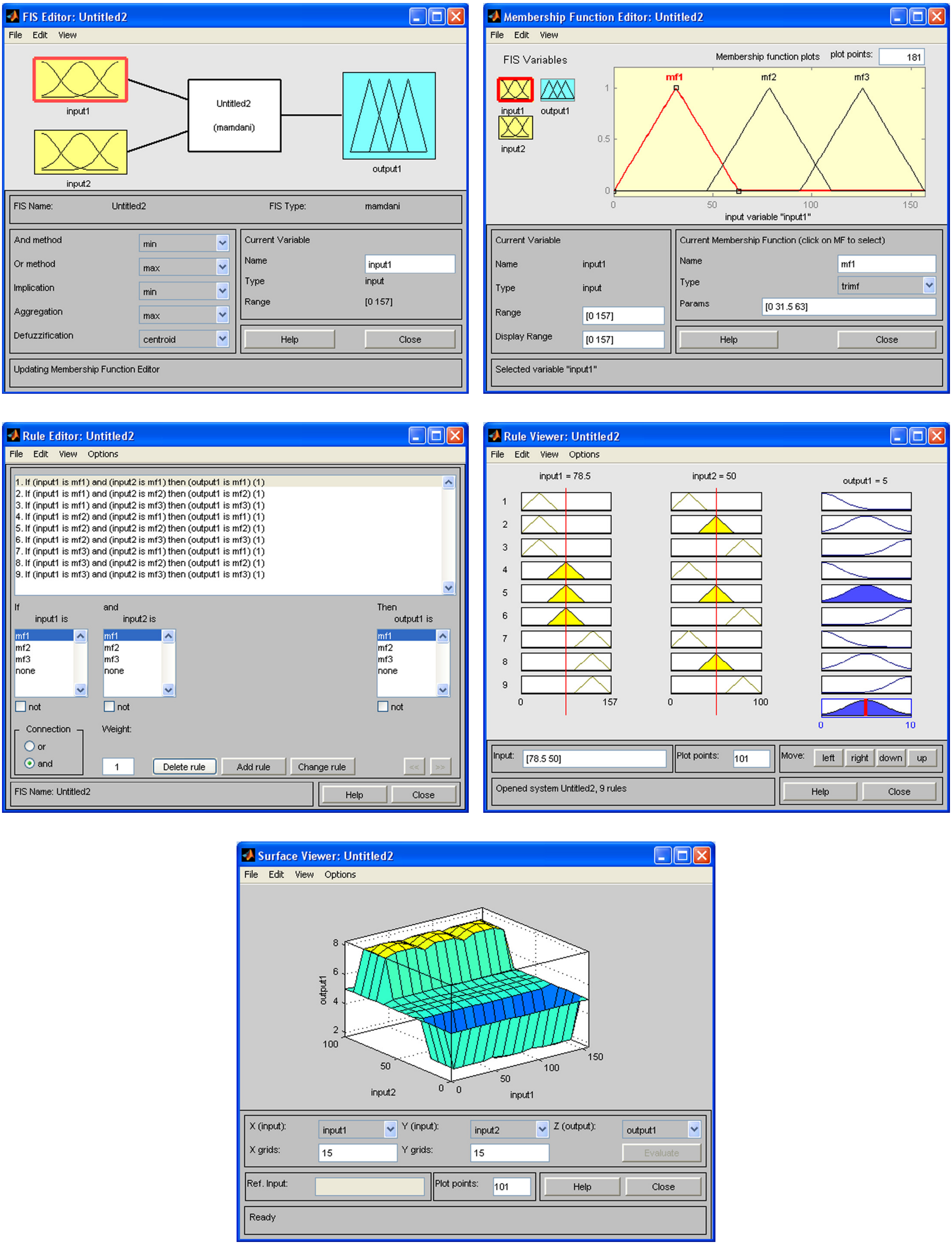

Fig. 6. Logical rule editor

The signals of mismatch of rotation velocity and speed of the mismatch change were set at the input of fuzzy controller, and attained the velocity setting voltage signal at the output.

Designing transients with fuzzy controller

Transient design and calculation was carried out using MatLab 7.11 software through simulating the system in Simulink program (Fig. 7).

Transients modes for simulating swivel head's velocity automatic control system with fuzzy controller were set as the same for the simulation with PI and PID controllers. The results of transients with fuzzy controller simulation under the given modes are shown in Fig. 8.

The results of the transients simulation for the set modes with different controllers are shown in Table 2.

Mode 1: Transient at startup under load (t = 0 s).

Mode 2: Transient at increasing setting signal (t = 5 s).

Mode 3: Transient at increasing load (t = 10 s).

Mode 4: Transient at uneven load (t = 15 s).

A comparative analysis of the transients quality indicator based on the results of simulating the drilling rig automatic control systems at the set modes showed that using swivel head's velocity control system with fuzzy controller significantly reduces the current change of transient response (time).

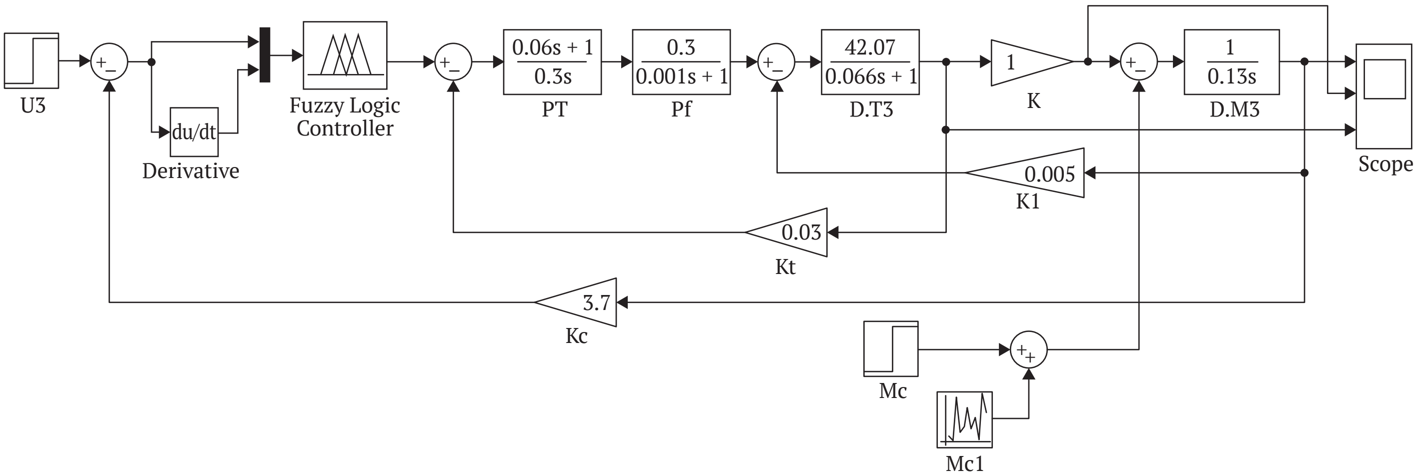

Fig. 7. Model of the system with fuzzy logic controller in MatLab

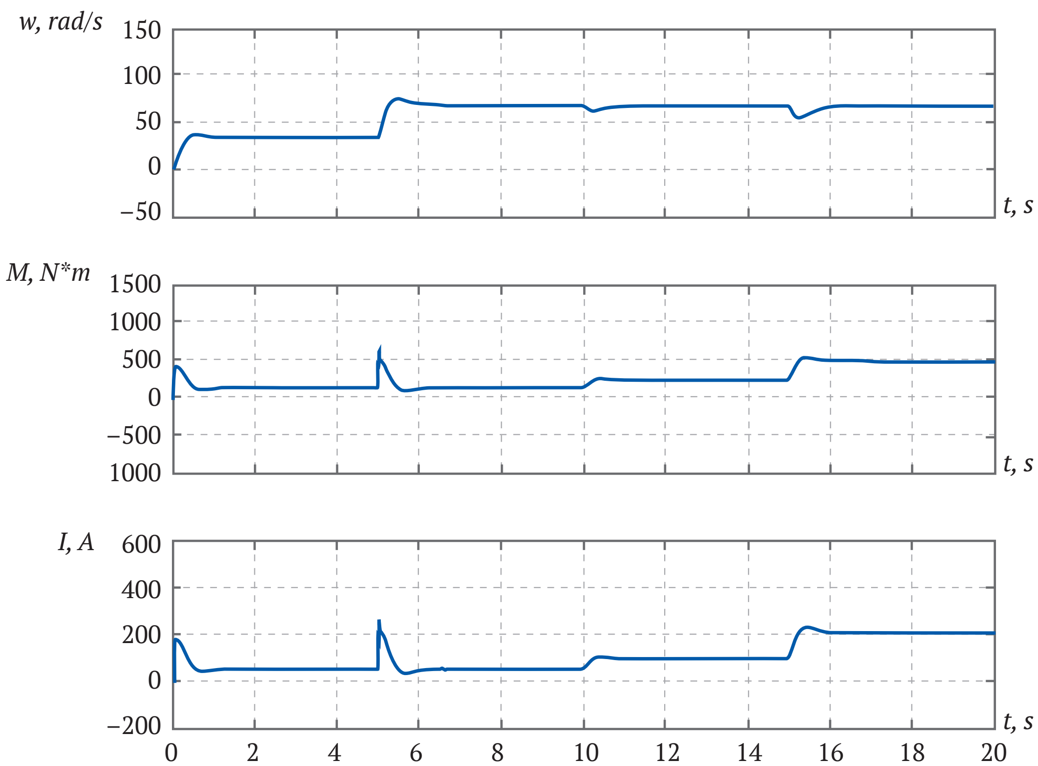

Fig. 8. Graphs of transients with fuzzy controller

Table 2

Transients control time

Operation modes	Controller type	Control (response) time, s		
		swivel head velocity	torque	current
Mode 1	PI controller	2.3	2.5	2.4
	PID controller (three-term controller)	2.3	2.8	2.5
	Fuzzy controller	2.3	1	1
Mode 2	PI controller	2.8	2.4	2.5
	PID controller (three-term controller)	2.4	3	3
	Fuzzy controller	1.4	1.1	1.4
Mode 3	PI controller	1.4	1.7	1.9
	PID controller (three-term controller)	1.8	1	2
	Fuzzy controller	1.1	0.7	0.7
Mode 4	PI controller	1.9	2.1	1.8
	PID controller (three-term controller)	2	2	2.2
	Fuzzy controller	1.3	2	1.3

Conclusions

The study substantiated the feasibility of successful applying simulation modeling for investigating the operation of swivel head electric drive, using the MatLab software environment. The results of the swivel head operation modes simulation with the standard controllers and the fuzzy controller showed that transients response (time) for the set modes of the automatic control system with the fuzzy controller decreased. The simulation results showed that the transient control time of the swivel head motor torque, and current change when using the swivel head velocity control with a fuzzy controller with increasing load depending on the rock hardness, decreased about two times. Implementation of the system of automatic control of the swivel head velocity of the drilling rig with application of the fuzzy controller will allow drilling rig vibration to be reduced. It will also provide effective protection of the swivel head electric (motor) drive from overload, increase the reliability of the equipment and productivity while drilling.

References

1. Ovsyannikov N.B., Pichuev A.V. Methods of forecasting of electric power load in mining industry. *Mining Informational and Analytical Bulletin*. 2015;(1):292–296. (In Russ.)

2. Klyuev R.V., Bosikov I.I., Gavrina O.A., Lyashenko V.I. Assessment of operational reliability of power supply to developing ore mining areas at a high-altitude mine. *Mining Science and Technology* (*Russia*). 2021;6(3):211-220. (In Russ.) https://doi.org/10.17073/2500-0632-2021-3-211-220

3. Sadridinov A.B. Analysis of energy performance of heading sets of equipment at a coal mine. *Mining Science and Technology* (*Russia*). 2020;5(4):367-375. (In Russ.) https://doi.org/10.17073/2500-0632-2020-4-367-375

4. Petrov V., Sadridinov A., Pichuev A. Analysis and modeling of power consumption modes of tunnelling complexes in coal mines. In: *E3S Web of Conferences*. *V^th^ International Innovative Mining Symposium*. 18 June 2020. 2020;174:01006. https://doi.org/10.1051/e3sconf/202017401006

5. Petrov V., Kuznetsov N., Morozov I. Experimental studies of energy technology indicators during ore crushing at a processing plant. In: *2020 IEEE International Conference on Advent Trends in Multidisciplinary Research and Innovation (ICATMRI)*. 2020. Pp. 1–4. https://doi.org/10.1109/ICATMRI51801.2020.9398320

6. Egorov A.N., Semenov A.S., Kharitonov Ya.S., Fedorov O.V. Efficiency of variable frequency drive in diamond mining. *Gornyi Zhurnal*. 2019;(2):77–82. (In Russ.) https://doi.org/10.17580/gzh.2019.02.16

7. Kuznetsov N.M., Shchutsky V.I. Rational of the electrical energy consumption at mining enterprises. *Apatity: Kola Science Centre of Russian Academy of Sciences*. 1997. 211 p. (In Russ.)

8. Fashchilenko V.N., Reshetnyak S.N. Resonant behavior of electric drives of mining machines. *Gornyi Zhurnal*. 2017;(7):80–83. (In Russ.) https://doi.org/10.17580/gzh.2017.07.15

9. Fashilenko V.N., Reshetnyak S.N. Synthesis of electromechanical systems of bodies cutting mining machines with the resonant mode of operation. *Mining Informational and Analytical Bulletin.* 2017;(S29):39–47. (In Russ.) https://doi.org/10.25018/0236-1493-2017-12-29-39-47

10. Shevyreva N.Yu. The influence of multistage filter compensation device on energy guality during the operation of drill rigs with variable-frequency electric drive. *Mining Informational and Analytical Bulletin.* 2015;(1):408–415. (In Russ.) URL: https://www.giab-online.ru/files/Data/2015/01/65_408-415_Shevyreva.pdf

11. Shevyrev Y.V., Pichuev A.V., Shevyreva N.Y. Improving energy performance in networks with semiconductor converters. In: *2019 International Conference on Industrial Engineering, Applications and Manufacturing* (*ICIEAM*). 25–29 March 2019. Sochi, 2019. Pp. 1–6. https://doi.org/10.1109/ICIEAM.2019.8743020

12. Do T.L. Research, assessment and proposals on resolving power quality problem for the power supply system of Lam Dong alumina refinery, Vietnam. *Mining Science and Technology* (*Russia*). 2021;6(2):121–127. https://doi.org/10.17073/2500-0632-2021-2-121-127

13. Kuznetsov N.M., Morozov I.N. Synthesis of the fuzzy controller of performance of the main ventilation installation of the mine. *Mining Informational and Analytical Bulletin.* 2018;(S48):336–345. (In Russ.) https://doi.org/10.25018/0236-1493-2018-11-48-336-345

14. Morozov I.N., Kirillov I.E. Using the theory of fuzzy sets in construction of automated system of managing grinding mining and processing enterprises. *Trudy Kolskogo nauchnogo centra RAN*. 2016;(6–7):141–147. (In Russ.) URL: https://cyberleninka.ru/article/n/ispolzovanie-teorii-nechetkih-mnozhestv-pri-postroenii-avtomatizirovannoy-sistemy-regulirovaniya-protsessa-izmelcheniya-gorno

15. Zhukovsky A.A., Nankin Y.A., Sushinsky V.A. *Drive and control systems of drilling rigs for open pits*. Moscow: Nedra Publ.; 1990. 223 p. (In Russ.)

Information about the authors

Nikolai M. Kuznetsov – Cand. Sci. (Eng.), Leading Researcher, Kola Science Centre of the Russian Academy of Science, Apatity, Russian Federation; ORCID 0000-0002-9440-8677, Scopus ID 56252352900, ResearcherID G-3754-2017; e-mail n.kuznetsov@ksc.ru

Ivan N. Morozov – Cand. Sci. (Eng.), Associate Professor, Murmansk Arctic State University, Murmansk, Russian Federation; ORCID 0000-0003-3488-8186, Scopus ID 57210912468, ResearcherID W-4918-2018

Received	17.10.2021
Revised	17.01.2022
Accepted	01.02.2022